

Two-Loop  $g^+ g^-$  Splitting Amplitudes in QCD

Zvi Bern

Department of Physics and Astronomy, UCLA  
Los Angeles, CA 90095-1547, USA  
E-mail: bern@physics.ucla.eduLance J. Dixon<sup>Y</sup>Stanford Linear Accelerator Center, Stanford University  
Stanford, CA 94309, USA  
E-mail: lance@slac.stanford.edu

David A. Kosower

Service de Physique Théorique, CEA (Saclay  
F-91191 Gif-sur-Yvette cedex, France  
E-mail: kosower@sph.saclay.cea.fr

**A bstract :** Splitting amplitudes are universal functions governing the collinear behavior of scattering amplitudes for massless particles. We compute the two-loop  $g^+ g^-$  splitting amplitudes in QCD,  $N = 1$ , and  $N = 4$  super-Yang-Mills theories, which describe the limits of two-loop  $n$ -point amplitudes where two gluon momenta become parallel. They also represent an ingredient in a direct  $x$ -space computation of DGLAP evolution kernels at next-to-next-to-leading order. To obtain the splitting amplitudes, we use the unitarity sewing method. In contrast to the usual light-cone gauge treatment, our calculation does not rely on the principal-value or Mandelstam-Leibbrandt prescriptions, even though the loop integrals contain some of the denominators typically encountered in light-cone gauge. We reduce the integrals to a set of 13 master integrals using integration-by-parts and Lorentz invariance identities. The master integrals are computed with the aid of differential equations in the splitting momentum fraction  $z$ . The poles of the splitting amplitudes are consistent with a formula due to Catani for the infrared singularities of two-loop scattering amplitudes. This consistency essentially provides an inductive proof of Catani's formula, as well as an ansatz for previously-unknown 1- pole terms having non-trivial color structure. Finite terms in the splitting amplitudes determine the collinear behavior of finite remainder terms in this formula.

**K eyw ords:** QCD, NNLO Computations, Jets, Collider Physics.

## 1. Introduction

Gauge theories form the backbone of the standard  $SU(3) \times SU(2) \times U(1)$  model of particle interactions. The computation of perturbative corrections in gauge theories is thus central to testing the standard model at high-energy colliders. Such computations are technically complicated, so a general understanding of properties of the results is very useful.

In the past decades, a number of new approaches have been developed to cope with this complexity, including helicity methods [1], color decompositions [2, 3, 4, 5, 6], recursion relations [7], ideas based on string theory [8, 9], and the unitarity-based method [10, 11, 12, 13]. The latter technique has been applied to numerical calculations, most recently the two-loop calculation of all helicity amplitudes for gluon-gluon scattering [14, 15].

The subject of two-loop calculations has seen tremendous technical progress in the last few years. Much of the progress has been facilitated by new techniques for performing loop integrals. Smirnov [16] and Tausk [17] gave closed-form expressions for the all-massless planar and non-planar double box integrals, respectively. Smirnov and Veretin [18] and Anastasiou et al. [19] provided algorithms for reducing the corresponding tensor integrals. More general reduction and evaluation techniques for integrals have followed as well [20, 21, 22, 23, 24]. Using these techniques, several groups have computed the basic two-loop QCD (and also QED) amplitudes for four external partons [25, 26, 27, 28, 29, 30, 31, 32, 15, 33, 34, 35], and for three partons and one external vector boson [36, 37, 22]. These amplitudes and matrix elements constitute one of the building blocks for next-to-next-to-leading order (NNLO) computations in perturbative QCD, in particular of the cornerstone processes  $e^+ e^- \rightarrow 3 \text{ jets}$  and  $p\bar{p} \rightarrow 2 \text{ jets}$ .

The two-loop amplitudes contain both ultraviolet and infrared singularities. Both are conventionally regulated using dimensional regularization. The infrared singularities correspond to the circulation of gluons in the loops that are nearly on shell and either soft or collinear with one of the external momenta (or to the circulation of other particles in the loops that are nearly on shell and collinear with one of the external momenta). The form and functional dependence of these singularities was predicted by Catani [38]. The *a priori* knowledge of these infrared singularities has been of great value in the explicit computations of two-loop amplitudes cited above.

The singularities in the virtual corrections have a counterpart in the infrared singularities of phase-space integrals of real-emission amplitudes. In the sum over all relevant (physically indistinguishable) amplitudes, unitarity in the form of the Kinoshita-Lee-Nauenberg theorem dictates that the singularities must cancel. The universality of the singularities in the integrals over real-emission amplitudes in turn reflects the universality of factorization of real-emission amplitudes in soft or collinear limits. For next-to-next-to-leading order (NNLO) calculations, the double-emission limits of tree amplitudes, and the single-emission limits of one-loop amplitudes, allow one to organize the singular phase-space integrations in a process-independent way. The universal functions governing these limits are all known [39, 40, 41, 42, 43, 44].

---

<sup>1</sup>Research supported by the U.S. Department of Energy under grant DE-FG03-91ER40662.

<sup>2</sup>Research supported by the U.S. Department of Energy under grant DE-AC03-76SF00515.

In this paper, we will compute the analogous functions, splitting amplitudes, governing the universal behavior of two-loop amplitudes as two gluon momenta become collinear. For example, in the time-like case where momenta  $k_a$  and  $k_b$  are both outgoing, we let  $k_a = zk_p$ ,  $k_b = (1-z)k_p$ , where  $k_p = k_a + k_b$  is the momentum of the nearly on-shell intermediate gluon  $P$ , and  $z$  is the longitudinal (or light-cone) momentum fraction carried by gluon  $a$ . Splitting amplitudes will be useful in checking two-loop computations beyond four external legs. A putative result for a higher-point amplitude must satisfy non-trivial constraints as momenta become collinear. They can also play a role in an alternative method of computing the NNLO corrections to the Altarelli-Parisi kernel governing the  $Q^2$  evolution of parton distributions and fragmentation functions [45]. The computation of this kernel is of great importance to a program of precision extraction of parton distribution functions from experimental data. It has been the object of an ongoing effort by Moch, Vermaseren and Vogt [46, 47], just recently completed [48]. The Mellin moments of the Altarelli-Parisi kernel are anomalous dimensions of leading-twist operators whose matrix elements give rise to parton distributions. One can compute them in a traditional manner, by computing ultraviolet divergences of loop corrections. Factorization implies, however, that one could compute the kernels in an infrared approach, directly in  $x$ -space [49, 50]. As in the computation of differential cross sections, there are both 'virtual' and 'real-emission' contributions to the kernel. The splitting amplitudes we compute in the present paper provide the doubly-virtual contributions to the NNLO kernel for evolution of the gluon distribution,  $P_{gg}^{(2)}(x)$  (at  $x \in 1$ ). Because the gluons have definite helicity, evolution of polarized distributions is equally accessible.

The computation of the Altarelli-Parisi kernel in  $N = 4$  supersymmetric gauge theories is also of interest, since its Mellin moments are the anomalous dimensions of classes of operators. The study of such anomalous dimensions is important to investigations of the anti-de Sitter/conformal field theory duality [51]. We gave the result for the splitting amplitude in  $N = 4$  supersymmetric gauge theory in an earlier Letter [52]. We will document that calculation in the present paper. The computation revealed an unexpected relation between splitting amplitudes at different loop orders: the two-loop splitting amplitude can be expressed algebraically in terms of the one-loop and tree splitting amplitudes, through  $O(\epsilon^0)$ , where  $\epsilon$  is the parameter of dimensional regularization,  $D = 4 - 2\epsilon$ . In the planar (large- $N_c$ ) limit, the four-point two-loop amplitude can be expressed in a similar 'iterative' form. This is very surprising because in a general massless field theory, the analytic structure of a two-loop amplitude can be considerably more complicated than that of one-loop amplitudes. Thus the two-loop amplitude in this theory is much simpler than expected. The splitting amplitude relation also led to a conjecture of a similar relation between one- and two-loop amplitudes with an arbitrary number of external legs.

To calculate the  $g \gamma g$  splitting amplitudes, we have used the unitarity-based method. The method is useful in general loop calculations in gauge theories. Its advantage over Feynman-diagram calculations is of course most obvious in those calculations which simply cannot be done by conventional techniques, such as that of infinite series of loop amplitudes [10, 11, 53]. The present calculation furnishes another example where the method has a clear advantage over conventional diagrammatic techniques. While the splitting amplitudes

tudes could be computed by conventional diagrammatic techniques, such a computation at two loops would probably require the use of light-cone gauge, because this gauge has simple collinear factorization properties, even in the presence of infrared singularities [54]. (An analysis in a covariant gauge is likely to be very difficult; for example, a generalization of the analysis in ref. [55] would require explicit knowledge of higher-point two-loop integrals.) As is well-documented in the literature [56, 57], use of light-cone gauge is fraught with subtleties and technical complications. Indeed, following the standard methods for dealing with light-cone gauge Feynman diagrams, along with any of the popular prescriptions needed to avoid ill-defined integrals, would lead to an answer with a surviving dependence on the prescription parameters, which cannot describe the collinear behavior of a gauge-invariant and prescription-parameter-independent amplitude. We will discuss these issues in more detail in section 3. The unitarity-based method avoids these complications, and ensures that the calculation can be done in a straightforward way using ordinary dimensional regularization. The insights furnished by the unitarity method also allow the systematic cancellation of ill-defined integrals appearing in more traditional light-cone gauge calculations [58].

To evaluate the loop momentum integrals we used integration-by-parts [59] and Lorentz invariance [20] identities implemented via the Laporta algorithm [23, 60] to solve the system of equations. With this technique the integrals can be reduced to a set of 13 master integrals. The master integrals are computed by constructing a set of differential equations in  $z$ , along the lines of refs. [18, 20].

We will organize the calculation in a color-stripped formalism, in which the color factors are separated from the kinematic content of amplitudes. At loop level, this leads to a hierarchy of terms, from terms leading in the number of colors, down through subleading contributions. The leading-color terms, which would dominate in the  $N_c \rightarrow 1$  limit, correspond to planar diagrams. These leading-color terms contain only a single color trace, with additional explicit powers of  $N_c$ . The two-loop splitting amplitude enters only into the collinear limit of single-trace terms (whether leading or subleading in color). The collinear limits of terms with multiple traces depend only on the tree-level and one-loop collinear splitting amplitudes. The full color-dressed splitting amplitude also factorizes into a color factor multiplied by a factor which is a function solely of the external momenta and helicities. The color factor for the  $g + g \rightarrow g + g$  splitting amplitude, in the language of Feynman diagrams, is always just a Lie algebra structure constant,  $f^{abc}$ . At two loops, the pure-glue result is purely leading-color; there are no subleading-color corrections. Adding quarks in the loops does generate subleading-color terms. However, non-planar diagrams do not give any contribution to the  $g + g \rightarrow g + g$  collinear behavior at two loops, because their color factors all vanish. (This feature will not hold for  $g + g \rightarrow q + q$  at three loops, and already fails to hold at two loops for splittings with external quarks,  $q + q \rightarrow q + q$ .)

As noted above, Catani [38] gave a formula which predicted the infrared singularities of renormalized two-loop amplitudes, which appear as poles through fourth order in  $\epsilon$ . One can take the collinear limit of the  $n$ -point formula, and compare it with the  $(n-1)$ -point formula, to obtain a prediction for the infrared singularities of the two-loop splitting amplitude. The Catani formula is expressed in terms of color-space operators. One term

arising at order  $1 =$  (denoted by  $\hat{H}_n^{(2)}$ ) contains a rather non-trivial color structure, and was known previously only for the four-point case. We have constructed a simple ansatz for its generalization to  $n$ -point amplitudes. A comparison of the Catani formula with our result requires an untangling of color correlations. We have performed this analysis, and find complete agreement. One can interpret this agreement as a proof of Catani's formula (including our ansatz for  $\hat{H}_n^{(2)}$ ) for the case of two-loop  $n$ -gluon amplitudes. The proof is inductive in the number of legs  $n$ , and requires certain reasonable assumptions about the types of functions that can appear in singular terms. (The functions should not vanish in all collinear limits. Such vanishing is unlikely to happen for functions which are equal to the tree amplitude times pure logarithms or polylogarithms, for example.) This proof complements the verification based on resummation given in ref. [61].

Given the consistency of our results with Catani's formula, we can subtract the singular behavior in  $\epsilon$ , to obtain a set of relations which control the finite remainder terms in the formula. We have checked that these relations are satisfied, up to overall normalization, by the finite remainder for the two-loop  $H_1^{(2)}$  gg splitting [62] for the case of identical-helicity gluons.

In the next section, we review the structure of gauge-theory amplitudes in their collinear limits. In section 3, we consider a hypothetical Feynman-diagram calculation, both in a covariant gauge and in light-cone gauge. We discuss the difficulties that would be encountered in these calculations, and how a unitarity-based method can circumvent them. In section 4, we review the unitarity-based sewing method, and present a detailed algorithm. (Appendix B describes a simple relabeling algorithm, used in the sewing process to bring integrands into a canonical form.) In section 5, we discuss the application of the sewing algorithm to the calculation of the two-loop splitting amplitude. In section 6, we describe the calculation of the required two-loop integrals, and the reduction of tensor integrals. We present our results in section 7. These contain the complete set of helicity-decomposed  $g_1^{(2)}$  gg splitting amplitudes in QCD with  $N_f$  fermions, as well as in  $N = 1$  and  $N = 4$  supersymmetric gauge theories. We present separately the collinear behavior of the finite terms in a two-loop amplitude. In section 8, we present the comparison of the singular parts of the color-trivial terms to those predicted by Catani's formula, as well as the collinear behavior of the finite remainder terms. (The precise definition of 'color-trivial' is given in that section. The full color dependence of the singular terms, including the ansatz for  $\hat{H}_n^{(2)}$ , and their collinear behavior, are discussed in appendix A.) We discuss the dressing of the splitting amplitudes with color factors, and the collinear behavior of the color-non-trivial parts of amplitudes, in section 9. We give some concluding remarks in the final section.

## 2. Splitting Amplitudes

Gauge-theory amplitudes are singular when external momenta become soft, or when a number of momenta become collinear. In these limits, the amplitudes factorize in a universal way. In collinear limits, the factorization is governed by splitting amplitudes depending only on the legs becoming collinear, and not on the remaining legs of the hard process. The

surviving hard amplitude, in turn, depends only on the merged leg, whose momentum is the sum of the collinear momenta. In this paper, we will consider the splitting amplitude governing the behavior of amplitudes as two momenta become collinear. (The tree-level behavior as three or four momenta become collinear has been derived by Cambell and Glover [40], Catani and Razzini [41], and by Del Duca et al. [63]. The one-loop behavior as three momenta become collinear has recently been considered by Catani, De Florian and Rodrigo [64].)

We find it most natural to discuss collinear factorization in the context of a trace-based color decomposition of the  $n$ -gluon amplitudes [2, 3, 4, 5]. Although the external gluons are in the adjoint representation, this color decomposition is given in terms of traces of matrices  $T^a$  in the fundamental representation of  $SU(N_c)$ , which we normalize by  $\text{Tr}(T^a T^b) = \delta^{ab}$ . We begin by discussing the behavior of terms leading in the number of colors,  $N_c$ , where we scale the number of fermions,  $N_f$ , with  $N_c$ . The full color behavior is a straightforward extension, which we defer to Section 9.

The loop expansion of the  $n$ -gluon amplitude is

$$A_n^{a_1 \dots a_n}(k_1; 1; \dots; k_n; n) = g^{n-2} \sum_{L=0}^{\infty} g^2 \frac{2e}{(4\pi)^2} A_n^{(L) a_1 \dots a_n}(k_1; 1; \dots; k_n; n); \quad (2.1)$$

where  $a_i$  is the color index of the  $i$ -th external gluon, and the factor of  $2e = (4\pi)^2 \frac{1}{L}$ , with  $e = 1 = 0.5772 \dots$ , corresponds to the normalization convention of ref. [38]. The trace-based color decomposition of the  $L$ -loop amplitude is

$$A_n^{(L) a_1 \dots a_n}(k_1; 1; \dots; k_n; n) = N_c^L \sum_{S_n = Z_n} \text{Tr}((1) \dots (n)) A_n^{(L)}((1); \dots; (n)) + O(N_c^{L-1}); \quad (2.2)$$

where  $A_n^{(L)}$  are  $L$ -loop color-ordered (sub-)amplitudes, where  $\text{Tr}(1 \dots n) = \text{Tr}(T^{a_1} \dots T^{a_n})$ ; and where  $S_n = Z_n$  runs over the non-cyclic permutations of  $1, 2, \dots, n$ . The latter correspond to the set of inequivalent traces. The permutation  $S_n$  acts both on the gluon momenta  $k_i$  and helicity labels  $a_i$ , implicit on the right-hand side of eq. (9.1). At tree level ( $L = 0$ ), expression (2.2) is exact, and has no subleading-color corrections. At loop-level ( $L > 0$ ), there are subleading-color terms containing products of two or more traces (see eqs. (9.4) and (9.9)). Also, the amplitudes must be evaluated in  $D = 4 - 2$  dimensions to regulate the virtual singularities. We extract in a prefactor the leading  $N_c^L$  behavior. The normalization of  $A_n$ , and hence of the splitting amplitudes we present below, differs from that in refs. [10, 11]. Note that  $A_n^{(L>0)}$  will in general contain terms proportional to powers of  $N_f = N_c$  and  $1 = N_c^2$ .

The color-ordered amplitudes in eq. (2.2) have a universal behavior as legs become collinear [65]. At tree level, the amplitudes behave as [66]

$$A_n^{(0)}(\dots; a^a; b^b; \dots) \stackrel{a \rightarrow b}{\sim} \text{Split}^{(0)}(z; a^a; b^b) A_{n-1}^{(0)}(\dots; P; \dots); \quad (2.3)$$

in the limit where the momenta  $k_a \rightarrow z k_p$  and  $k_b \rightarrow (1-z) k_p$  with  $k_p = k_a + k_b$ . Here  $\text{Split}^{(0)}(z; a^a; b^b)$  is a tree-level splitting amplitude. Legs  $a$  and  $b$  carry helicities  $a$  and

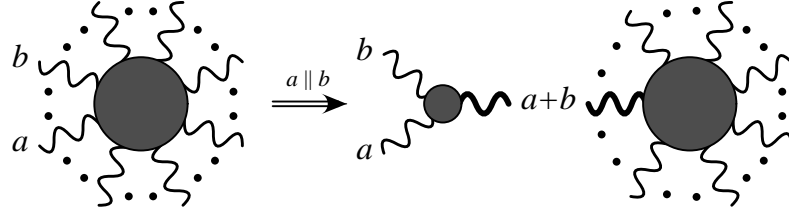


Figure 1: The collinear factorization of a tree-level amplitude. The thick line represents a slightly off-shell gluon.

, while the merged leg  $P$  carries helicity  $\pm$ . In the sum  $\sum$  runs over the two helicities of the intermediate state. The factorization of an  $n$ -point tree amplitude into a splitting amplitude and an  $(n-1)$ -point amplitude (2.3) is depicted schematically in figure 1.

The pure-gluon tree-level splitting amplitudes are [67, 4, 66]

$$\text{Split}^{(0)}(z; a^+; b^-) = 0; \quad (2.4)$$

$$\text{Split}^{(0)}(z; a^+; b^+) = \frac{1}{P \frac{z}{z(1-z)} \text{habi}}; \quad (2.5)$$

$$\text{Split}^{(0)}(z; a^+; b^-) = \frac{z^2}{P \frac{z}{z(1-z)} [ab]}; \quad (2.6)$$

$$\text{Split}^{(0)}(z; a^+; b^+) = \frac{(1-z)^2}{P \frac{z}{z(1-z)} [ab]}; \quad (2.7)$$

These splitting amplitudes are expressed in terms of spinor inner products [1, 66],  $h_i j_i = h_i j j^+ i$  and  $[ij] = h_i^+ j j^- i$ , where  $j j^- i$  are massless Weyl spinors of momentum  $k_i$ , labeled by the sign of the helicity. The spinor products are antisymmetric, with norm  $j h_i j_i j = j [ij] j = \frac{1}{2} s_{ij}$ , where  $s_{ij} = 2 k_i \cdot k_j$ . A key advantage of the spinor formalism is that it makes the square-root behavior of the splitting amplitudes manifest. The remaining tree-level splitting amplitudes, with  $\pm = \pm$ , may be obtained from the above ones by parity, which states (for general loop order  $L$ ) that

$$\text{Split}^{(L)}(z; a^+; b^-) = \text{Split}^{(L)}(z; a^+; b^-)_{\text{habi} \neq [ab]}; \quad (2.8)$$

In quoting explicit results in this paper, we use parity to assume that the intermediate state  $P$  always has positive helicity,  $\pm = +$ . As we shall discuss further in section 9, Bose symmetry implies that the color-stripped splitting amplitude is antisymmetric under exchange of its two arguments (including  $z \leftrightarrow 1-z$ ),

$$\text{Split}^{(L)}(1-z; b^+; a^+) = \text{Split}^{(L)}(z; a^+; b^+); \quad (2.9)$$

This relation allows us to obtain the results for  $P^+ \rightarrow a^+ b^-$  from those for  $P^+ \rightarrow a^- b^+$ .

At one loop the structure is similar. In this case the the collinear limits are [10, 55, 65]

$$\begin{aligned} A_n^{(1)}(:::; a^+; b^-; :::) &\stackrel{a^+ b^-}{=} \text{Split}^{(0)}(z; a^+; b^-) A_{n-1}^{(1)}(:::; P^+; :::) + \\ &+ \text{Split}^{(1)}(z; a^+; b^-) A_{n-1}^{(0)}(:::; P^+; :::); \end{aligned} \quad (2.10)$$

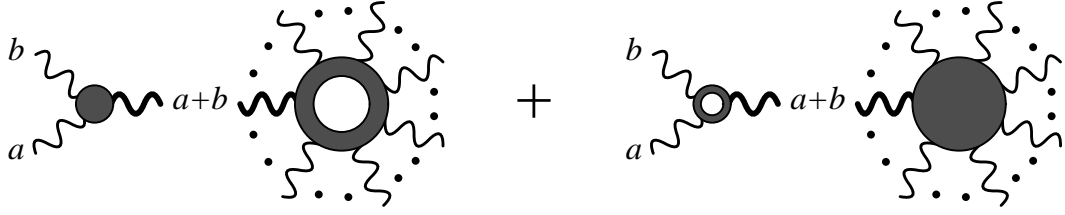


Figure 2: Two types of terms appear in the collinear factorization of a one-loop amplitude. The thick lines represent slightly off-shell gluons.

where  $\text{Split}^{(1)}$  is a one-loop splitting amplitude. Figure 2 displays eq. (2.10) schematically.

Except for  $\text{Split}_-(z; a^-; b^-)$ , which vanishes at tree level (along with  $\text{Split}_+(z; a^+; b^+)$ ), the ratio of the  $g^+ g^-$  one-loop splitting amplitudes to the tree-level ones is well-defined. The ratio depends trivially on the Lorentz invariant  $s_{ab}$ , and non-trivially on  $z$ , but it does not involve spinor products. For the helicity configuration whose tree splitting amplitude vanishes we have,

$$\text{Split}^{(1)}(z; a^-; b^-) = + \hat{c} \frac{p}{z(1-z)} \frac{\text{hab}}{[ab]^2} \frac{2}{(1-2)(2-2)(3-2)} \frac{2}{s_{ab}} \frac{1}{1} \frac{N_f}{N_c} ; \quad (2.11)$$

where

$$\hat{c} = \frac{e}{2} \frac{(1+z)^2(1-z)}{(1-2)} : \quad (2.12)$$

Notice that in the  $\epsilon$ -expansion of  $(s_{ab})^2$ ,  $\ln(s_{ab})$  appears. For timelike kinematics, this expression has an imaginary part according to the prescription,

$$\ln(s_{ab}) = \ln s_{ab} \quad i ; \quad s_{ab} > 0 : \quad (2.13)$$

The remaining splitting amplitudes, for  $= +$ , are conveniently written in terms of their ratios to the tree-level ones,

$$\text{Split}^{(1)}(z; a^+; b^+) = r_S^{(1);N=4}(z; s_{ab}) \text{Split}^{(0)}(z; a^+; b^+); \quad (2.14)$$

where

$$r_S^{(1);N=4}(z; s) = r_S^{(1);N=4}(z; s) + \hat{c} \frac{2}{s} \frac{2z(1-z)}{(1-2)(2-2)(3-2)} \frac{1}{1} \frac{N_f}{N_c} ; \quad (2.15)$$

$$r_S^{(1);N=4}(z; s) = r_S^{(1);N=4}(z; s) ; \quad (2.16)$$

and

$$r_S^{(1);N=4}(z; s) = \hat{c} \frac{2}{s} \frac{1}{2} \frac{1}{z} \frac{z}{\sin(\pi)} + \sum_{m=1}^{\infty} 2^{2m-1} L_{2m-1} \frac{z}{z-1} \# \\ = \hat{c} \frac{1}{2} \frac{2}{z(1-z)(-s)} + 2 \ln z \ln(1-z) \frac{z}{z-1} + O(z) : \quad (2.17)$$

(Here,  $r_n$  is the Riemann zeta function.) The label  $N = 4$  on  $r_s^{(1);N=4}$  means that it is the appropriate function for  $N = 4$  super-Yang-Mills theory, for both  $++$  and  $+$  cases (see also section 7.1). At one loop this expression also happens to serve as the splitting amplitude for pure  $N = 1$  super-Yang-Mills theory, for both nonvanishing cases,

$$r_s^{(1)++;N=1}(z;s) = r_s^{(1)+;N=1}(z;s) = r_s^{(1);N=4}(z;s) : \quad (2.18)$$

This relation will be violated at two loops. The parameter  $R$  selects the particular variant of dimensional regularization (see eq. (7.1)). For  $R = 1$  the scheme is the 't Hooft-Veltman (HV) [68] scheme, while for  $R = 0$  it is the four-dimensional helicity [8, 69] (FDH) scheme. We always quote results for supersymmetric theories in the FDH scheme, which is related to, but distinct from, Siegel's dimensional reduction scheme [70]. As noted above, the normalization of the splitting amplitudes differs from that in ref. [10]; to recover the earlier normalization for  $\text{Split}^{(1)}$ , replace  $\hat{c}$  by  $c$ , defined in eq. (2.12) of that reference. To recover the earlier normalization of  $r_s^{(1)}$ , replace  $\hat{c}$  by unity.)

These one-loop splitting amplitudes were first obtained from the collinear limits of four-point amplitudes [10]. Subsequently they were obtained to all orders in  $\epsilon$ , as required for NNLO calculations [55, 42, 43]. We will express divergent parts of the two-loop splitting amplitudes in terms of one-loop quantities. Hence we have retained all the terms in the expansion in these expressions.

At two loops, the subject of this paper, the amplitudes behave as [65],

$$\begin{aligned} A_n^{(2)}(:::; a^a; b^b; :::) &\stackrel{akb}{=} \text{Split}^{(0)}(z; a^a; b^b) A_{n-1}^{(2)}(:::; P; :::) + \\ &+ \text{Split}^{(1)}(z; a^a; b^b) A_{n-1}^{(1)}(:::; P; :::) + \\ &+ \text{Split}^{(2)}(z; a^a; b^b) A_{n-1}^{(0)}(:::; P; :::) ; \quad (2.19) \end{aligned}$$

where  $\text{Split}^{(2)}$  is the two-loop splitting amplitude. One of the goals of this paper is to calculate this two-loop splitting amplitude in QCD. To do so we will use the unitarity sewing method [10, 11, 12], as applied to splitting amplitudes [43]. In a previous paper we presented the result of this calculation for the special case of  $N = 4$  super-Yang-Mills theory. For this theory the unique two-loop splitting amplitude has the remarkable property of being an iteration of the one-loop result (2.17), which led to a conjecture that a similar iterative property holds for the planar contributions to amplitudes [52]. This conjecture was shown to be correct for the four-point amplitude using a previously-derived [71] expression for the two-loop integrand. In section 7 we shall present the explicit values of the two-loop splitting amplitudes for  $g \rightarrow gg$  in QCD, as well as in  $N = 4$  and  $N = 1$  supersymmetric gauge theories.

As in the one-loop case, we write the two-loop splitting amplitudes in terms of their ratios  $r_s$  to the corresponding tree-level splitting amplitudes (when the latter do not vanish). Taking  $\epsilon = +$  by parity, we define  $r_s^{(2)}$  via,

$$\text{Split}^{(2)}(z; a^a; b^b) = r_s^{(2)a^a b^b}(z; s_{ab}) \text{Split}^{(0)}(z; a^a; b^b) : \quad (2.20)$$

We give the explicit expansions of the functions  $r_s^{(2)}(a, b)$ , as Laurent expansions in  $\epsilon$ , for the various theories in question, in eqs. (7.16), (7.28), (7.29) and (7.38), and the expression for  $\text{Split}^{(2)}(z; a, b)$  in eq. (7.43).

Although we shall not discuss higher-loop splitting amplitudes here, we remark that the obvious  $L$ -loop generalization of the collinear behavior,

$$A_n^{(L)}(:::; a^a; b^b; :::) \stackrel{akb}{=} \sum_{L=0}^{\infty} X^L \text{Split}^{(L)}(z; a^a; b^b) A_{n-1}^{(L-1)}(:::; P; :::); \quad (2.21)$$

can indeed be proven correct [65]. These splitting amplitudes govern the collinear behavior of the entire amplitude, including all multiple color trace terms. We will discuss this more fully in section 9. With our normalizations the leading-color contributions to  $\text{Split}^{(1)}$  are of order  $N_c^0$ , but in general the splitting amplitudes have contributions of higher order in  $1=N_c^2$ , as well as quark-loop contributions of order  $(N_f=N_c)^p$ , with  $p \leq L$ , or higher in  $1=N_c^2$ .

### 3. Difficulties with Feynman Diagram Approach

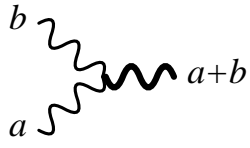


Figure 3: The three-point vertex diagram for obtaining the tree-level splitting amplitude. The thick line represents an on-shell gluon.

Before turning to our calculation of the two-loop  $g! gg$  splitting amplitudes using the unitarity-based sewing method, it is instructive to consider how one would proceed using a standard Feynman diagram approach. Heuristically, one might try to 'factorize' an  $n$ -point amplitude on the collinear pole, i.e. to construct the  $L$ -loop splitting amplitudes by summing up all  $L$ -loop Feynman diagram with three external legs, one of which is on-shell. While this might seem to be the most straightforward approach, a number of complications arise in practice, as we shall see in this section. In section 5 we shall sidestep these complications using the unitarity-based sewing procedure [10, 11, 12, 13], outlined in section 4. This method has previously been applied to splitting amplitudes at one loop [65, 43].

#### 3.1 Tree-Level Splitting Amplitudes

At tree level, factorization works without any subtleties. That is, we can compute the splitting amplitude directly from the Feynman diagram three-point vertex depicted in figure 3. The only diagrams for an  $n$ -point amplitude with a pole in  $s_{ab}$  are those containing this vertex as one factor. Such calculations have appeared elsewhere, for example in ref. [66].

As two color-adjacent momenta  $k_a$  and  $k_b$  become collinear, we factorize an  $n$ -point tree amplitude on the  $s_{ab}$  kinematic pole in terms of a three-point vertex and an  $(n-1)$ -point amplitude,

$$A_n^{(0)}(1; 2; :::; a; b; :::; n) \stackrel{akb}{=} (a)'' (b) V_i \frac{X''(P)''(P)}{s_{ab}} + \frac{\partial}{\partial''(P)} A_{n-1}^{(0)}(1; 2; :::; P; :::; n); \quad (3.1)$$



Figure 4: Three non-vanishing Feynman diagrams contributing to the pure-glue splitting amplitude. The thick gluon line is slightly off-shell.

where the kinematics is the same as in eq. (2.3). In setting up the calculation the merged leg should be left slightly off-shell. Otherwise the putative splitting amplitude would be ill-defined, since the  $1=s_{ab}$  pole diverges. This basic structure is independent of the particle type, although we have written eq. (3.1) for the case of an intermediate gluon. Here " $\langle P \rangle$ " is the polarization vector for the gluon  $P$  with helicity  $\pm$ . For the case of  $g \rightarrow gg$ , the ordinary Feynman gauge three-point vertex is

$$V(k_a, k_b) = \frac{i}{p^2} (k_a \cdot k_b) + (2k_b + k_a) \cdot (2k_a + k_b) : \quad (3.2)$$

After inserting an explicit representation of the helicity states [1], we obtain from eq. (3.1) precisely the collinear behavior (2.3), together with the explicit values of the splitting amplitudes (2.4)–(2.7). In this limit the helicity algebra in the numerator of the vertex causes it to vanish like  $\frac{p}{s_{ab}}$ , partially canceling the pole in  $s_{ab}$ . Physically, this cancellation is due to an angular momentum mismatch between  $\langle P \rangle$  and  $k^a + k^b$ . Overall, we are left with the  $1=\frac{p}{s_{ab}}$  behavior evident in the splitting amplitudes. Other gauge choices, such as light-cone gauge or the non-linear Gervais-Neveu gauge [72], give the same final result as Feynman gauge.

### 3.2 Difficulties at Loop Level

The simplicity of a conventional diagrammatic calculation at tree level might lead one to believe that a similar approach should work at loop level. Such a calculation would involve Feynman diagrams of the type depicted in Figure 4. This expectation, however, turns out to be incorrect. At loop level, the situation is not quite this simple.

In covariant gauges, such as Feynman gauge, one immediately runs into trouble [55], because there are contributions to collinear behavior from Feynman diagrams of the form shown in Figure 5, with no single-particle pole in  $s_{ab}$ . The required pole emerges only after carrying out the loop integration. Moreover, the  $\epsilon$ -expansion of some of the integrals has discontinuous behavior as  $s_{ab} \rightarrow 0$ , because of the interchange of this limit with the limit  $\epsilon \rightarrow 0$ .

The appearance of more complicated loop integrals is reflected in the structure of the known results for the splitting amplitudes (2.15)–(2.17), which contain polylogarithms in the variable  $z$ . Such functions simply cannot occur in the integrals encountered in the triangle or bubble graphs in Figure 4, which in a covariant gauge produce only logarithms, in the variable  $s_{ab}$ . Clearly, the polylogarithms must come from elsewhere. They do in fact arise from non-factorizing diagrams of the type shown in Figure 5 [55]. This peculiar

absence of factorization is tied to the presence of soft and collinear virtual divergences in the theory, reflected as poles in the loop amplitudes. At one loop, the non-factorizing pieces may be reconstructed using knowledge of all the possible integral functions that appear in amplitudes, along with the universal structure of the infrared divergences. Indeed, such a reconstruction was used to prove universal factorization of the one-loop amplitudes [55] and to compute their explicit values [42]. This reconstruction, however, does not generalize straightforwardly to higher loops.

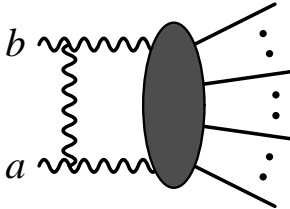


Figure 5: In covariant gauges, diagrams without single-particle factorization can contribute to the splitting amplitude.

As the next logical choice of a method for calculating a splitting amplitude directly from Feynman diagrams, one might turn to light cone-gauge. This gauge is known [73, 54] to have simple factorization properties. A key advantage of light-cone gauge is that only physical states propagate. This can help clarify various formal properties. Moreover, light-cone gauge vertex integrals do contain polylogarithms of the type appearing in the one-loop splitting amplitude. Light-cone gauge has a long history and has been used to address a wide variety of problems. For example, the first proofs of factorization in QCD between the hard and soft parts of a process were performed in this gauge [54]. Another important example is the next-to-leading order (NLO) calculation of the Altarelli-Parisi evolution kernel in  $x$ -space [73, 74, 75, 76]. Light-cone gauge has also been used for more formal purposes, such as the proof of finiteness of maximally supersymmetric ( $N = 4$ ) Yang-Mills gauge theories [77].

In describing the collinear limit of amplitudes, light-cone gauge is useful because, as a physical gauge, it can prevent the non-factorizing graphs of figure 5 from contributing. In a general covariant gauge, such graphs would inevitably mix under residual gauge transformations with the graphs in figure 4.

In light-cone gauge, the one-loop splitting amplitude is given by the sum of the three Feynman diagrams shown in figure 4. In this gauge there are no ghost contributions. Furthermore, all cactus diagrams, as well as bubbles attached to the massless external lines  $a$  and  $b$ , vanish in dimensional regularization, leaving only the three diagrams shown. The light-cone gauge Feynman vertices are the same as those in Feynman gauge. The propagator is now

$$D = \frac{i\gamma}{p^2 + i} \quad (3.3)$$

where the light-cone projector is,

$$d = \frac{n \cdot p + p \cdot n}{p \cdot n} : \quad (3.4)$$

Here  $p$  is the particle momentum,  $n$  is the Minkowski metric, and  $n$  is a nullvector ( $n^2 = 0$ ) defining the light-cone direction.

In carrying out a light-cone gauge calculation, one quickly runs into well-known technical difficulties [56] arising from regions of loop integration where the light-cone denominator

$p \cdot n - \hat{p}$  vanishes. The light-cone denominators introduce a new set of singularities in the Feynman integrals, some of which are not regulated by dimensional regularization. In order for a generic light-cone gauge diagram to be well-defined, a prescription for dealing with these singularities is needed. For example, the principal-value (PV) prescription replaces

$$\frac{1}{p \cdot n} \stackrel{!}{=} \lim_{! \rightarrow 0^2} \frac{1}{p \cdot n + i} + \frac{1}{p \cdot n - i} ; \quad (3.5)$$

where  $i$  is a regulator parameter. Another choice, better founded in field theory, is the Mandelstam-Leibbrandt prescription [77, 56]. A comparison of these two prescriptions may be found in ref. [78].

The introduction of an additional prescription in a splitting amplitude calculation is problematic for a number of reasons:

The additional prescription complicates the calculation, and requires the computation of more difficult Feynman integrals.

At higher loops the validity of the prescription is less clear [57].

After expanding in small  $\epsilon$ , the results contain factors of  $\ln \epsilon$ , where  $\epsilon$  is the prescription parameter. In general these cancel only after combining virtual and real emission contributions.

Further to the last point, a calculation of the splitting amplitudes that retains dependence on a prescription parameter cannot match the splitting amplitudes extracted from the collinear limits of scattering amplitudes. An on-shell  $n$ -point scattering amplitude is gauge invariant, and depends only on the external momenta and on the dimensional regulator parameter  $\epsilon$ , not on any light-cone prescription parameter  $\epsilon$ . The same is true of its collinear limits. Thus loop splitting amplitudes defined via the collinear limits of scattering amplitudes cannot depend on the parameter  $\epsilon$ .

If we had been computing the Altarelli-Parisi kernel, which receives contributions from both virtual and real emission contributions, then the dependence on  $\epsilon$  would cancel between them [74, 75, 76, 78]. However, since we are interested in computing the collinear behavior of the virtual contributions on their own, in general the dependence would not cancel. This difficulty makes it unclear how the desired splitting amplitudes can emerge from a light-cone gauge calculation.

It is helpful to consider a few examples in order to illustrate the structure of integrals with light-cone denominators, and to help explain how we will later sidestep these difficulties, using the unitarity-based sewing method.

### 3.3 One-Loop Light-Cone Integral Examples

Consider the scalar integrals shown in figure 6. In the figure, an arrow on an internal line indicates the insertion of the light-cone factor  $1 = (p_i \cdot n)$ , with the momentum carried by the marked line. Such integrals appear in a light-cone gauge calculation of the one-loop splitting amplitude, using the Feynman diagrams of figure 4. We shall see that there is a

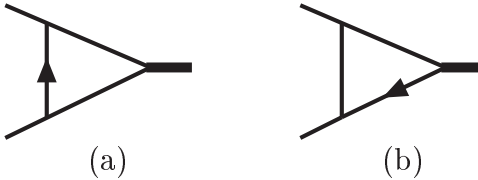


Figure 6: One-loop triangle diagrams containing light-cone denominators. The arrow indicates the line containing a light-cone denominator. Integral (a) contains an unregulated singularity, but does not appear in the unitarity-based sewing method.

big difference between the two types of integrals in figure 6; one is properly regulated by dimensional regularization without any additional prescriptions, and one is not [78].

The explicit expressions for the two integrals are,

$$J^{(a)}(z; s) = i \int_{-z}^z \frac{d^D p}{p^2 (p - k_1)^2 (p - k_1 - k_2)^2 (p - k_1)^n} ; \quad (3.6)$$

$$J^{(b)}(z; s) = i \int_{-z}^z \frac{d^D p}{p^2 (p - k_1)^2 (p - k_1 - k_2)^2 p^n} ; \quad (3.7)$$

where  $s = (k_1 + k_2)^2 = 2k_1 \cdot k$  and, for consistency with the collinear kinematics,  $z$  is defined by

$$k_1 \cdot n = z (k + k_2) \cdot n ; \quad k \cdot n = (1 - z) (k + k_2) \cdot n ; \quad (3.8)$$

For  $J^{(a)}(z; s)$  the light-cone denominator involves the loop momentum between the two massless legs, while for  $J^{(b)}(z; s)$  the light-cone denominator involves a loop momentum adjacent to the merged on-shell external leg.

In order to evaluate these integrals it is helpful to make use of their properties as  $n$  is rescaled [43], which imply that

$$J^{(a)}(z; s) = \frac{1}{(-s)^{1+}} \frac{f^{(a)}(z)}{(k_1 + k_2) \cdot n} ;$$

$$J^{(b)}(z; s) = \frac{1}{(-s)^{1+}} \frac{f^{(b)}(z)}{(k_1 + k_2) \cdot n} ; \quad (3.9)$$

where  $f^{(a)}, f^{(b)}$  are functions to be determined. Without loss of generality we may set

$$(k_1 + k_2) \cdot n = s : \quad (3.10)$$

At the end of the evaluation we can use eq. (3.9) to replace one factor of  $1=(-s)$  with  $1=[(k_1 + k_2) \cdot n]$ . (The splitting amplitudes are independent of  $n$ , so the light-cone vector  $n$  must cancel from final expressions.)

One might be tempted to switch to light-cone coordinates, as is commonly done when performing light-cone gauge calculations. In these coordinates we take  $p^+ = p \cdot n$  and  $p^- = p \cdot n$  where  $n$  is dual to  $n$ , i.e.

$$n = (n_0; n) ; \quad n = (n_0; n) : \quad (3.11)$$

In light-cone coordinates, the integral  $J^{(b)}(z; s)$ , for example, is given by

$$J^{(b)}(z; s) = i \int_0^Z \frac{d^D p^2}{D=2} dp^+ dp^- \frac{1}{p^2 (p - k_1)^2 (p - k_1 - k_2)^2 p^+}; \quad (3.12)$$

which is ill-defined because of the unregulated longitudinal integral  $dp^+ = p^+$ . However, with this choice of coordinates we have switched to a version of dimensional regularization where only the transverse coordinates are regulated. This does not correspond to covariant dimensional regularization:  $dp^+ dp^- d^D p^2 \neq d^D p$ . This difficulty is relatively minor, and may be dealt with by reverting to covariant dimensional regularization. Alternatively, we could introduce the principal-value prescription, to justify intermediate steps, but then remove it prior to performing the final Feynman-parameter integration (see for example eq. (34) of ref. [78]). In either case, care is required because of the ill-defined nature of expressions.

Even covariant dimensional regularization, however, does not succeed to properly regulate all light-cone integrals. Let us first compare the behavior of  $J^{(a)}$  and  $J^{(b)}$  in their momentum-space forms (3.6) and (3.7). In momentum space, singularities arise whenever two or three denominator factors vanish. The light-cone denominator vanishes when  $p$  becomes proportional to  $n$ ,  $p \parallel n$ . In this region  $p^2$  also vanishes, but the other two denominators do not vanish. The singularity that arises here thus looks very much like the collinear singularity that arises when  $p$  becomes collinear with  $k_1$ ,  $p \parallel k_1$ . This singularity is regulated by covariant dimensional regularization, and so we may expect the same to be true for the new singularity that arises in the presence of the light-cone denominator. This will indeed turn out to be the case. In contrast, for  $J^{(a)}$ , after shifting the momentum  $p^0 = p - k_1$  we can see that in the soft region  $p^0 \parallel 0$  we have four vanishing denominators, which is indicative of the difficulties that will be encountered in evaluating this integral.

We can see the difficulty with  $J^{(a)}$  more explicitly using its Feynman-parameterized form. We begin by Schwinger parameterizing,

$$J^{(a)}(z; s) = i \int_0^Z \prod_{i=1}^4 dt_i \frac{d^4 p}{2} \exp \frac{h}{(t_1 + t_2 + t_3)p^2 - 2p \cdot (t_1 k_1 + t_3 k_1 + t_3 k_2)} \frac{i}{t_4 p - n + \frac{1}{2}s + t_4 k_1 - n}; \quad (3.13)$$

To integrate out the loop momentum we perform the shift

$$p = p^0 + \frac{t_2 k_1 + t_3 k_1 + t_3 k_2}{T} + \frac{t_4 n}{2T}, \quad (3.14)$$

where  $T = t_1 + t_2 + t_3$ . (Note that the Schwinger parameter  $t_4$  associated with the light-cone denominator is absent from  $T$ .) Wick rotating and then integrating out the shifted loop momentum  $p^0$  gives

$$J^{(a)}(z; s) = \int_0^Z \prod_{i=1}^4 dt_i \frac{Y^4}{T} \frac{d^D p}{D=2} \exp \frac{(t_2 + t_3)t_3 s}{T} \frac{t_4 (t_2 k_1 + t_3 k_1 + t_3 k_2)}{T} \frac{n}{T} + \\ + t_3 s + t_4 k_1 - n$$

$$= \int_0^z \prod_{i=1}^3 dt_i T^{D=2} \exp \frac{t_1 t_3 s}{T} + \frac{s t_4 (t_3(1-z) - t_1 z)}{T} ; \quad (3.15)$$

where we have used the replacements (3.8) and (3.10) to obtain the last line. The integral over the Schwinger parameter  $t_4$  associated with the light-cone denominator is now trivial, and yields

$$J^{(a)}(z; s) = \int_0^z \prod_{i=1}^3 dt_i T^{D=2+1} \frac{1}{s(t_1 z - t_3(1-z))} \exp \frac{t_1 t_3 s}{T} ; \quad (3.16)$$

As usual we may convert the Schwinger parameters to Feynman parameters by defining  $a_i = t_i = T$  and integrating out the overall scale  $T$ , yielding a compact Feynman parameter representation,

$$J^{(a)}(z; s) = (1 + ) (s)^2 \int_0^z \prod_{i=1}^3 da_i \frac{1}{a_j} \frac{x^3}{a_1 z - a_3(1-z)} \frac{(a_1 a_3)^{-1}}{a_1 z - a_3(1-z)} ; \quad (3.17)$$

The reader will observe that for timelike kinematics, the integrand blows up inside the region of integration. For example, if  $z = 1/2$  there is a singularity at  $a_1 = a_3$ . This singularity could be regulated by analytically continuing in  $z$ ; in the space-like region, where  $z > 1$ , it is in fact absent. This is not, however, the only singularity in the integrand. It is also singular in the corner of the integration region where  $a_2 = 1$ , as can be made manifest by changing variables  $a_2 = 1 - v$ ,  $a_1 = vu$ ,  $a_3 = v(1 - u)$ , with jacobian  $v$ ,

$$J^{(a)}(z; s) = (1 + ) (s)^2 \int_0^z dv du v^{-2} \frac{[u(1-u)]^{-1}}{1-u-z} ; \quad (3.18)$$

The singularity as  $v \rightarrow 0$  is stronger than the  $v^{-1}$  that would correspond to a logarithmic divergence, and would give rise to a pole in  $v$ . Formally, analytic continuation in  $v$  will regulate this divergence (in fact the  $v$  integral will not give rise to a pole at all), but this requires a large analytic continuation, and effectively happens through the subtraction of an infinite constant. (There is of course no associated bare coupling here into which such an infinite constant could be absorbed.) Note that this pathology is independent of  $z$ , and so cannot be cured by analytically continuing in the latter variable.

The principal-value prescription (3.5) is a widely-used method to deal with this problem. For this integral it would give rise to a 'naked'  $1/v$  singularity. Absent such a prescription, which as discussed above we must avoid for other reasons, care would be required in a complicated calculation to ensure that all integrals are continued in a consistent manner, and that these continuations do not violate any symmetries. It would be much simpler if we do not have to confront this issue at all. As we shall see, our approach to the calculation indeed allows us to avoid integrals like  $J^{(a)}$  altogether.

In contrast, the integral  $J^{(b)}$  in figure 6(b) is properly regulated by dimensional regularization. To see this explicitly, follow similar steps as in the computation of  $J^{(a)}$  to obtain,

$$J^{(b)}(z; s) = (1 + ) (s)^2 \int_0^z \prod_{i=1}^3 da_i \frac{1}{a_j} \frac{x}{a_2 z + a_3} \frac{(a_1 a_3)^{-1}}{a_2 z + a_3} ; \quad (3.19)$$

In this case, the integrand diverges no worse than  $a_i^{-1}$  near any boundary, and so dimensional regularization renders the integral finite for small negative  $w$  without infinite subtractions. Indeed, this integral is well-defined and its value is [43],

$$J^{(b)}(z; s) = 2 \frac{(1 + \dots)^2 (1 - \dots)}{(1 - 2 \dots)} (s)^2 \left( \frac{1}{z} - \frac{1}{2} - \frac{1}{2} \ln z + \frac{1}{2} \ln^2 z + \text{Li}_2(1 - z) \right) + O(\dots); \quad (3.20)$$

so there is no need for an additional prescription here. We will also encounter the integral  $J^{(b)}(1 - z)$ . In the space-like case, with  $1 - z < 0$ , the latter's integrand will be singular inside the region of integration. As explained above, this can be regulated by analytic continuation in  $z$  from  $z < 1$ .

Although it is not necessary, it is still possible to use an additional prescription for dealing with the light-cone denominator singularity in  $J^{(b)}$ . Had we, for example, used the principal-value prescription we would have obtained instead

$$J_{PV}^{(b)}(z; s) = (1 + \dots)(s)^2 \int_0^{Z_1 Y^3} \prod_{i=1}^X da_i \prod_j \frac{1}{a_j} (a_1 a_3)^{-1} \frac{a_2 z + a_3}{(a_2 z + a_3)^2 + (s)^2}; \quad (3.21)$$

following the discussion in e.g. ref. [78]. For  $z = 0$  this integral evaluates to

$$J_{PV}^{(b)}(z; s) = (s)^2 \left( \frac{(1 + \dots)^2}{z} - \frac{1}{2} + \ln \frac{1}{s} - 2 \ln z - \ln \frac{1}{s} \ln z + \ln^2 z + \text{Li}_2(1 - z) \right) + O(\dots); \quad (3.22)$$

Compared with the result in dimensional regularization (3.20), the  $1/z$  singularity arising from the light-cone denominator has been traded for a  $\ln z$  singularity. The  $\ln z$  would then appear in the result for the splitting amplitude. As mentioned earlier, such a result cannot match the splitting amplitude describing the collinear limits of gauge-invariant, dimensionally-regulated one-loop amplitudes, because the latter depend only on  $s$ , not  $z$ . We therefore wish to avoid additional prescriptions, which are in any event unnecessary for  $J^{(b)}$ . They would be required only for integrals like  $J^{(a)}$ .

What distinguishes the integrals (a) and (b) in figure 6? Could it be that the appearance of ill-defined integrals like (a) is purely an artifact of the gauge choice and would not appear in a more physical construction of the splitting amplitudes? We will see that the answer to the latter question is yes.

A general difficulty with diagrammatic approaches is that gauge-invariant results are chopped up and separated into gauge-dependent pieces by the decomposition into diagrams. For example, for a fully on-shell scattering amplitude calculation at tree level, each light-cone gauge Feynman diagram contains light-cone denominators. Yet by gauge invariance their sum must be free of such denominators. Unitarity then implies that similar cancellations should happen at loop level. For splitting amplitudes, one leg is off-shell. Hence the cancellation of light-cone denominators is not complete; nevertheless, there will be a partial cancellation. In order to understand which light-cone denominators may appear and which should not, we use unitarity.

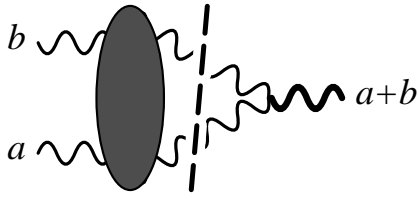


Figure 7: The two-particle cut of a one-loop splitting amplitude. The cut is represented by the dashed line. On the left-hand side all legs, including the cut ones, are on-shell. On the right-hand side the merged leg represented by a thick line is slightly off-shell.

The two-particle cut of the one-loop splitting amplitude is depicted in Figure 7. Using the Cutkosky rules [79] we obtain,

$$\text{Absp Split}^{(1)}(z; a; b) = \frac{d^D p}{(2^D)^2} \left[ \delta^2(p^2) + \delta^2(p_1^2) + \delta^2(p_2^2) A_4^{(0)}(a; b; p_2; p_1) \right] d(p_1) d(p_2) V(p_1; p_2); \quad (3.24)$$

where  $p_1 = p$ ,  $p_2 = p - k_a - k_b$ , the vertex  $V$  is defined in eq. (3.2),  $d$  is the physical state projector given in eq. (3.4), and  $\delta^2(p^2) = \delta^0(p^0) \delta^2(p^2)$ . This is the only non-trivial cut of the one-loop splitting amplitude and therefore yields the complete absorptive part. On the left-hand side of the cut,  $A_4^{(0)}$  is a gauge-invariant amplitude | all legs including the cut ones are on-shell. Any light-cone denominator appearing to the left of the cut must therefore be spurious: gauge invariance dictates that light-cone denominators cannot appear after combining all Feynman diagrams, because such denominators would not appear in a covariant gauge. Because the full one-loop splitting amplitude can be reconstructed from its absorptive part, the light-cone denominator appearing in the integral in Figure 6(a) must also be spurious (absent from the sum over all diagrams) in the full calculation, not just the absorptive part. In contrast, light-cone denominators on the cut lines are introduced by the Cutkosky rules via the sum over polarizations across the cut line,

$$\sum_{\text{X}} \delta^{(1)}(p) \delta^{(1)}(p) = \frac{p \cdot n + n \cdot p}{p \cdot n} = d; \quad (3.25)$$

This physical state projector is the on-shell version of the one appearing in the light-cone gauge propagator (3.3). The light-cone denominators that appear here can survive. This is the type of light-cone denominator that appears in the integral of Figure 6(b). (Indeed, as noted earlier, some light-cone denominators must survive in order to get an answer of the sufficient polylogarithmic complexity.)

The unitarity argument indicates that only light-cone denominators associated with a cut line need survive. (In the multi-loop case, denominators associated with lines to the right of all cuts can also survive.) Thus it should be possible to perform calculations where dangerous light-cone denominators of the sort depicted in Figure 6(a) do not appear. The unitarity-based sewing method, which we present in section 4, has exactly this property.

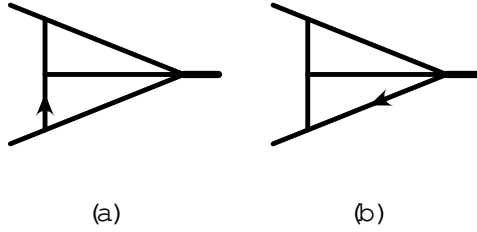


Figure 8: Sample three-point integrals at two loops containing light-cone denominators. Integral (a) is ill-defined without additional prescriptions, but integral (b) is rendered finite by dimensional regularization alone.

### 3.4 Two-Loop Light-Cone Integrals

At two loops we encounter a similar situation: some integrals are properly regulated solely by covariant dimensional regularization, and others are not.

As concrete examples consider the two-loop integrals in figure 8, given by

$$L^{(a)}(z; s) = i \int_0^z \frac{d^D p}{(2\pi)^D} \frac{d^D q}{(2\pi)^D} \frac{1}{p^2 (p - k_1)^2 (p + q)^2 (q + k_1 + k_2)^2 (q + k_1)^2 (p - k_1)^2} ; \quad (3.26)$$

$$L^{(b)}(z; s) = i \int_0^z \frac{d^D p}{(2\pi)^D} \frac{d^D q}{(2\pi)^D} \frac{1}{p^2 (p - k_1)^2 (p + q)^2 (q + k_1 + k_2)^2 (q + k_1)^2 p} ; \quad (3.27)$$

In our calculation of the two-loop splitting amplitude from the unitarity sewing method, we encounter only integrals similar to  $L^{(b)}$ . Following similar steps as at one loop, we obtain the Feynman parametrized form,

$$L^{(a)}(z; s) = (1 + 2) (s)^{2/2} \int_0^z \int_{i=2}^1 \frac{da_i}{Y^6} \frac{1}{a_i} \int_j^X \frac{a_j}{z [a_6 (a_2 + a_3) + a_3 (a_2 + a_4)]} \frac{a_2 a_6}{a_2 a_6} ; \quad (3.28)$$

where

$$= (a_2 + a_4) (a_3 + a_5) + a_6 (a_2 + a_3 + a_4 + a_5) ; \quad (3.29)$$

This integral has an insufficiently regulated divergence in the region  $a_5 \rightarrow 0$ . To see this, make the change of variables  $a_5 = 1 - v$ ,  $a_{j=2,3,4,6} = vb_j$ , for which the jacobian is  $v^3$ :

$$L^{(a)}(z; s) = (1 + 2) (s)^{2/2} \int_0^z \int_{i=2,3,4,6}^1 \frac{dv}{Y^6} \frac{db_i}{b_i} \frac{1}{b_i} \int_j^X \frac{b_j}{v} v^{2/3} \frac{b^3}{z [b_6 (b_2 + b_3) + b_3 (b_2 + b_4)]} \frac{b_2 b_6}{b_2 b_6} ; \quad (3.30)$$

where

$$b = vb_3 (b_2 + b_4) + vb_6 (b_2 + b_3 + b_4) + (1 - v) (b_2 + b_4 + b_6) ; \quad (3.31)$$

Like  $J^{(a)}$  of the previous subsection, the integral has a power-law divergence for  $v \rightarrow 0$  which would require a large analytic continuation, or equivalently the subtraction of an

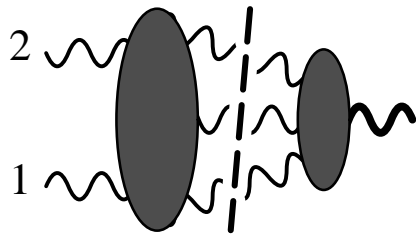


Figure 9: The three-particle cut of a two-loop splitting amplitude. On the left-hand side of the cut, the amplitude is gauge invariant since all legs including the cut ones are on-shell.

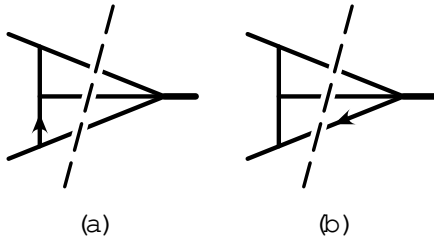


Figure 10: The three-particle cut of the two-loop three-point integrals of figure 8.

infinite constant. This divergence is again independent of  $z$ , and hence cannot be cured by analytic continuation in that variable.

On the other hand, for integral (b) in figure 8 we have the Feynman parametrized form

$$L^{(b)}(z; s) = \frac{(1 + z^2)(s^2 - 2)}{z^6 \prod_{i=2}^0 (a_i s^i + 1)} \prod_j \frac{a_j}{a_2 a_6 + z [a_4 a_6 + a_5 (a_2 + a_4 + a_6)]} \frac{(a_2 a_3 a_6)^{1/2}}{a_2 a_6 + z [a_4 a_6 + a_5 (a_2 + a_4 + a_6)]}; \quad (3.32)$$

In this case the integral is well-defined; at all boundaries, the integrand goes like  $v^{1-m}$ ,  $m = 1, \dots, 4$ . For example, as  $a_3 = 1 - v \rightarrow 1$ , the presence of  $a_3$  in the numerator lessens the singularity to  $v^1$ .

But need we concern ourselves with the possible appearance of ill-defined integrals like  $L^{(a)}$ ? As at one loop, light-cone denominators at two loops can be separated into two categories, depending on whether they appear in unitarity cuts or not. For example, consider the three-particle cut of a two-loop splitting amplitude shown in Figure 9. The three-particle cuts of the two integrals in Figure 8 are shown in Figure 10. Since all legs of the four-point amplitude on the left-hand side of the cut, including the cut ones, are fully on-shell, then following the same logic as in the one-loop case, the light-cone denominator appearing in the integral in Figure 8(a) is a light-cone gauge artifact which can be eliminated. (This type of argument cannot be used on the right-hand side of the cut, because the emerged leg is off-shell.) The light-cone denominator appearing in Figure 8(b), on the other hand, is allowed because it corresponds to a physical-state projector on a cut line.

The use of the unitarity-based sewing method, which we describe in detail in the following section, allows us to avoid the use of any prescription for light-cone denominators



Figure 11: Additional three-point integrals at two loops containing light-cone denominators. Both integrals are well-defined using dimensional regularization alone.

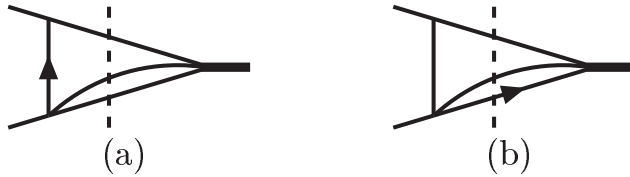


Figure 12: The three-particle cuts of the two-loop three-point integrals of Figure 11.

in the calculations in following sections. But one can also imagine applying the insights above to a more standard diagrammatic calculation in light-cone gauge. One could proceed as follows: introduce one of the standard prescriptions for dealing with light-cone denominator singularities. Then, attempt to combine diagrams algebraically to remove those light-cone denominators which by unitarity cannot appear in the desired quantity. Once all denominators leading to ill-defined integrals have canceled, one can remove the additional prescription (for example, by taking  $\epsilon \rightarrow 0$  in the PV prescription), and only then perform the loop integrals.

The unitarity arguments above can be applied not only to ill-defined integrals, but also to rule out certain well-defined integrals. As an example, consider the two integrals in Figure 11. Both turn out to be well-defined (for integral (a), this is clear from momentum-space power-counting). If we examine their cuts, shown in Figure 12, however, we see that integral (a) has a light-cone denominator to the left of the cut, and hence cannot appear. Integral (b) has a light-cone denominator on the cut, and hence is not ruled out by the unitarity argument. Indeed, it is the master integral  $W_{\text{edge}}(z; s)$  of Figure 31, whose explicit expansion in  $\epsilon$  is given in eq. (6.49).

In summary, the unitarity cuts point to a method that sidesteps the prescription issues associated with light-cone denominators, because only a restricted set of integrals appear. In the next section we explain in some detail how to construct loop-momentum integrands using the unitarity method. In our calculation of two-loop splitting amplitudes in sections 5 and 6, such loop integrals are reduced to a linear combination of master integrals. There are several equivalent bases that are convenient for different aspects of the calculation; one of the equivalent forms contains only integrals well-defined using dimensional regularization alone, and not requiring any additional prescriptions. All singular boundaries lead to logarithmic singularities in the  $\epsilon \rightarrow 0$  limit, just as for the integral  $J^{(b)}$  discussed in the previous subsection, or the integral  $L^{(b)}$  above.

## 4. Review of the Unitarity-Based Sewing Method

### 4.1 Overview

The unitarity of the scattering matrix in a quantum field theory is the statement that probability is conserved. It is an essential property of any sensible and consistent theory. It relates the non-forward part  $T$  of the scattering matrix  $S$  to its square,  $i(T - T^Y) = T^Y T$ , where  $T$  is defined via  $S = 1 + iT$ . In Feynman diagrams, unitarity is expressed by the Cutkosky rules [79, 80], which express the ‘imagine’ or absorptive part of a diagram<sup>1</sup> in terms of phase-space integrals over products of lower-loop diagrams. The product is given by ‘cutting’, replacing specified sets of propagators by delta functions in the propagator momentum. Loop amplitudes are computed, of course, by summing over appropriate collections of Feynman diagrams. Their absorptive parts are given by sums of products of lower-loop diagrams. Collecting all diagrams on each side of a cut into amplitudes, we see that the absorptive parts of loop amplitudes are just sums over products of lower-loop amplitudes.

This observation is particularly powerful in gauge theories (and in gravity as well). In gauge theories, there are extensive cancellations between different diagrams in the computation of scattering amplitudes for on-shell states. These simplifications can be made manifest at early stages of a tree-level calculation using the spinor helicity representation for gauge-boson polarization vectors. (These simplifications may be understood using twistor space [9].) The final answers in massless theories are particularly simple, sometimes simpler than the expression for a single Feynman diagram out of the hundreds or thousands that contribute, and have a natural expression in terms of spinor products. We may then express the cut of an on-shell one-loop amplitude, given by a product of on-shell tree amplitudes (or a sum of such products), in simple form as well. This simplicity carries through order-by-order in perturbation theory. The sewing technique aims to exploit this simplicity, by turning the process around, and building loop amplitudes out of their cuts, in turn given by lower-loop amplitudes.

The full amplitude can in principle be reconstructed using dispersion relations. For general gauge theories in four dimensions, the dispersive reconstruction of an amplitude suffers from an additive ambiguity related to divergent ultraviolet behavior. One can add a rational function, free of cuts, to the amplitude. This problem has traditionally hampered the use of dispersion relations to obtain complete amplitudes. It is solved in massless theories<sup>2</sup> through the use of dimensional regularization, which effectively tames the ultraviolet behavior of the bare integrand [81] and thereby removes the need for explicit subtractions. This represents a third role for the dimensional regulator beyond its usual roles as a regulator for ultraviolet and infrared divergences. The sewing technique we review is equivalent to the use of dispersion relations in dimensional regularization, although for practical purposes it is preferable to make use of ordinary Feynman-integral techniques for

<sup>1</sup>By ‘imagine’ we mean the discontinuities across branch cuts.

<sup>2</sup>In massive theories, there is an additional source of ambiguities (from masses inside bubbles on external legs). When there is only one mass in a calculation, this problem can be resolved through simple adjustments [12].

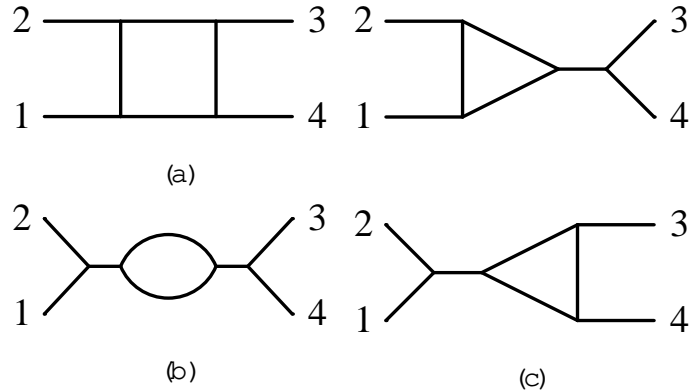


Figure 13: Color-ordered Feynman diagrams for the one-loop four-point amplitude in  $\text{Tr}^3$  field theory: (a) the box diagram (b) the s-channel bubble diagram (c) the s-channel triangle diagrams. The two t-channel triangle diagrams and the t-channel bubble diagram are not shown explicitly. Bubbles on external legs vanish in dimensional regularization and are not shown here either.

performing the necessary integrations rather than doing explicit dispersion integrals. (At one loop, for example, knowledge of the complete decomposition of n-point integrals in dimensional regularization in terms of a basis of known integrals [82] reduces the problem to an algebraic one.) Sewing back together cut amplitudes, with the cut lines on shell but treated exactly in  $D = 4 - 2$  dimensions, will reproduce the full gauge-theory answer. (The different ways of continuing the amplitude to  $D$  dimensions correspond to the use of different variants of dimensional regularization, such as CDR [83], HV [68], or FDH [8, 69].) One can then expand in  $\epsilon$  to obtain the answer through  $\mathcal{O}(\epsilon^0)$ , including the rational terms. A more pedestrian way to understand how the rational terms are included properly is to observe that in dimensional regularization, these terms are not purely rational, but rather are rational functions of the momentum invariants, multiplied by  $(s)^L$  at  $L$  loops, for some invariants (e.g. as in eq. (3.23)). At  $\mathcal{O}(\epsilon^0)$ , this factor contains a logarithm, and hence an imaginary part for  $s > 0$ . Only when the  $\epsilon \rightarrow 0$  limit is taken at the end of the calculation, does the term become purely a rational function, free of discontinuities.

#### 4.2 Sewing at One Loop

Consider first the sewing method at one loop. Before explaining it in generality, it will be useful to examine the procedure in a simple example. In each example here and in later subsections, we will make contact with standard methods by starting with an amplitude expressed in terms of conventional Feynman diagrams. In the examples, we will work in a massless  $\text{Tr}^3$  field theory (with transforming under the adjoint of  $SU(N_c)$ ), but as discussed above the method applies to general theories, and indeed is relatively more powerful precisely in field theories with many redundant variables in their covariant form, such as gauge theories and gravity.

Let us start by considering the four-point one-loop amplitude. The full amplitude has Bose symmetry, which just as in the gauge-theory case we can exhibit most concisely by rewriting it as a sum over color permutations of a more basic quantity. The leading-color

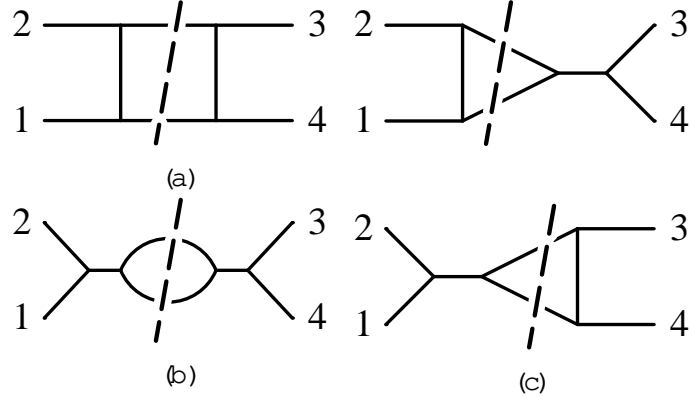


Figure 14: Diagrams depicting the s-channel cut of the one-loop four-point amplitude in  $\text{Tr}^3$  field theory.

contributions (leading in a  $1 \Rightarrow N_c$  expansion) involve only planar diagrams. We will focus on these contributions in the examples. In particular, we focus on the coefficient of the color trace  $\text{Tr}(T^{a_1} T^{a_2} T^{a_3} T^{a_4})$  given by color-ordered diagrams [66, 13] with the 1234 ordering of legs.

There are seven color-ordered diagrams contributing to this one-loop partial amplitude. The ones with cuts in the s channel are depicted in Figure 13. The ordered amplitude has cuts in only two channels, s and t. If we examine the s channel, we see that only four of the diagrams contribute to the cut: the box, two triangles, and one of the bubbles. Similarly, four diagrams contribute to the cut in the t channel. The s-channel cut may be obtained by replacing the propagators cut in Figure 14 via

$$\frac{1}{p^2 + i} \rightarrow 2i^+ (p^2); \quad (4.1)$$

This replacement converts the loop integral to one over the phase space of the two cut legs, which are placed on shell. We can also see that the sum of terms factors, so that on each side of the cut we obtain a tree amplitude as the sum of diagrams, as shown in Figure 15. In each channel, the cut is thus given by a phase space integral of the product of two tree amplitudes,

$$A^{(1)}(1;2;3;4) = \frac{\int d^D p_1 d^D p_2}{(2\pi)^D} \left( \frac{p_1^2}{s_{12}} + \frac{p_2^2}{s_{14}} + \frac{(p_1^2)^D}{s_{12}^D} (p_1 + p_2 + k_1 + k_2) \right) A^{(0)}(1;2;p_1;p_2) A^{(0)}(p_1; p_2; 3; 4);$$

where

$$A^{(0)}(1;2;3;4) = i \frac{1}{s_{12}} + \frac{1}{s_{14}}; \quad (4.2)$$

and we have suppressed powers of the three-scalar coupling.

The sewing procedure reverses this process. We start, for example, in the s channel. Multiply the tree amplitude on the left-hand side of Figure 15 by that on the right-hand side,

$$A^{(0)}(1;2;p_1;p_2;3;4) A^{(0)}(p_1; p_2; 3; 4) = \frac{1}{s_{12}} + \frac{1}{s_{14}} - \frac{1}{s_{34}} - \frac{1}{s_{14}}; \quad (4.3)$$

where  $\gamma_1 = \gamma_2 - k_1 - k_2$ . Put in the two propagators crossing the cut, and integrate over the loop momentum  $\gamma$  to yield,

$$\begin{aligned} & \frac{d^D \gamma}{(2\pi)^D} \frac{1}{s_{12}} + \frac{1}{s_1} \frac{1}{\gamma^2} \frac{1}{s_{34}} \frac{1}{s_4} \frac{1}{(\gamma + k_1 + k_2)^2} \\ &= \frac{d^D \gamma}{(2\pi)^D} \frac{1}{s_{12}^2} \frac{1}{\gamma^2 (\gamma + k_1 + k_2)^2} + \frac{1}{s_{12}} \frac{1}{\gamma^2 (\gamma - k_4)^2 (\gamma + k_1 + k_2)^2} + \\ & \quad + \frac{1}{s_{12}} \frac{1}{(\gamma + k_1)^2 \gamma^2 (\gamma + k_1 + k_2)^2} + \frac{1}{(\gamma + k_1)^2 \gamma^2 (\gamma - k_4)^2 (\gamma + k_1 + k_2)^2} : \end{aligned} \quad (4.4)$$

Similarly, from the t-channel cut, we obtain,

$$\begin{aligned} & \frac{d^D \gamma}{(2\pi)^D} \frac{1}{s_{23}^2} \frac{1}{\gamma^2 (\gamma + k_2 + k_3)^2} + \frac{1}{s_{23}} \frac{1}{\gamma^2 (\gamma - k_1)^2 (\gamma + k_2 + k_3)^2} + \\ & \quad + \frac{1}{s_{23}} \frac{1}{(\gamma + k_2)^2 \gamma^2 (\gamma + k_2 + k_3)^2} + \frac{1}{(\gamma + k_2)^2 \gamma^2 (\gamma - k_1)^2 (\gamma + k_2 + k_3)^2} : \end{aligned} \quad (4.5)$$

The first three terms have no cut in the s channel, but the last term does: it is given by the residue of the poles as  $\gamma = k_1$  and  $\gamma + k_2$  simultaneously go on shell,

$$\frac{1}{2(\gamma - k_1) \gamma k_2 (\gamma - k_1) \gamma} : \quad (4.6)$$

Alternatively, we can shift  $\gamma \rightarrow \gamma + k_1$ , upon which the last term becomes identical to the last term in eq. (4.4).

We cannot simply add the contributions from the s and t channels, because this would correspond to the sum of eight diagrams, double-counting the box diagram 13(a), given by the last terms in eqs. (4.4) and (4.5). Accordingly, we must find a function which has the correct cuts in all channels. We can do this either before or after integration, although in general it is easier to do it before loop integration. One way is simply to sum both

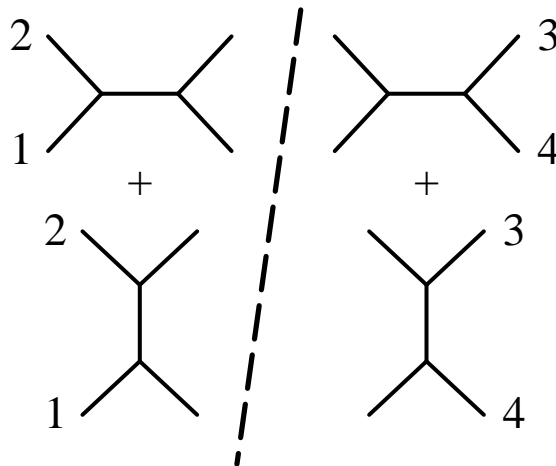


Figure 15: The s-channel cut of the one-loop four-point amplitude in  $\text{Tr}^3$  field theory, seen as a product of tree amplitudes.

contributions, and then remove the overlap: terms in one cut channel which also have a ‘cut’ | in the sense of having the propagators which give rise to a cut | in the other channel. One can alternatively think of this as ‘merging’ the two expressions, taking a term if present in either cut or in both, but taking it only once in the latter case.

The net effect is to drop one of the two equivalent terms; we obtain the sum of the remaining terms for the ordered one-loop amplitude,

$$\begin{aligned}
 A_Z^{(1)}(1;2;3;4) = & \frac{d^D \delta}{(2\pi)^D} \frac{1}{s_{12}^2} \frac{1}{\delta^2 (1 + k_1 + k_2)^2} + \frac{1}{s_{12}} \frac{1}{\delta^2 (1 - k_4)^2 (1 + k_1 + k_2)^2} + \\
 & + \frac{1}{s_{12}} \frac{1}{(1 + k_1)^2 \delta^2 (1 + k_1 + k_2)^2} + \frac{1}{(1 + k_1)^2 \delta^2 (1 - k_4)^2 (1 + k_1 + k_2)^2} + \\
 & + \frac{1}{s_{23}^2} \frac{1}{\delta^2 (1 + k_2 + k_3)^2} + \frac{1}{s_{23}} \frac{1}{\delta^2 (1 - k_1)^2 (1 + k_2 + k_3)^2} + \\
 & + \frac{1}{s_{23}} \frac{1}{(1 + k_2)^2 \delta^2 (1 + k_2 + k_3)^2} ;
 \end{aligned} \tag{4.7}$$

exactly as would have emerged from a Feynman-diagram computation. Of course, in a <sup>3</sup> field theory, there are no cancellations between different diagrams, so the sewing method is also equivalent in complexity to the usual approach. In gauge theories, the sewn on-shell tree amplitudes are much simpler objects than the one-loop diagrams, and so the sewing approach helps minimize the complexity of intermediate steps.

In the above examples, the procedures for sewing and removing any overlaps or double-counting are completely mechanical. Note that none of them make any reference (to use an old-fashioned language) to double dispersion relations. Indeed, only in an abstract sense are dispersion relations used at all, since we do not perform the dispersion integrals explicitly, but rather implicitly via construction of appropriate Feynman integrals. We will next explain how to formalize these procedures, and then give an algorithm which can be used to implement them in practice. ¶

To formalize the sewing procedure, introduce the basic promotion operator  $A$ . It will be applied to products of amplitudes (or to terms from a product). It represents the combined operations of summing over helicity states (and over different particle states if appropriate), re-expressing spinor products in terms of the cut momentum, multiplication by the cut-crossing propagators, and completion of dot products in denominators to standard propagator denominators. It does not introduce the phase-space integral over the product of amplitudes. The result of the promotion operation is an integrand which depends on the external momenta and on the loop momentum. Note that the sum over intermediate states must in general be carried out in  $D = 4 - 2$  dimensions, and that it is a sum only over physical states. This implicitly introduces a physical projection operator. In calculations of full amplitudes, the resulting operators leave little trace, but in calculations of splitting amplitudes such as the one we carry out in the present paper, these operators will give rise to light-cone-like denominators in integrals.

We will also need to introduce the cut-projection operator  $P_s$ , which yields the part of its argument that has a cut in the  $s$  channel, where  $s$  denotes an arbitrary invariant

of  $m$  consecutive external momenta. At one loop, it extracts the joint pole term in two propagator denominators  $\frac{1}{s_1 s_2}$ , where  $(s_1 + s_2)^2 = s$ . It corresponds to requiring that a pair (any pair) of propagators yielding a cut in the  $s$  channel be present in the diagram.

In a computation with  $n$  external massless momenta, there are in general  $n(n-3)/2$  independent invariants in  $D$  dimensions. Denote by  $C$  the ordered set of these invariants,

$$C = \{s_{12}, s_{23}, s_{13}, \dots\} \quad (4.8)$$

(We will denote the number of elements in  $C$  by  $n_C$ .) We will sew the channels in the specified order, with the notation  $s_j \in C$  denoting the  $j$ -th invariant in  $C$ . The optimal ordering (from the viewpoint of computational efficiency) depends on the process and the particle content of the theory, but of course the final answer is independent of this ordering. Let  $K_j = k_{a_j} + \dots + k_{b_j}$  be the momentum whose square is the given invariant  $s_j$ . The first momentum (within the cyclic order of external momenta) we will denote  $a_j$ , and the last momentum by  $b_j$ . The momentum before  $a_j$  will be labeled  $a_j - 1$ , and the one after  $b_j$ ,  $b_j + 1$ .

The analytic behavior in different invariants is independent even if the invariants are related by Gram determinant conditions arising from the restriction to four dimensions. Thus even if we take all external momenta to be in four dimensions, we must still take the full set of  $D$ -dimensional invariants.

The complete integrand of the one-loop amplitude  $A^{(1)}(1, \dots, n)$  is then given by the sum over all channels,

$$I^{(1)} = \sum_{j=1}^{n_C} Q_j \prod_{l=1}^{j-1} 1 \prod_{l=j+1}^m P_{s_l} P_{s_j} \frac{k}{A^{(0)}(s_j; a_j, \dots, b_j; \dots, K_j)} A^{(0)}(s_j + K_j; b_j + 1, \dots, a_j - 1; \dots) \quad (4.9)$$

That is, we sum over all channels, each time removing all terms already found in previous channels. The amplitudes in this equation must in general have the *sewn legs* (' or '+  $K_j$ ) in  $D$  dimensions. Whether the external legs are taken to be in four dimensions or in  $D$  dimensions depends on the variant of dimensional regularization employed. In practice, it is best to use a four-dimensional scheme, and convert later if necessary.

Indeed, there are several practical aspects not addressed by the formal expression above. These include questions of diagram labeling, classification, and the use of a basis for organizing numerators of terms in the integrand. As the formal expression hints, none of these tools are intrinsically required by the unitarity-based sewing method. The cut projection can be performed by extracting residues of poles; and the promotion involves simple algebraic manipulations. Furthermore, non-manifestly vanishing expressions still vanish, and do not affect the final answer. In a practical calculation, however, we would like the cut projection to be simple, ideally just amounting to the identification of the formal coefficient of a pole. We would like to avoid the appearance of complicated expressions which actually vanish. Furthermore, the integrand produced by the sewing method will ultimately be fed to an integration machinery which does require the corresponding

diagrams to be labeled and classified by topology. We therefore might as well incorporate these aspects into an algorithm.

To do so, start with all color-ordered graphs with a maximum number of propagators containing the loop momenta. We will call these ‘parent’ diagrams. All other topologies can be obtained by canceling propagators, that is by multiplying the numerator by an inverse propagator. These we will call ‘daughter’ diagrams; below, we will also include the parent in its set of all daughters. At one loop, if all external particles are massless, there is in fact only one parent diagram. (Recall that we are restricting attention to processes where all internal masses vanish.) If we have two or more massive external particles (for example,  $W$  bosons), we will have different parent diagrams corresponding to the different ways of attaching the massive legs to the loop. At two loops, there are  $n(n+1)/2$  planar parent diagrams when all external particles are massless. (Integrals that reduce to products of one-loop integrals, such as bow tie integrals, have intrinsically two-loop integrals as parent diagrams.) Examples are shown in figure 16.

Each cut will in general start with a different labeling of any given parent diagram, because the loop momentum ‘ $m$ ’ may denote a different propagator. The algorithm will make use of a simple relabeling operation, reviewed in appendix B, to bring these into canonical form. The labeling of propagators must incorporate a notation for the parent diagram, because the algebraic relations of dot products to inverse propagators differ from diagram to diagram.

The external gluon legs we may choose to treat using form al polarization vectors  $u_i(k_i)$ , or using the spinor-helicity method. The external fermion legs we may choose to treat using form al spinor wavefunctions  $u(k_i)$ ,  $u(k_i)$ , or again using a helicity basis. Either choice (or a mixture) may be employed with the algorithm we will present below. The basis one should use for expressing numerator polynomials depends slightly on the external leg treatment, because there can be different numbers of independent invariants from which the polynomials are built. The algebraic processing of expressions will also be somewhat different. In all cases, the basis at one loop will contain all inverse propagators containing the loop momentum. These are sufficient to express all dot products of the loop momentum with external momenta. Note that Levi-Civita tensors involving the loop momentum can be converted to Gram determinants (and thence to dot products) by multiplying by another Levi-Civita tensor involving only external momenta. (The latter object is just another

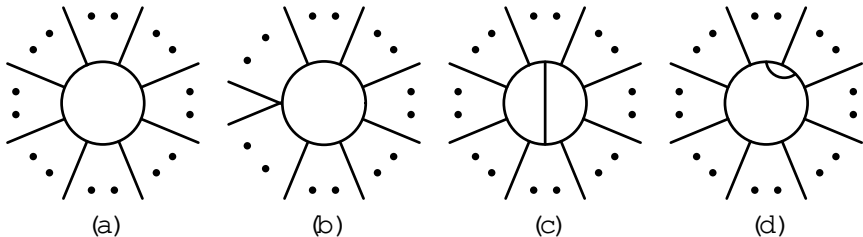


Figure 16: Examples of parent and daughter diagrams: (a) a parent diagram at one loop; (b) a daughter diagram at one loop, which is a daughter of the diagram in (a); (c) and (d) parent diagrams at two loops.

constant as concerns the manipulations we perform.) We will also need the square of (2)-dimensional components of the loop momentum,  $(\gamma_2)^2$ . We must add dot products of the loop momentum with several external polarization vectors (if any). These will not give rise to expressions that can cancel propagator denominators. (We could have taken these to be in  $D$  dimensions, after all, in which case they would clearly be independent.) In all algebraic manipulations, one should be sure to use momentum conservation, eliminating one external momentum, and re-expressing invariants in terms of an independent set, in order to avoid the appearance of zero in obscure forms. (For formalexpressions  $\gamma_j \cdot k$ , one should pick a momentum other than  $k_j$  to eliminate, so as to impose the on-shell conditions too.)

For example, in computing the an  $n$ -point gluon amplitude, we can pick the standard labeling to have the loop momentum between legs  $n$  and 1. If we treat all external legs in the spinor-helicity basis, then the basis set will simply be,

$$f^2; (\gamma - k_1)^2; (\gamma - k_1 - k_2)^2; \dots; (\gamma - k_1 - \dots - k_n)^2; (\gamma_2)^2 g; \quad (4.10)$$

if we choose to treat legs  $1; \dots; j$  using form alpolarization vectors, we should add

$$f''_1 \quad \gamma; \dots; j \quad g \quad (4.11)$$

to this set.

Amplitudes with fermions in a loop arise from sewing amplitudes with pairs of external fermions on either side of a cut. Sewing will include closing a fermion loop. (The usual minus sign must be included explicitly.) This yields a spinor trace, which can be expanded in terms of dot products and Levi-Civita tensors. The latter can be converted to dot products as described above. Internal fermions thus do not require any new basis elements.

Amplitudes with external fermions will contain different terms, factors of a 'spinor string' consisting of an external spinor wavefunction (either form alu,  $u$  or in the helicity basis), a product of gamma matrices dotted into various  $D$ - or four-vectors (momenta, polarization vectors, the light-cone vector, or other spinor strings), and an ending spinor wavefunction. Roughly speaking, we need to perform sufficient manipulations on these to ensure that no difference of two such objects contains a factor of an inverse propagator. A basis for spinor strings involving spinor wavefunctions can be obtained by commuting loop momenta to the left; commuting  $\gamma_2$ , if present, to the next position; and commuting form alpolarization vectors (if present) to an ordered sequence following them. The spinor string can end with either a spinor carrying an external momentum or the light-cone vector, or another external fermion wavefunction. Alternatively, one can convert the spinor string to a trace by multiplying by appropriate spinorial factors involving only external momenta and spins, and then expanding the trace into dot products and Levi-Civita tensors as above. (The spinorial factors are just spinor products in a helicity basis.) In this case, no spinor strings are needed in the basis.

The projection  $P_{s_j}$  of the promoted integrand in eq. (4.9) back onto the same channel which was sewn, ensures that no (spurious) terms lacking a cut in the sewn channel are generated. This projection is not really needed in the purely formalexpression, but ensures

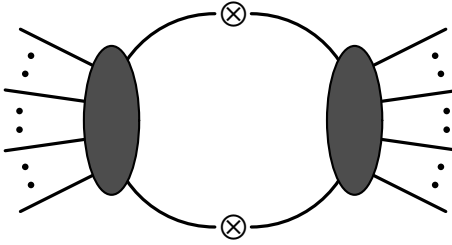


Figure 17: Sewing together two tree-level amplitudes to produce a contribution to the one-loop integrand.

that algebraic manipulations when working in the basis required for a practical algorithm do not create unwanted terms.

The basis will be used to identify terms that have cuts in different channels. A term with uncanceled propagators corresponding to the cut channel will have a cut in that channel.

For a practical algorithm, one may proceed as follows:

1. Form the ordered set of all independent channels in  $D$  dimensions. (That is, in determining the independence of different invariants, one should use only momentum conservation, and not integer-dimension-specific Gram determinant relations.)
2. Associate a labeling of internal lines to each distinct Feynman integral parent which has a daughter appearing in the integrand. (Because of cancellations in gauge theories, not every topology that appears in the set of the usual Feynman diagrams for a given process will necessarily appear in the sewn integrand.)
3. For each parent integral, form a basis set for expanding numerators, consisting of the inverse propagators; the square of the  $(-2)$ -dimensional components of the loop momentum,  $(\not{k}_2)^2$ ; and dot products of the loop momentum with any form of external polarization vectors. For external fermions with form wavefunctions, spinor strings should be added as described above.
4. Initialize the integrand's value to zero.

We will form the integrand by iterating over channels. For a color-ordered amplitude, each channel corresponds to a consecutive set of external momenta,  $k_{a_1}; \dots; k_{b_j}$ , the cut invariant being  $s_j = (k_{a_j} + \dots + k_{b_j})^2$ .

For each channel,

5. Sew. Form the product of the two on-shell tree amplitudes  $A^{(0)}(\not{k}_1; a_j; \dots; b_j; \not{k}_2)$  and  $A^{(0)}(\not{k}_2; b_j + 1; \dots; n; 1; \dots; a_j - 1; \not{k}_1)$ , where  $\not{k}_1 + \not{k}_2 + \not{K}_j = 0$ , summing over the products of amplitudes for the different particle types and helicities that can circulate in the loop. The sum must in general be performed in  $D = 4 - 2$  dimensions. Use

polarization-vector identities (eq. (3.25), etc.),

$$X = \frac{1}{2} \frac{u(\gamma) u(\gamma)^\dagger + u(\gamma^\dagger) u(\gamma)^\dagger}{n + n^\dagger}; \quad (4.12)$$

to express everything in terms of the cut momentum  $\gamma$ . Here,  $n$  is the light-cone reference vector. (If all external legs are on shell, different  $n_i$  may be used for different cut legs if desired, and indeed the light-cone denominators can be removed algebraically.) The dimensionality of  $\gamma$  depends on the variant of dimensional regularization (see eq. (7.1)). Multiply by 1 when a fermion loop is created by sewing. Put in the propagators crossing the cut,  $\frac{1}{\gamma}$  for each cut leg. Complete dot products in the denominator to form propagator denominators adjacent to the cut,  $2 \gamma \cdot k_1^\dagger (\gamma \cdot k_1)^2$ , the  $+$  corresponding to  $k_1$  on the left side of the cut, the  $-$  sign to those on the right side of the cut. Rewrite the expression in terms of the basis set, and expand sums so that each term can be classified as the daughter of a single parent diagram. The sewing operation is depicted schematically in figure 17. In eq. (4.9), it corresponds to the promotion operator  $P_{s_j}$ .

6. Put into canonical form. Use momentum conservation to reduce the number of cut-crossing momenta (now loop momenta) appearing in spinor traces, and then expand spinor traces and all dot products in terms of the basis. (As explained above, this expansion may not always be necessary.) When using the spinor-helicity method for external polarization vectors, or explicit helicity states, we will obtain spinor strings of the form  $h j_1 \bar{j}_2 \gamma^\dagger j_3 \bar{j}_4$  etc. As explained above, one can complete these to a trace, then convert the trace to dot products and Levi-Civita tensors. The latter should be converted to Gram determinants (and thence to dot products) by multiplying (and dividing) by a Levi-Civita tensor involving only external momenta. (Spinor strings involving only external momenta need not be manipulated, obviously.)
7. Relabel. For each term in the sewn expression for a given channel, relabel the momenta to the standard labeling for its parent integral. Where required, insert factors of squared momenta in the numerator and denominator to match a 'parent' diagram. In some cases, it will be possible to obtain different parents by inserting different factors; it doesn't matter which one is picked.
8. Clean. Remove all terms which have no cut in the current channel. (Such terms might have been introduced by earlier algebraic manipulations.) That is, using a canonical basis as described above, remove any terms which do not contain both cut propagators. This step corresponds to the operator  $P_{s_j}$  in eq. (4.9).
9. Merge. Remove all terms in the current-channel sewn expression that already appear in the net integrand. That is, remove any term which has cuts in a previously-processed channel. Using a canonical basis as described above, it suffices to pick out and remove terms that have a pair of propagators corresponding to a cut in a

previously-processed channel. This step corresponds to the operator  $\sum_{l=1}^Q j_l 1 \quad P_{s_l}$  in eq. (4.9).

10. Accumulate. Add the remaining terms in the current-channel  $s_n$  expression to the integrand. This step corresponds to the sum in eq. (4.9).
11. Continue with the next channel at step # 5.

In special cases (for example, massless supersymmetric theories at one loop), it may be possible to compute the cuts using four dimensional helicity states, and to make use of spinor-helicity simplifications for the cut-crossing momenta [10, 11]. (It is always possible to use such simplifications for the external momenta at an early stage of the calculation.) In this case, one must re-express spinor products involving  $\gamma_1$  and  $\gamma_2$  in terms of dot products of these momenta with other vectors,  $\gamma_1 \cdot i [\gamma_1 \cdot b] \gamma_2 \cdot j [\gamma_2 \cdot b]$ . (This is always possible because the cut-crossing momenta will appear with opposite phase weight in the two tree amplitudes on either side of the cut.) It may also happen that some channels are redundant; this will happen when all integrals appearing in the answer have cuts in multiple channels. In the computation of splitting amplitudes, one side of the cut will have an on-shell tree amplitude, while the other side contains a tree-level splitting amplitude. The sewing procedure will introduce physical-projector denominators. These resemble light-cone gauge denominators. In the computation of on-shell amplitudes, these physical-projector denominators will disappear algebraically. (This is a consequence of gauge invariance.) In the computation of splitting amplitudes, in contrast, these denominators will survive into the integration, and in fact play a crucial role in obtaining the right sort of integral. However, as discussed in section 3, at one loop they will only arise in lines corresponding to cut momenta. As we have seen in the example of the  $1+2$  splitting amplitude, integrals with such projectors have no singularities beyond those regulated by dimensional regularization.

In general, the integrand has cuts in many different channels. Indeed, the resulting loop amplitudes are expressed in terms of polylogarithmic functions that have discontinuities in several different invariants. Accordingly, any given term in the integrand may have combinations of propagators leading to cuts in different channels, and thus might emerge from sewing in any of those channels. The different ways of sewing must all yield the same answer. The simplest way of seeing this is to consider a gedanken calculation of a one-loop amplitude from Feynman diagrams. We can extract the cut of the sum of all diagrams in any given channel. Putting the cut legs on shell, the sums of diagrams on either side will yield a product of tree amplitudes. Because of their origin in a unique expression, however, reconstructions of the analytic functions from different channels will yield the same answer.

In terms of the cut projection operator introduced earlier, this amounts to the statement that

$$P_{s_1} \overset{\text{k}}{A}_1(s_2) A_2(s_2) = P_{s_2} \overset{\text{k}}{A}_3(s_1) A_4(s_1); \quad (4.13)$$

where  $A(s)$  is an abbreviation for the amplitude with two adjacent legs  $\gamma_{1,2}$  satisfying  $\gamma_1 \cdot \gamma_2 = s$ . Checking the consistency of different cuts in intermediate steps, as expressed by this equation, is a good way of verifying the correctness of code implementing the algorithm.

The consistency of di  
erent cuts also shows that the order of evaluation of channels, i.e. the ordering in  $C$  in eq. (4.8), does not affect the final result. For example, if we were to evaluate two channels in the order  $fs_1; s_2 g$ , we would obtain,

$$\overset{\text{k}}{A}_3(s_1)\overset{\text{k}}{A}_4(s_1) + (1 - P_{s_1}) \overset{\text{k}}{A}_1(s_2)\overset{\text{k}}{A}_2(s_2); \quad (4.14)$$

(Recall that the projection back onto the  $s_2$  channel is not really needed in the formal expression, and has been omitted here.) In the other order, we would obtain

$$\overset{\text{k}}{A}_1(s_2)\overset{\text{k}}{A}_2(s_2) + (1 - P_{s_2}) \overset{\text{k}}{A}_3(s_1)\overset{\text{k}}{A}_4(s_1); \quad (4.15)$$

The difference of the two evaluations is

$$P_{s_2} \overset{\text{k}}{A}_3(s_1)\overset{\text{k}}{A}_4(s_1) - P_{s_1} \overset{\text{k}}{A}_1(s_2)\overset{\text{k}}{A}_2(s_2); \quad (4.16)$$

which vanishes using eq. (4.13).

Many terms (all, in an  $N = 4$  supersymmetric theory) may have cuts in more than one channel. The cut consistency condition can be used to cross-check these terms, and is often of great utility in debugging computer code implementing a calculation. Note that when using the spinor-helicity techniques, the use of non-trivial (Gram determinant) identities may be required to show cut consistency.

Each  $s_2$  and integrated cut is gauge invariant independently when all external legs are on shell. Its absorptive part is, after all, equal to the phase-space integral of a gauge-invariant non-forward matrix element. The dispersion integral of such a quantity is gauge invariant as well. At the integrand level, this is reflected in the disappearance of any dependence on the light-cone vector  $n$  introduced by the sum over gluon polarizations. (One typically needs to make use of momentum conservation to see this explicitly.) The same statement is not true if we are computing an object with off-shell legs, as is the case for the splitting amplitude. In that case, some light-cone denominators will survive. As we will discuss in a later subsection, others will cancel algebraically, and it is possible to predict in advance which must disappear.

The procedure we have described above is not the only way to merge information from di  
erent cuts to yield a single function with the correct cuts in all channels. One can also imagine performing the merging step after integration. That is, one could integrate the  $s_2$  integrand in each channel separately, and then search for a function whose branch-cut discontinuities match those found in each of the separate invariants. This requires the use of a nonredundant basis of master integrals. Operationally, one would rewrite the result of integration in each channel in terms of this basis, throwing away integrals with no discontinuity in the given channel. One could verify cut consistency by checking that the coefficients of a given master integral with discontinuities in multiple channels are in fact the same in the di  
erent computations in these channels. In combining channels, one would then take the result from any of the channels (that is, pick one, rather than adding together the di  
erent contributions). This is in fact the procedure that was presented in ref. [11]. It may be advantageous for some calculations, though in general it will require

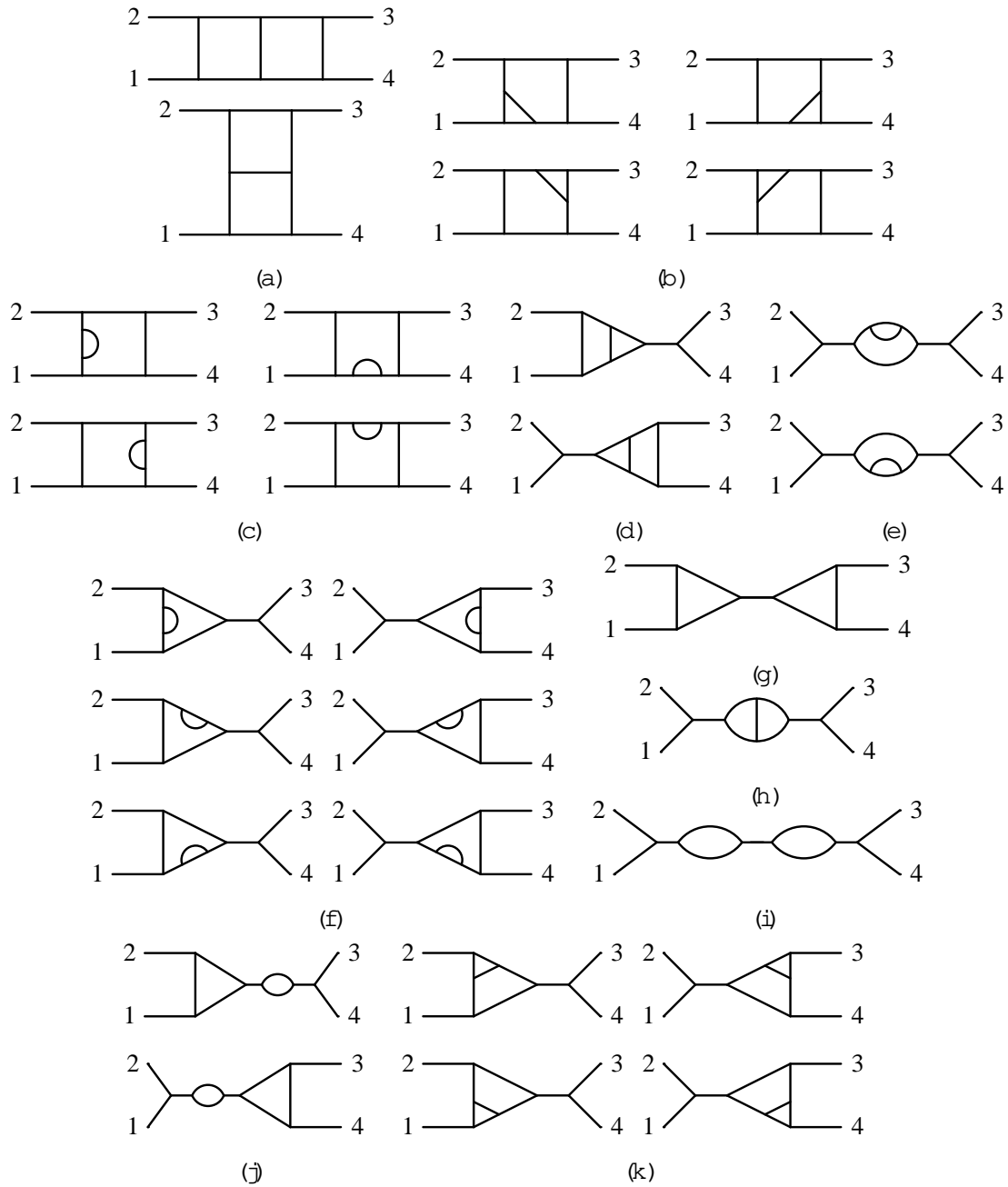


Figure 18: Color-ordered Feynman diagrams for the two-loop four-point amplitude in  $\text{Tr}^3$  field theory: (a) planar box diagrams (b) triangle-in-box diagrams (c) bubble-in-box diagrams (d) s-channel ladder triangle diagrams (e) s-channel bubble-in-bubbles. (f) s-channel bubble-in-triangle diagrams (g) s-channel triangle-pair diagrams (h) s-channel lizard-eye bubble (i) s-channel double bubble (j) s-channel triangle-bubble diagrams (k) s-channel triangle-in-triangles. The corresponding t-channel diagrams for (d)-(k) are not shown explicitly.

the computation of super-uous integrals. As with the basic sewing procedure, there are adjustments that would be required in a two-loop computation, which we will discuss in the next subsection.

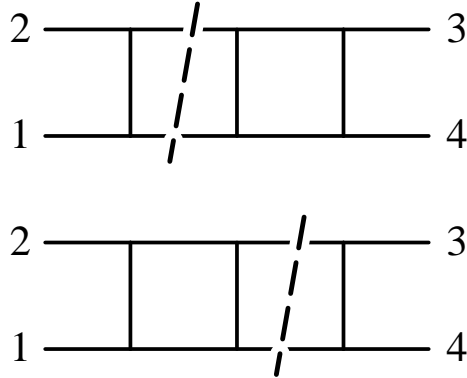


Figure 19: The s-channel two-particle cuts of the planar double box.

### 4.3 Sewing at Two Loops

As for the one-loop case, we start our two-loop discussion with the example of a four-point amplitude. We again consider the contribution with a given ordering of the external legs, and restrict attention to planar diagrams. In the one-loop example, we saw that we must pay attention to potential double-counting in assembling contributions from different channels. At two (and higher) loops, we must also confront potential double-counting in contributions to a given channel. To understand how this arises, start once more with the Feynman diagrams for this planar ordered amplitude, shown in figure 18.

Consider in particular the planar double box shown in figure 18(a). It has both two- and three-particle cuts. The two-particle cuts, shown in figure 19, contain a product of a one-loop amplitude and a tree amplitude, with four external legs apiece. There are two separate cuts.

The three-particle cut in the planar double box is a sum of two terms, shown in figure 20. It corresponds to a product of two five-point tree amplitudes. The complication here arises from the fact that a given term in the two-loop amplitude may contribute to both terms in the two-particle cut; both terms in the three-particle cut; or to both two- and three-particle cuts. In such a case, when we reconstruct the original integrand, we must count it only once. A simple analogy would be an integrand of the form  $X^2$ ; since cutting is analogous to differentiation, we would have

$$[X^2]_{\text{cut}} = 2X \downarrow_{\text{cut}} X; \quad (4.17)$$

and promoting the latter back to an integrand requires a factor of 1/2 just as it would for integration. Note that if we denote the cut momenta by  $\gamma_{1,2,3}$ , then the terms which contribute to both two- and three-particle cuts necessarily contain the propagators

$$\frac{1}{\gamma_1^2 \gamma_2^2 \gamma_3^2 (\gamma_1 + \gamma_2)^2 (\gamma_2 + \gamma_3)^2}; \quad (4.18)$$

using the labeling of legs in the three-particle cut.

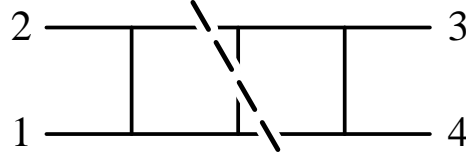
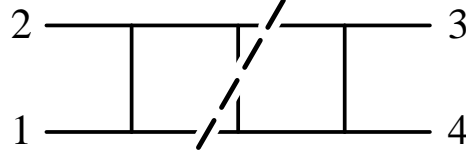


Figure 20: The s-channel three-particle cuts of the planar double box.

We will focus here on the leading-color (planar) contributions to the two-loop amplitude, though of course an analogous procedure applies to the subleading contributions (which include non-planar integrals). Let us begin the sewing procedure with the two-particle cuts in the s channel. We must take the one-loop amplitude (4.7), with legs (3;4) replaced by legs ( $\gamma_2; \gamma_1$ ), and  $\gamma$  replaced by  $p$  in the integral, and sew it to the tree amplitude  $A^{(0)}(\gamma_1; \gamma_2; 3; 4)$ , obtaining

$$\begin{aligned}
 & \sum_i \frac{d^D p}{(2^-)^D} \frac{d^D \gamma}{(2^-)^D} \\
 & \frac{1}{s_{12}^2} \frac{1}{p^2 (p + k_1 + k_2)^2} + \frac{1}{s_{12}} \frac{1}{p^2 (p^-)^2 (p + k_1 + k_2)^2} + \\
 & + \frac{1}{s_{12}} \frac{1}{(p + k_1)^2 p^2 (p + k_1 + k_2)^2} + \frac{1}{(p + k_1)^2 p^2 (p^-)^2 (p + k_1 + k_2)^2} + \\
 & + \frac{1}{[(\gamma + k_1)^2]^2} \frac{1}{p^2 (p^- - k_1)^2} + \frac{1}{(\gamma + k_1)^2} \frac{1}{p^2 (p^- - k_1)^2 (p^- - k_1)^2} + \quad (4.19) \\
 & + \frac{1}{(\gamma + k_1)^2} \frac{1}{(p + k_2)^2 p^2 (p^- - k_1)^2} \frac{1}{(\gamma + k_1 + k_2)^2 \gamma^2} \frac{1}{s_{34}} + \frac{1}{(\gamma - k_4)^2}
 \end{aligned}$$

where we have relabeled  $\gamma_1 \leftrightarrow \gamma$ . Restricting attention to those terms with explicit powers of  $1=s_{12}^2$  or  $1=s_{12}^3$ , we have

$$\begin{aligned}
 & \sum_i \frac{d^D p}{(2^-)^D} \frac{d^D \gamma}{(2^-)^D} \frac{1}{s_{12}^2 (\gamma + k_1 + k_2)^2 \gamma^2} \frac{1}{s_{12}} \frac{1}{p^2 (p + k_1 + k_2)^2} + \frac{1}{p^2 (p^-)^2 (p + k_1 + k_2)^2} + \\
 & + \frac{1}{(p + k_1)^2 p^2 (p + k_1 + k_2)^2} + \frac{1}{p^2 (p + k_1 + k_2)^2 (\gamma - k_4)^2} + \quad (4.20)
 \end{aligned}$$

These terms are sufficient to illustrate the issues associated with potential double-counting.

There is a similar contribution from sewing  $A^{(0)}(1; 2; \gamma_2; \gamma_1)$  to  $A^{(1)}(\gamma_1; \gamma_2; 3; 4)$ . If we now take the cut of the expression (4.19), however, we discover that we can cut not only the  $\gamma$  loop, but also the  $p$  loop. The corresponding terms would appear not only in this sewing, but also in the other contribution (with the loop amplitude on the right-hand side

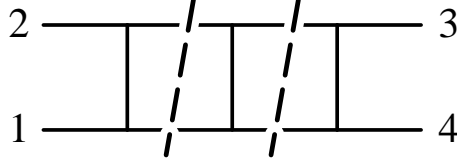


Figure 21: The s-channel 'double' two-particle cuts of the planar double box.

of the cut). This would be a source of double-counting. To correct for it, we must subtract from the sum of the two contributions those terms that can be cut both ways. These are the terms extracted by a 'double cut' (shown in figure 21), again in the sense of requiring that the propagators giving rise to a two-particle cut be present in both the ' and p loops,

$$\frac{i}{s_{12}} + \frac{i}{s_{p1}} \quad \frac{i}{s_{12}} \quad \frac{i}{s_p} \quad \frac{i}{s_{34}} \quad \frac{i}{s_{4'}} ; \quad (4.21)$$

or promoted back to a two-loop integral,

$$i \int^Z \frac{d^D p}{(2^-)^D} \frac{d^D \gamma}{(2^-)^D} \frac{1}{s_{12}^2 (\gamma + k_1 + k_2)^2 \gamma^2 p^2 (p + k_1 + k_2)^2} \\ \frac{1}{s_{12}} + \frac{1}{(p + k_1)^2} + \frac{1}{(p - \gamma)^2} + \frac{1}{(\gamma - k_4)^2} + ; \quad (4.22)$$

which is identical to the term  $s$  in eq. (4.20), obtained from the first of the two-particle cut contribution. Counting the contribution only once then gives eq. (4.22) as the result of combining the two two-particle cut contributions.

Next, we must consider the three-particle cuts. We begin with the product of two two-point amplitudes,

$$A^{(0)}(1;2;\gamma_3;\gamma_2;\gamma_1) = i \frac{1}{s_{\gamma_2 \gamma_3} s_{\gamma_1 1}} + \frac{1}{s_{\gamma_1 \gamma_2} s_{12}} + \frac{1}{s_{\gamma_1 \gamma_2} s_{\gamma_3 2}} + \frac{1}{s_{\gamma_2 \gamma_3} s_{12}} + \frac{1}{s_{\gamma_1 1} s_{\gamma_3 2}} ; \quad (4.23)$$

and  $A^{(0)}(\gamma_1; \gamma_2; \gamma_3; 3; 4)$ .

Let us focus on the terms containing a factor of  $1 = s_{12}^2$ . These are

$$i \int^Z \frac{d^D \gamma_1}{(2^-)^D} \frac{d^D \gamma_3}{(2^-)^D} \frac{1}{s_{12}^2} \frac{1}{\gamma_1^2 \gamma_3^2 (\gamma_1 + \gamma_3 + k_1 + k_2)^2} \\ \frac{1}{[(\gamma_3 + k_1 + k_2)^2]^2} + \frac{2}{(\gamma_3 + k_1 + k_2)^2 (\gamma_1 + k_1 + k_2)^2} + \frac{1}{[(\gamma_1 + k_1 + k_2)^2]^2} ; \quad (4.24)$$

The first and last of these terms correspond to the diagrams of figure 18(e). The middle term corresponds to the diagram of figure 18(h); but it appears in the product with a (superfluous) factor of 2. This factor is due precisely to the fact that this term can be cut in two different ways, corresponding to the two terms depicted in figure 22. We must remove this double counting, by subtracting those terms which contribute twice; this leaves

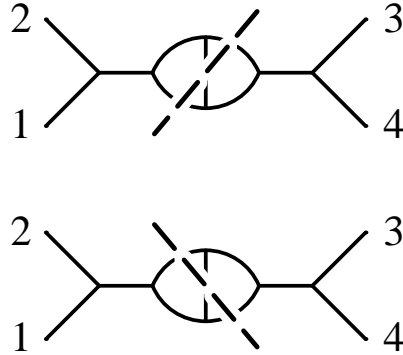


Figure 22: The s-channel three-particle cuts of the lizard-eye bubble.

us with

$$\begin{aligned} i^Z & \frac{d^D \gamma_1}{(2^-)^D} \frac{d^D \gamma_3}{(2^-)^D} \frac{1}{s_{12}^2} \frac{1}{\gamma_1^2 \gamma_3^2 (\gamma_1 + \gamma_3 + k_1 + k_2)^2} \\ & \frac{1}{[(\gamma_3 + k_1 + k_2)^2]^2} + \frac{1}{(\gamma_3 + k_1 + k_2)^2 (\gamma_1 + k_1 + k_2)^2} + \frac{1}{[(\gamma_1 + k_1 + k_2)^2]^2} : \end{aligned} \quad (4.25)$$

Finally, we must combine the two- and three-particle cuts. Again, we can add the two contributions, and remove terms which appear in both, for example by removing terms in the three-particle cuts which have (any) two-particle cut. Of the terms listed explicitly in eq. (4.25), only the middle term has a two-particle cut. Removing it (thereby performing the required merging), and relabeling  $\gamma_1 \leftrightarrow \gamma_3$ ,  $p \leftrightarrow k_1 \leftrightarrow k_2$ , we obtain,

$$\begin{aligned} i^Z & \frac{d^D p}{(2^-)^D} \frac{d^D \gamma}{(2^-)^D} \frac{1}{s_{12}^2} \frac{1}{\gamma^2 (p + k_1 + k_2)^2} \\ & \frac{1}{s_{12}^2} \frac{1}{p^2 (\gamma + k_1 + k_2)^2} + \frac{1}{p^2 (p - \gamma)^2 (\gamma + k_1 + k_2)^2} + \\ & + \frac{1}{(p + k_1)^2 p^2 (\gamma + k_1 + k_2)^2} + \frac{1}{p^2 (\gamma - k_4)^2 (\gamma + k_1 + k_2)^2} + \\ & + \frac{1}{(p - \gamma)^2 [p^2]^2} + \frac{1}{(p - \gamma)^2 [(\gamma + k_1 + k_2)^2]^2} + ; \end{aligned} \quad (4.26)$$

again in exact agreement with the terms that would emerge from a Feynman-diagram calculation. (The reader may wonder why the first and last terms in eq. (4.25), which correspond to the diagrams in figure 18(e), do not contain two-particle cuts. Naively, these diagrams do contain two-particle cuts; but a closer inspection shows that such a cut would have a bubble on an external line; such bubbles are scale-free and hence vanish in dimensional regularization.)

Note that not all contributions will require these subtractions to match overlaps; for example, the t-channel cut of the planar double box shown in figure 23 has only one contribution, a three-particle cut.

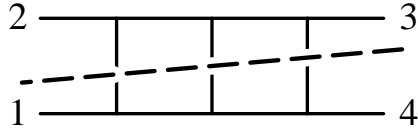


Figure 23: The t-channel cut of the planar double box.

In practice, it appears to be more efficient to start with the two-particle cuts, and then merge in additional terms from the three-particle cuts. In addition to the cut projection operator  $P_s$ , which yields the part of its argument that has any cut (two- or three-particle) in the specified channels, we will also make use of four additional projection operators. These are  $P_s^{(2)}$ , which extracts terms containing a two-particle cut;  $P_s^{(3)}$ , those containing a three-particle cut;  $P_{sjj}^{(2)}$ , those containing a 'double cut', that is whose two-particle cut can be cut again (for example, figure 21); and  $P_s^{(3)}$ , those containing a contribution to both terms in the three-particle cut (corresponding to terms which have all the propagators cut in figure 21 and the center propagator in addition). Note that these projection operators do not necessarily remove terms with other cuts; for example,  $P_s^{(2)}$  may yield an expression containing three-particle cuts in addition to the two-particle cut. In cases where there is only a single two-particle cut, or where there is only a single contribution to the three-particle cuts,  $P_{sjj}^{(2)}$  and  $P_s^{(3)}$  are understood to vanish.

$\mathbf{k}$

Using these projection operators, we can define a complete promotion operator  $\mathbf{C}_c$  for a given channel,

$$\begin{aligned}
 & \mathbf{C}_c A^{(1)}(f_{ig}; a_j; \dots; b_j) A^{(0)}(b_j + 1; \dots; a_j - 1; f_{ig}) = \\
 & \quad 1 - \frac{1}{2} P_{sjj}^{(2)} \mathbf{C}_c A^{(0)}( \cdot; a_j; \dots; b_j; \cdot - K_j) \\
 & \quad \quad \quad A^{(1)}( \cdot + K_j; b_j + 1; \dots; a_j - 1; \cdot ) + \quad (4.27) \\
 & \quad \quad \quad + A^{(1)}( \cdot; a_j; \dots; b_j; \cdot - K_j) \quad \quad \quad i \\
 & \quad \quad \quad A^{(0)}( \cdot + K_j; b_j + 1; \dots; a_j - 1; \cdot ) + \\
 & \quad + 1 - P_s^{(2)} \mathbf{C}_c \frac{1}{2} P_s^{(3)} \\
 & \quad \quad \quad A^{(0)}( \cdot_1; \cdot_2; a_j; \dots; b_j; \cdot_1 - \cdot_2 - K_j) \\
 & \quad \quad \quad A^{(0)}( \cdot_1 + \cdot_2 + K_j; b_j + 1; \dots; a_j - 1; \cdot_2; \cdot_1 );
 \end{aligned}$$

where  $A^{(1)}$  denotes the integrand for the one-loop amplitude. Here we consider only the planar case, so that all cut-crossing momenta are color-adjacent; but the construction generalizes in a straightforward way to non-planar amplitudes. As in the example discussed earlier, the role of the factors of  $1/2$  in front of  $P_{sjj}^{(2)}$  and  $P_s^{(3)}$  is to remove double-counting that occurs in cutting, ensuring that each term contributes to the integrand with the correct coefficient.

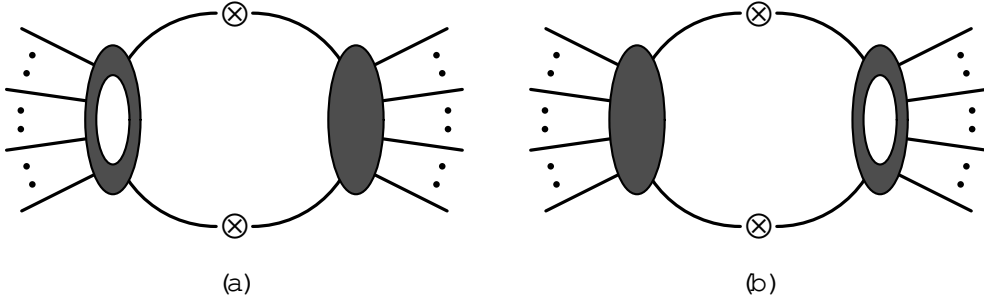


Figure 24: The two contributions wherein one sews a one-loop amplitude to a tree-level amplitude to produce a contribution to the two-loop integrand.

Using this complete promotion operator, the complete integrand for the two-loop amplitude  $A^{(2)}(1;:::;n)$  is given by an expression very similar in form to that for the one-loop amplitude (4.9),

$$I^{(2)} = \sum_{j=1}^{N^c} \sum_{k=1}^{Q_j-1} \frac{1}{P_{s_1} \dots P_{s_j}} \frac{k}{C} A^{(1)}(f_{ig}; a(s_j); ::; b(s_j)) A^{(1)}(b(s_j) + 1; ::; a(s_j) - 1; f_{ig}); \quad (4.28)$$

but with the complete promoted cut being used where the basic one was in the one-loop case.

A practical algorithm is similar in structure to that at one loop, but requires additional merging over two- and three-particle cuts. The first three steps (construct ordered set of all channels, determine labelings, initialize integrand to zero) are the same. As in the one-loop case, from a formal point of view, the relabelings below are not required by the method, but since we will ultimately be feeding the resulting integrands to an integration machinery, we might as well incorporate the standardization at an early stage in the calculation.

In the two-loop case, ‘irreducible numerators’ appear. These are dot products of loop momenta and external momenta that cannot be written as linear combinations of inverse propagators. Such terms must be added to the basis of expressions described just before the one-loop algorithm. With this modification, the algorithm again continues after the first four set-up steps by iterating over all channels. For each channel  $(k_{a_j}; ::; k_{b_j})$ ,

5. Sew first two-particle cuts. Form the product of the integrand for the on-shell one-loop amplitude  $A^{(1)}(1; a_j; ::; b_j; 2)$  and the tree amplitude  $A^{(0)}(1; b_j + 1; ::; n; 1; ::; a_j - 1; 1)$  (where  $1 + 2 + K_j = 0$ ), summing over the different particle types and helicities that can circulate in the loop. The sum must in general be performed in  $D = 4 - 2$  dimensions. Use the polarization-vector identities (4.12) to express everything in terms of the cut momenta  $1; 2$  and the light-cone vector  $n$ . (As in the one-loop case, this will introduce physical projectors into the integrand.) Multiply by 1 for each fermion loop is created by sewing. Put in the propagators crossing the cut,  $\frac{i}{k}$  for each cut leg. Note that in general four-dimensional Fierz identities may not be used. Fermion traces over internal fermion lines should be performed first,

re-expressing the result in dot products, with summation over gluon polarizations performed afterwards. Rewrite terms using the basis expressions, and expand sums so that each term can be classified as the daughter of a single parent diagram. Complete dot products in the denominator to form propagator denominators adjacent to the cut,  $2' \cdot k_i$  ( $k_i^2$ ), the  $+$  corresponding to  $k_i$  on the left side of the cut, the  $-$  sign to those on the right side of the cut. The sewing operation is depicted schematically in figure 24(a), and corresponds to the promotion of the second term in brackets in eq. (4.27).

6. Put into canonical form. Use momentum conservation to reduce the number of cut-crossing momenta (now loop momenta) appearing in spinor traces, and then expand spinor traces and all dot products in terms of the basis. (As explained above, this expansion may not always be necessary.) When using the spinor-helicity method for external polarization vectors, or explicit helicity states, we will obtain spinor strings of the form  $h j_1 \bar{j}_2 \cdots \bar{j}_3 j_4$ . As explained earlier, one can complete these to a trace, then convert the trace to dot products and Levi-Civita tensors. The latter can be converted to Gram determinants (and thence to dot products) by multiplying (and dividing) by a Levi-Civita tensor involving only external momenta. (Spinor strings involving only external momenta need not be manipulated, obviously.)
7. Relabel. For each term obtained in step 6, relabel the momenta to the standard labeling for its parent integral. Where required, insert factors of squared momenta in the numerator and denominator to match a 'parent' diagram. In some cases, it will be possible to obtain different parents by inserting different factors; it doesn't matter which one is picked.
8. Sew second two-particle cuts. Form the product of the on-shell tree amplitude  $A^{(0)}(\ell_1; a_j; \dots; b_j; \ell_2)$  and the integrand for the on-shell one-loop amplitude  $A^{(1)}(\ell_2; b_j + 1; \dots; n; 1; \dots; a_j - 1; \ell_1)$  (where  $\ell_1 + \ell_2 + K_j = 0$ ), again summing over the different particle types and helicities that can circulate in the loop. As in step 5, put in fermion minus signs and the cut propagators, complete dot products to propagators, and rewrite terms using basis expressions. The sewing operation is depicted schematically in figure 24(b), and corresponds to the promotion of the first term in brackets in eq. (4.27).
9. Put into canonical form. Use momentum conservation, the cut condition, and expansion of spinor traces, along the lines of step 6.
10. Relabel. For each term obtained in step 9, relabel the momenta to the standard labeling for its parent integral, inserting factors of squared momenta in the numerator and denominator where required.
11. Merge two-particle cuts, removing double-counting. To the result obtained in step 7, add those terms obtained in step 10 not present in the result from step 7. (Equivalently, add the results of steps 7 and 10, and then subtract terms present in both

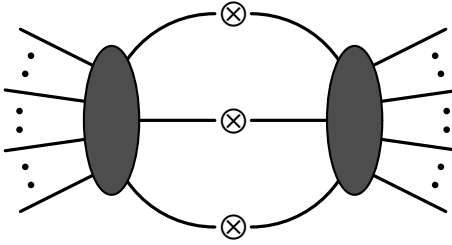


Figure 25: Sewing together two tree-level amplitudes to produce the three-particle cut contribution to the two-loop integrand.

expressions. These latter terms are those with two pairs of propagators present, i.e. those cut through in the ‘double’ two-particle cut.) This step corresponds to the operator  $(1 - \frac{1}{2}P_{s,jj}^{(2)})$  in eq. (4.27), and yields the sewn two-particle cut in the given channel.

12. Sew three-particle cuts. Form the product of on-shell tree amplitudes  $A^{(0)}(\gamma_2; \gamma_1; a_j; \dots; b_j; \gamma_3)$  and  $A^{(0)}(\gamma_3; b_j + 1; \dots; n; 1; \dots; a_j - 1; \gamma_1; \gamma_2)$  (where  $\gamma_1 + \gamma_2 + \gamma_3 + K_j = 0$ ), summing over the different particle types and helicities for the  $\gamma_i$ . As in step 5, put in fermion minus signs and the cut propagators, complete dot products to propagators, and rewrite terms using basis expressions. This operation is depicted schematically in figure 25, and corresponds to the promotion operation in the last term in eq. (4.27).
13. Put into canonical form. Use momentum conservation, the cut condition, and expansion of spinor traces, along the lines of step 6.
14. Relabel. For each term obtained in step 13, relabel the momenta to the standard labeling for its parent integral, inserting factors of squared momenta in the numerator and denominator where required.
15. Remove double-counting. Multiply by one-half those terms (if any) which contribute to both terms in the three-particle cuts. These are the terms that contain all five propagators  $1 = \gamma_1^2$ ,  $1 = \gamma_2^2$ ,  $1 = \gamma_3^2$ ,  $1 = (\gamma_1 + \gamma_2)^2$ , and  $1 = (\gamma_2 + \gamma_3)^2$ . As before, in general, identification of these terms may require expansions of numerators, and use of momentum-conservation identities. This step corresponds to the operator  $(1 - \frac{1}{2}P_s^{(3)})$  in eq. (4.27), and yields the sewn three-particle cut in the given channel.
16. Merge two- and three-particle cuts. To the two-particle cut obtained in step 11, add those terms in the three-particle cut not present in the two-particle cut. (Equivalently, add the two expressions, then subtract those terms in the three-particle cut also present in the two-particle cut, corresponding to the action of the operator  $P_s^{(2)}$  in eq. (4.27).) This yields the complete sewn expression (4.27) in the current channel.
17. Clean. Remove all terms which have no cut in the current channel. (Such terms might have been introduced by earlier algebraic manipulations.) Using a canonical basis as

described above, remove any term which do not contain both cut propagators. This step corresponds to the operator  $P_{s_j}$  in eq. (4.28).

18. Merge. Remove all terms in the current-channel  $\text{sew}_n$  expression that already appear in the net integrand. That is, remove any term which has cuts in a previously-processed channel. Using a canonical basis as described above, it succeeds to pick out and remove terms that have a pair or triplet of propagators corresponding to a cut in a previously-processed channel. This step corresponds to the operator  $\sum_{l=1}^Q \sum_{j=1}^{l-1} P_{s_l}$  in eq. (4.28).
19. Accumulate. Add the remaining terms in the current-channel  $\text{sew}_n$  expression to the integrand. This step corresponds to the sum in eq. (4.28).
20. Continue with the next channel at step # 5.

As in the one-loop case, one could alternatively do the merging after integration rather than before. One again needs a non-redundant basis of master integrals; but here, one needs to adjust the coefficients of some integrals to account for the double-counting issues discussed in the earlier example, and handled in steps 11 and 15 of the two-loop algorithm above. The master integrals must be chosen so that each is associated with a definite overall correction for double-counting; and one must keep track of the original set of cut lines in each term, alongside the integral result. In performing integral reductions, one must eliminate integrals in which cut propagators are cancelled. In the computation of a given cut in an amplitude, one first needs to merge the different two-particle cuts, as there is now more than one contribution. Those master integrals with two contributions to the three-particle cuts in the given channel would have their coefficients decreased by a factor of two. The three-particle cuts must then be merged with the two-particle cuts to obtain the full set of terms for the given channel. One can check cut consistency between different channels just as at one loop. Master integrals with discontinuities in two or more channels must appear with the same coefficient in each channel. The merging of contributions from different channels also proceeds in the same manner as at one loop: for those master integrals with discontinuities in multiple channels, one would take the result from any of the channels (that is, pick one, rather than adding together the different contributions).

#### 4.4 Merging with Legs Off Shell

When computing splitting amplitudes, we have an off-shell leg in the problem, and not all light-cone denominators cancel from the final integrand as they do for fully on-shell scattering amplitudes. For two-loop splitting amplitudes, one side of the cut will have an on-shell tree or one-loop amplitude integrand, while the other side contains a tree-level splitting amplitude or one-loop splitting amplitude integrand. The three-particle cuts require the use of 1 ! 3 tree-level splitting amplitudes, which should be calculated in light-cone gauge. This introduces additional light-cone gauge denominators into certain integrals. As at one loop, sewing gluons across the cut using eq. (4.12) will introduce similar denominators. These denominator factors will survive into the integration, and in

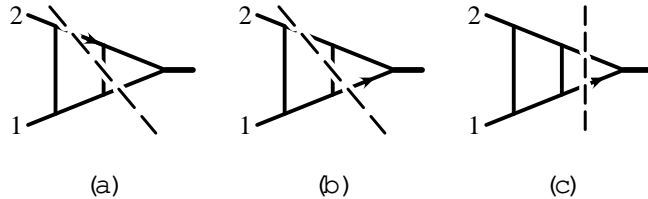


Figure 26: The three-particle cut (a) contains a light-cone denominator on the leg indicated by an arrow, but the two-particle cut (c) will not contain one on that leg. Cut consistency demands that the light-cone denominator indicated in (a) must cancel from all terms where the two-particle cut (c) does not vanish. The light-cone denominator arising in the three-particle cut indicated in (b) is compatible with the ones in the two-particle cut (c) and therefore does not need to cancel.

fact play a crucial role in obtaining the right ‘complexity’ of integrals. However, as we shall discuss in section 5, they will only arise in lines corresponding to cut momenta or connected directly to the on-shell vertex.

The presence of non-cancelling light-cone denominators does not alter the merging procedure described above: these denominators simply go along for the ride. Following the discussion in section 3, we may expect all surviving light-cone denominators to produce integrals properly regulated by covariant dimensional regularization, and this is indeed the case in the calculation we have performed. In contrast, a light-cone gauge Feynman diagram approach would contain ill-defined diagrams requiring an additional prescription such as the PV or ML prescriptions. The ill-defined contributions may cancel in the sum over all diagrams before integration, if a great deal of care were taken to align momenta properly across different diagrams, as guided by the unitarity cuts.

As discussed in section 4.2, if all legs are on shell then all light-cone denominators cancel from the integrands of each cut. Even if some legs are off shell, some light-cone denominators (introduced by the physical-state projector a cut) can be canceled prior to integration by combining information from different cuts. The possibility of these cancellations is dictated by cut consistency. If a given term in an integrand has a cut in more than one channel then it must appear with the same coefficient in each such cut. A light-cone denominator absent in a term in any one of the cuts must also cancel in all other cuts. This cancellation may, however, not be manifest. To cancel the denominators, in general, momentum conservation rearrangements are required. We note that in performing the calculation it is generally helpful to explicitly cancel as many light cone-denominators as possible, to reduce the number and complexity of integral types that need to be evaluated. (This goes beyond the automatic absence of dangerous light-cone denominators discussed at the end of section 3.)

As an example, consider the contributions to the two-loop splitting amplitude depicted in Figure 26, with both two- and three-particle cuts. In the cuts a light-cone denominator will appear on each gluon line. The three-particle cut contains contributions with the light-cone denominators indicated in Figure 26(a) and (b). However, if these contributions also have the two-particle cut indicated in Figure 26(c), then the light-cone denominator indicated in (a) must cancel algebraically in the three-particle cut after suitably combining

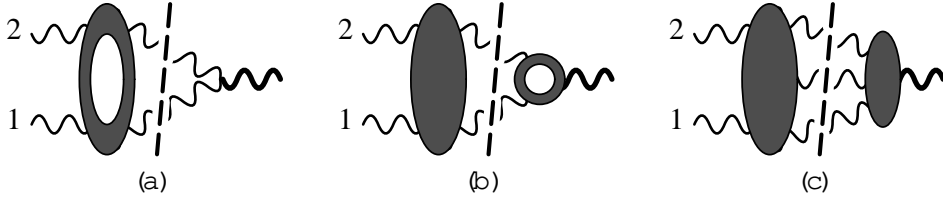


Figure 27: The three contributing cuts.

term  $s$  using momentum conservation. The reason is cut consistency: in terms which have both two- and three-particle cuts, we must obtain identical results. In the two-particle cut (c) everything to the left of the cut is gauge invariant, and cannot contain light cone denominators. (If we consider, instead of figure 26, a contribution for which either of the two cut propagators in (c) are absent, then we cannot determine from that two-particle cut whether the denominator in (a) should cancel or not. However, by considering the other contribution to the three-particle cut we find that the absence of the top cut propagator in (c) allows the denominator in (a) to be present; but in the absence of the bottom cut propagator alone, the denominator in (a) has to cancel.) More examples of arguments of this type can be found in the discussion of the types of integral topologies encountered in figure 30 in section 6.

## 5. Generation of Splitting Amplitude Integrands

Using the unitarity-based method described in the previous section we have generated the integrand for the two-loop splitting amplitude. Here, instead of sewing together two on-shell amplitudes, we sew an on-shell amplitude to a splitting amplitude. The tree splitting amplitudes are given by a current with one leg on shell [7], or equivalently, an amplitude with one leg on shell divided by the squared momentum of that leg. In general, the current should be evaluated in light-cone gauge. It can be computed either recursively [7], or via color-ordered Feynman rules. In a computation of the one-loop splitting amplitude, only the  $1!2$  tree splitting amplitude enters; in the computation of the two-loop one, both the  $1!2$  and  $1!3$  splitting amplitudes enter. The  $1!2$  tree-level splitting amplitude is basically just a vertex, and so has the same expression in both covariant and light-cone gauges; but the expression for the  $1!3$  amplitude is not the same in different gauges [41, 84].

The  $1!3$  splitting amplitude governs the universal behavior of tree-level gauge-theory amplitudes in triply-collinear limits, where three color-adjacent momenta  $k_{1,2,3}$  become collinear, and all invariants  $t_{123}, s_{12}, s_{23}$  are comparably small. These limits have been described previously in refs. [40, 41].

There are three basic types of contributions we need to consider:

- (a) two-particle cuts with an on-shell one-loop four-point amplitude integrand sewn onto the tree-level  $1!2$  splitting amplitude, depicted in figure 27 (a);
- (b) two-particle cuts with an on-shell tree-level four-point amplitude sewn onto the one-loop  $1!2$  splitting amplitude integrand, depicted in figure 27 (b);



Figure 28: Examples of non-planar contributions to the two-loop  $g \! \! \! / \, gg$  splitting amplitude, all of which have vanishing color factors.

(c) three-particle cuts with an on-shell tree-level three-point amplitude sewn onto the tree-level  $1 \! \! \! / \, 3$  splitting amplitude, depicted in figure 27(c).

In our calculation, there is a cut in only one channel (the invariant  $s_{12}$  in figure 27), so cross-channel projection and consistency issues do not arise. However, the three contributing cuts do need to be constructed and merged as described in the previous section, as there are terms that are common to different contributions. As in the one-loop case, the light-cone denominators inserted by the physical projection operators on the cut are crucial to getting the correct answer. This is also true for the light-cone denominator on a line connected to the on-shell vertex, contained in the  $1 \! \! \! / \, 3$  splitting amplitude. Its absence would result in different and inconsistent integrands emerging from the two- and three-particle cuts.

In principle, non-planar topologies could enter into the  $g \! \! \! / \, gg$  splitting amplitude, for example the crossed triangle graphs shown in figure 28. However, it turns out that all such non-planar graphs, for both pure-glue and fermion-loop contributions, have vanishing color factors: one simply dresses the diagrams with their color factors and performs the color algebra to demonstrate this. Accordingly, we only need to sew amplitudes into planar configurations for our calculation. As we shall show in section 9, the only color factor that arises in the pure-glue contributions is the leading-color one, namely  $C_A^2 = N_c^2$ , for the simple reason that there are no other color Casimirs at this order. The fermion-loop contributions can be divided into leading-color ( $C_A N_f = N_c N_f$ ) and subleading-color ( $(C_A - 2C_F)N_f = N_f = N_c$ ) terms. Both types arise from planar diagrams. Each planar diagram contributing to the subleading-color terms can be drawn with the virtual gluon on the inside of the fermion loop, whereas each for the leading-color terms can be drawn with the virtual gluon on the outside. (Some diagrams with bubble insertions can be drawn both ways, and are proportional to  $C_F = (N_c^2 - 1)/(2N_c)$ .) We discuss the full color dressing of the splitting amplitudes in section 9.

For splitting amplitudes with external quarks,  $g \! \! \! / \, q\bar{q}$  and  $q \! \! \! / \, q\bar{q}$ , the non-planar color factors no longer vanish. Non-planar two-loop three-point integrals with light-cone denominators will be required. However, these integrals should be amenable to the same methods used in the present computation.

In carrying out the calculation, we group terms in each sewn cut into different integral topologies, according to their propagators and light-cone denominators. To reduce the number of independent topologies, we perform a partial-fraction decomposition when

certain multiple light-cone-denominators appear. For example, if  $p_1 + p_2 = k_1 + k_2$  for two internal momenta  $p_1, p_2$ , we substitute

$$\frac{1}{p_1 \cdot n \cdot p \cdot n} \cdot \frac{1}{(k_1 + k_2) \cdot n \cdot p_1 \cdot n} + \frac{1}{p_2 \cdot n} : \quad (5.1)$$

Although the physical-state projectors for a two-particle cut generate two different light-cone denominators, the use of eq. (5.1) allows us to consider only one at a time. For triplets of light-cone denominators associated with a three-particle cut, only two have to be considered at a time. We also use a symmetry of the integrals under  $k_1 \leftrightarrow k_2$  ( $z \leftrightarrow 1-z$ ) to restrict the number of integral topologies to those described in figure 30 in the next section.

After relabeling momenta circulating in the seven cut (see appendix B) to match the labeling used by the integration routine for a given topology (see the next section), we obtain an integrand of the form

$$\frac{f(p^2; p \cdot q, \frac{q^2}{p^2} p \cdot k \cdot "i \cdot p; "j \cdot q)}{i p_i^2} : \quad (5.2)$$

ignoring factors that come out of the integral such as  $"i \cdot "j$ . Here  $p$  and  $q$  are the loop momenta;  $i p_i^2$  is shorthand for the set of both Feynman propagators and light-cone denominators for the topology. The polarization vectors for particles  $i = 1, 2; P$  are denoted by  $"i$ , and are taken to satisfy the light-cone-gauge condition  $"i \cdot n = 0$ , as well as the transverse condition  $"i \cdot k = 0$ . Note that although  $k_P$  is slightly off shell, any terms arising from  $"p \cdot k \neq 0$  will not be sufficiently singular in the  $k_P^2 \neq 0$  limit to contribute to the splitting amplitude, and hence we may as well set  $"p \cdot k$  to zero.)

In the dot products of polarization vectors with loop momenta,  $"i \cdot p$  and  $"i \cdot q$ , the  $D$ -dimensional loop momenta are effectively projected into four dimensions, because the external physical polarizations are four dimensional. Following the discussion of ref. [8], we write the loop momenta in these dot products as linear combinations of four independent momenta:  $k_1, k_2, n$ , and the dual vector

$$v \cdot "i \cdot p = c_1^p "i \cdot k + c_2^p "i \cdot k + c_n^p "i \cdot n + c_v^p "i \cdot v : \quad (5.3)$$

Then we have, for example,

$$"i \cdot p = \frac{p}{k} "i \cdot k + c_2^p "i \cdot k + c_n^p "i \cdot n + c_v^p "i \cdot v : \quad (5.4)$$

where

$$\begin{aligned} c_1^p &= \frac{1}{2k_1 \cdot k \cdot k_1 \cdot n} k_2 \cdot n \cdot p \cdot 1 \not{k} \cdot k_1 \cdot n \cdot p \cdot 2 \not{k} \cdot k_1 \cdot k \cdot p \cdot n; \\ c_2^p &= \frac{1}{2k_1 \cdot k \cdot k_2 \cdot n} k_2 \cdot n \cdot p \cdot 1 \cdot k \cdot k_1 \cdot n \cdot p \cdot 2 \not{k} \cdot k_1 \cdot k \cdot p \cdot n; \\ c_n^p &= \frac{1}{2k_2 \cdot n \cdot k \cdot n} k_2 \cdot n \cdot p \cdot 1 \not{k} \cdot k_1 \cdot n \cdot p \cdot 2 \cdot k \cdot k_1 \cdot k \cdot p \cdot n; \\ c_v^p &= \frac{1}{2k_1 \cdot k \cdot k_1 \cdot n \cdot k \cdot n} "i \cdot 1 \cdot 2 \cdot 3 \cdot p \cdot k_1^{-1} k_2^{-2} n^3 = \frac{1}{2k_1 \cdot k \cdot k_1 \cdot n \cdot k \cdot n} p \cdot v : \quad (5.5) \end{aligned}$$

After this substitution we use momentum conservation to express each integrand in terms of a basis consisting of:

1. inverse propagators;
2. light-cone denominators and numerators;
3. irreducible numerators (dot products of loop momenta with  $k_1$  and  $k_2$  which cannot be written in terms of inverse propagators); and
4. dot products of loop momenta with the dual vector (5.3), coming from  $c_v^p$  and  $c_v^q$ .

Following the merging procedure described in the previous section, at the integrand level, we obtained a single expression with correct cuts in all channels. Using the formula in section 4 of ref. [8], we then replaced dot products of loop momenta with the dual vector,  $p \cdot v$  and  $q \cdot v$ , by other elements of the basis. (These formulae are valid at the level of integrals, not integrands, so they should only be applied after checking cut consistency.) Typical propagator momenta, light-cone dot products, and irreducible numerators that appear in the calculation are given in eqs. (6.4) and (6.6). This produces an expression ready to be integrated. We describe the integration method in the next section.

## 6. Integrals

### 6.1 Introduction

All the integrals encountered in our computation of the two-loop splitting amplitudes are 3-point integrals with one external massive leg, and two massless legs. The massless legs carry momenta  $k_1$  and  $k_2$ . The massive leg carries momentum  $k_p = k_1 + k_2$  with  $k_p^2 = (k_1 + k_2)^2 = 2k_1 \cdot k_2 + s$ . We consider the time-like case,  $s > 0$ . For the space-like case, we take the splitting to be  $(k_1) \cdot (k_p) + k_2$ , with  $k_p^2 = s < 0$ . Here  $(k_p)$  and  $k_2$  carry longitudinal momentum fractions  $x$  and  $1-x$  respectively, with  $x = 1-z$ . The space-like case may be obtained from the time-like case using analyticity. As there is no other dimensionful parameter in the problem, the dependence on  $s$  is determined by dimensional analysis to be  $/ (s)^2$ . To reach the physical range  $0 < x < 1$ , it is also necessary to continue the momentum fraction  $z$  to values larger than 1, as we shall discuss in section 7.4.

In addition to standard propagator factors of the form  $1-p^2$  in the denominator, and tensors in the numerator, there can also be denominator factors from light-cone gauge (or physical state projection, of the form  $1=(p \cdot n)$  where  $n$  is the light-cone gauge vector,  $n^2 = 0$ ). The vector  $n$  is also used to define the collinear momentum fraction  $z$ , according to the kinematic relations (3.8). We also rescale  $n$  so that it obeys eq. (3.10),  $k_p \cdot n = -s$ .

Two-loop 3-point integrals containing light-cone denominator factors have not been encountered previously, and contain non-trivial dependence on  $z$ . For the case of a gluon splitting to two gluons, we shall see that the non-planar topologies all have vanishing color factor, and hence the corresponding integrals do not need to be calculated. The integrals from the planar topologies can be reduced to a set of 13 master integrals, using identities based on integration by parts (IBP) [59] and Lorentz invariance [20]. The master integrals

can be evaluated as Laurent expansions in  $x$  with the aid of differential equations in  $z$ , along the lines of refs. [18, 20].

The Laurent expansions of each master integral, through the order in  $z$  required to obtain the splitting amplitudes to order  $z^0$ , can be expressed in terms of logarithms, plus the polylogarithmic functions defined [85] by,

$$Li_n(x) = \sum_{i=1}^{\infty} \frac{x^i}{i^n} = \int_0^z \frac{x}{t} Li_{n-1}(t); \quad (6.1)$$

$$Li_2(x) = \int_0^z \frac{x}{t} \ln(1-t); \quad (6.2)$$

Here we need  $Li_n(x)$ , for  $n = 2, 3, 4$ , and the argument  $x$  can be  $z, 1-z$  or  $(1-z)/z$ . (For  $n < 4$ , identities relate some of these polylogarithms to each other.) For the order  $z^1$  terms in the splitting amplitudes, the corresponding set of functions (with  $n$  extending up to 5) is not sufficient; instead harmonic polylogarithms [86, 20] are required.

In section 6.2 we describe the procedure for reducing the two-loop three-point integrals with light-cone denominators to master integrals, and give a list of master integrals required for the  $g^+ g \rightarrow gg$  splitting amplitude. In section 6.3 we illustrate how to derive differential equations for the master integrals, and present the differential equations. We also give the Laurent expansions of the master integrals.

## 6.2 Reduction Procedure

A typical integral encountered is the two-loop nested double triangle integral with two light-cone denominators inserted,

$$L(1; 2; 3; \dots; 9) = \int_0^z \frac{d^D p}{D=2} \frac{d^D q}{D=2} \prod_{i=1}^9 \frac{1}{(p_i^2)^{n_i}}; \quad (6.3)$$

where  $D = 4 - 2\epsilon$ ,

$$\begin{aligned} p_1 &= q; & p_2 &= q + k_1 + k_2; & p_3 &= p; & p_4 &= p - k_1 - k_2; \\ p_5 &= p - k_1; & p_6 &= p + q; \\ p_7^2 &= q \cdot n; & \hat{p} &= 2q \cdot k; & p_9^2 &= (p - k_1 - k_2) \cdot n; \end{aligned} \quad (6.4)$$

and the  $n_i$  are integers. The momentum routings for this integral are depicted in figure 29(a). The on-shell external momentum  $k_1 + k_2$  flows in from the right of the diagram, and splits into on-shell momenta  $k_1$  and  $k_2$  flowing out to the left. The uncircled numbers adorning the internal lines label the internal momenta  $p_i$ , whose squares are the ordinary denominators  $p_i^2$ ,  $i = 1, 2, \dots, 6$ , appearing in eq. (6.3). The circled numbers correspond to the light-cone denominators, in this case  $p_7^2$  and  $p_9^2$ , which are linear in  $n$ . Associated with each circled number is an arrow on an internal line. The arrow is a reminder of the direction of the internal momentum which is Lorentz-contracted with  $n$  to form the light-cone denominator. One of the  $p_i^2$  in eq. (6.3) is not shown in figure 29(a):  $p_8^2 = 2q \cdot k$ . In this

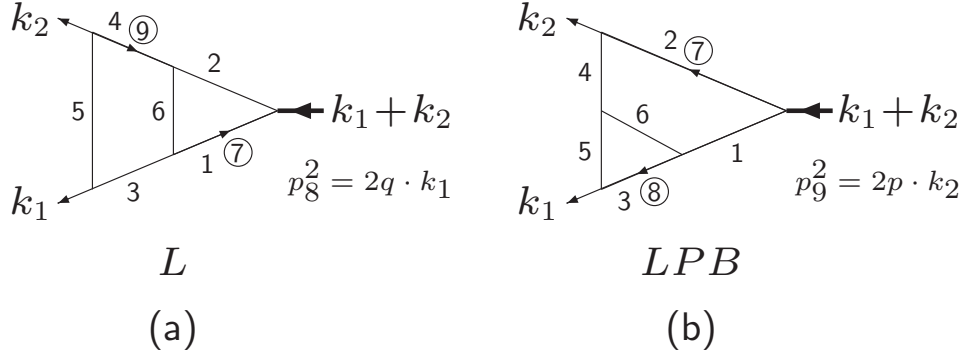


Figure 29: (a) The planar double triangle integral  $L (i)$  defined in eq. (6.3). (b) The planar double triangle integral  $LPB (i)$  defined in eq. (6.5). In each case  $k_1$  and  $k_2$  are the two outgoing massless external lines. The internal lines, or 'ordinary' propagators, labelled with an uncircled integer  $i$ ,  $i \in \{1, 2, \dots, 6\}$ , carry momenta  $p_i$ . The special light-cone denominator factors  $p_i$  in which can be present are marked with an arrow on an internal line, and the corresponding integer label is circled. The arrow serves to remind one of the direction of the loop momentum used in their definition. Propagators 8 (in case (a)) and 9 (in case (b)) do not appear in denominators in these integrals. The expressions for  $p_8^2$  and  $p_9^2$  are given explicitly.

topology, it only appears in the numerator, i.e.  ${}_8 = 0$ . It will appear as an irreducible numerator in the tensor integrals arising from the numerator algebra generated in evaluating the cuts. Its presence is also required to close the IBP equations.

We also encounter the 'pentabox' integral topology [87] (but with one ordinary propagator cancelled), again with two light-cone denominator insertions,

$$LPB (1; 2; 3; \dots; 9) = \frac{d^D p}{D=2} \frac{d^D q}{D=2} \sum_{i=1}^9 \frac{1}{(p_i^2)^i}; \quad (6.5)$$

where

$$\begin{aligned} p_1 &= q; & p_2 &= q + k_1 + k_2; & p_3 &= p; & p_4 &= q + k_1; \\ p_5 &= p - k_1; & p_6 &= p + q; \\ p_7^2 &= (q + k_1 + k_2) \cdot n; & \hat{p} &= p \cdot n; & \hat{p}^2 &= 2p \cdot k; \end{aligned} \quad (6.6)$$

The momentum routings for this integral are depicted in Figure 29(b). In this case  $p_7^2$  and  $p_9^2$  are the circled, light-cone denominators, and  $p_8^2$  only appears in the numerator,  ${}_9 = 0$ .

Besides the two types of integrals depicted in Figure 29, there are several more types, which differ from either  $L$  or  $LPB$  only in the location of the light-cone denominators. All the light-cone configurations are shown in Figure 30. The leftmost two cases,  $L$  and  $LPB$ , are equivalent to Figure 29(a) and Figure 29(b). The momentum routings and the labels for the external legs and for propagators 1 to 6 are exactly the same as in Figure 29, so we have suppressed them in Figure 30. The remaining cases define the integrals  $D (i)$ ,  $F (i)$ ,  $G (i)$ ,  $H (i)$ ,  $J (i)$  and  $M (i)$ , by analogy to eqs. (6.3) and (6.5). As in the  $L$  and  $LPB$  cases, one extra propagator, linear in the loop momentum but not a light-cone denominator, is

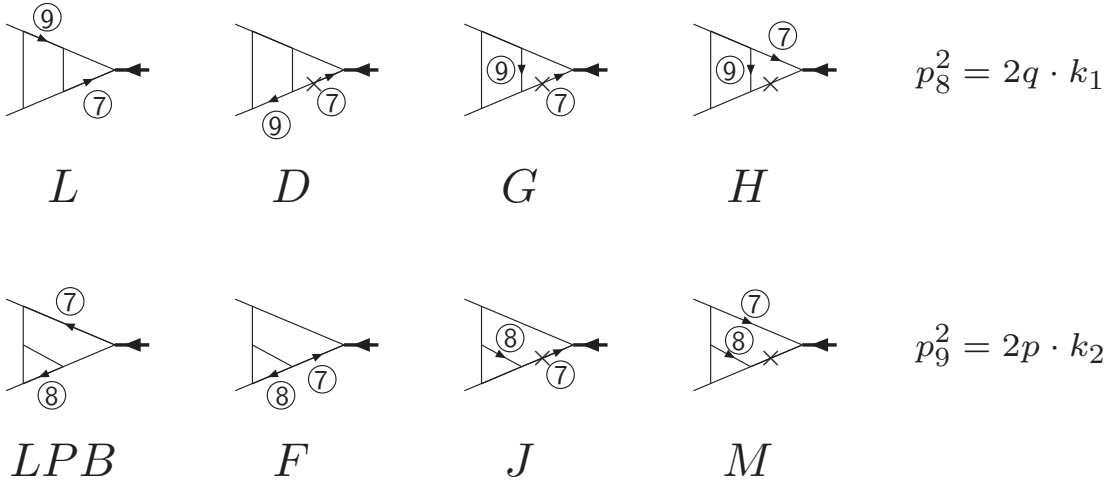


Figure 30: List of required light-cone denominator insertions for the  $g \rightarrow gg$  splitting amplitude. The leftmost two cases are equivalent to Figure 29(a) and Figure 29(b). The labels for the external legs and for propagators 1 to 6 are suppressed. The expression for the extra propagator required for tensor reductions is the same for L, D, G and H topologies:  $p_8^2 = 2q \cdot k_1$ . The extra propagator for LPB, F, J and M topologies is  $p_9^2 = 2p \cdot k_2$ . For the D, G, H, J and M topologies, the ‘’ sign indicates that the marked ordinary propagator is not required in the denominator, only in the numerator.

required for tensor integral reduction and for the IBP equations to close; the expression for this propagator is shown explicitly in the figure.

The symbol ‘’ on a line in Figure 30 indicates that that ordinary propagator never appears in the denominator, when the light-cone denominators indicated by the arrows are present. As discussed in section 4.4, the unitarity cuts guarantee these facts. For example, suppose the propagator marked with a ‘’ in the J topology were present. Then such an integral has a 2-particle cut to the right of the circled propagator 8. (If propagator 2, which also must be present in the 2-particle cut, did not appear in the denominator, then the integral would become a massless external leg integral, which vanishes trivially in dimensional regularization.) But we know that no light-cone projectors should appear to the left of such a cut, so either the circled propagator 8 or the unmarked propagator must be absent in J. If the circled propagator 8 is absent from the denominator, we consider the integral to belong to the F topology instead.

Note that we have not explicitly shown integrals that are related to the ones in Figure 30 by the external leg permutation  $k_1 \leftrightarrow k_2$ , which also takes  $z \leftrightarrow 1 - z$ . We always use this permutation to map such integrals into those shown in Figure 30.

There are three independent external four-vectors in the light-cone integrals,  $k_1, k_2$  and  $n$ . Due to momentum conservation, the same number of vectors appear in the two-loop four-point integrals needed for  $2 \rightarrow 2$  scattering,  $k_1 + k_2 \rightarrow k_3 + k_4$ . In fact,  $n$  may be thought of as a fictitious momentum vector  $k_3$ , if desired. Then the derivation of IBP and Lorentz invariance identities follows straightforwardly from previous work on four-point

integrals [59, 18, 20, 19]. The IBP equations for the L topology are derived by considering

$$0 = \sum_{i=1}^Z \frac{d^D p}{D=2} \frac{d^D q}{D=2} \frac{\partial}{\partial a} b \frac{Y^9}{(p_i^2)^i} ; \quad (6.7)$$

where the  $p_i^2$  are given in eq. (6.4),  $a$  2 fp ; $q$   $g$  are the two independent loop momenta, and  $b$  can be any of the five available vectors, b 2 fp ; $q$  ; $k_1$  ; $k_2$  ; $n$   $g$ . Thus for each value of  $f_{ig}$ , there are  $2^5 = 32$  IBP equations, which are linear in the L (i). They can be written as

$$0 = (0 \ 2 \ 3 \ 4 \ 5 \ 6 \ 9) + (4(s \ 3)4^+ \ 53 \ 5^+ + (6(1 \ 3)6^+ + 9s9^+); \quad (6.8)$$

$$0 = (3 \ 6 + (3(1 \ 6)3^+ \ 4(s \ 2 \ 3 + 6)4^+ + 5(1 + 3 \ 6 + 8)5^+ \ 6(1 \ 3)6^+ \ 97 \ 9^+); \quad (6.9)$$

$$0 = (3 + 5 + 35 \ 3^+ + 4(s \ 3 + 5)4^+ \ 53 \ 5^+ \ 6(3 \ 5 + 8)6^+ + 9zs9^+); \quad (6.10)$$

$$0 = (4 \ 5 \ 3(s \ 4 + 5)3^+ \ 45 \ 4^+ + 54 \ 5^+ + (6(1 \ 2 + 4 \ 5 + 8)6^+ + 9(1 \ z)s9^+); \quad (6.11)$$

$$0 = (3(s \ 9)3^+ \ 49 \ 4^+ + 5((1 \ z)s \ 9)5^+ + 6(s \ 7 \ 9)6^+); \quad (6.12)$$

$$0 = (1 \ 6 + (1(3 \ 6)1^+ \ 2(s \ 1 \ 4 + 6)2^+ + 6(1 \ 3)6^+ + (7(s \ 9)7^+ \ 8(3 \ 5)8^+); \quad (6.13)$$

$$0 = (D \ 2 \ 1 \ 2 \ 6 \ 7 \ 8 + 2(s \ 1)2^+ \ 6(1 \ 3)6^+); \quad (6.14)$$

$$0 = (18 \ 1^+ \ 2(s + 8)2^+ \ 6(3 \ 5 + 8)6^+ + 7zs7^+); \quad (6.15)$$

$$0 = (1 \ 2 + (1(s \ 2 + 8)1^+ + 2(1 + 8)2^+ + 6(1 \ 2 + 4 \ 5 + 8)6^+ + (7(1 \ z)s7^+ \ 8zs8^+); \quad (6.16)$$

$$0 = (17 \ 1^+ + 2(s \ 7)2^+ + 6(s \ 7 \ 9)6^+ + 8zs8^+); \quad (6.17)$$

Here  $i$  are operators taking  $i! \ i \ 1$ ; for instance, in eq. (6.8) the expression  $53 \ 5^+$  is shorthand for the term  $5L(1; 2; 3 \ 1; 4; 5 + 1; 6; 7; 8; 9)$ .

Three Lorentz invariance identities for each value of  $f_{ig}$  can also be derived, by requiring

$$0 = \sum_{i=1}^Z \frac{d^D p}{D=2} \frac{d^D q}{D=2} j \ k_1 \frac{\partial}{\partial k_1} + k_2 \frac{\partial}{\partial k_2} + n \ \frac{\partial}{\partial n} \frac{Y^9}{(p_i^2)^i}; \quad (6.18)$$

where

$$\begin{aligned} 1 &= k_1 k_2 \ k_2 k_1; \\ 2 &= k_1 n \ n k_1; \\ 3 &= k_2 n \ n k_2; \end{aligned} \quad (6.19)$$

The three identities are

$$0 = (2 + 4 \ 5 \ 8) \ 2(s + 1 + 28)2^+ \ 4(s \ 3 + 25)4^+ + 53 \ 5^+ +$$

$$+ \gamma(zs + z_1 - z_2 + 8)7^+ - \gamma(zs - (1 - z)3 - z_4 + 5)9^+ ; \quad (6.20)$$

$$0 = z(5 - \gamma + 8 - 9) + \gamma(7 + 8)2^+ + \gamma(s - 3 + 5 - 9)4^+ \\ - 5z35^+ + \gamma z s 9^+ ; \quad (6.21)$$

$$0 = \gamma_2 + \gamma_4 - (5 + 8)z - (\gamma + 9)(1 - z) - \gamma_2(s + 1 - 7 + 8)2^+ \\ - \gamma_4(5 + 9)4^+ + \gamma_5((1 - z)s + z_4 - 9)5^+ \\ - \gamma_8(zs + z_1 - z_2 - 7)8^+ + \gamma_9(1 - z)s 9^+ : \quad (6.22)$$

There are analogous sets of equations for the other integral topologies: LPB, D, G, H, F, J and M.

The next step is to solve the linear system of IBP and Lorentz equations for each topology. We use a Gauss elimination algorithm first introduced by Laporta [23]. We have used a customized version of this algorithm [60], written in MAPLE [88] and FORM [89]. After performing the reductions, we obtain 13 master integrals for the  $g! gg$  problem:

$$\begin{aligned} L(1;1;1;1;0;0;0;0;0) &= \text{Spec}(s) = \frac{2s^2}{(1 - z)^2} B_{\text{tie}}(s) ; \\ L(1;0;0;1;0;1;0;0;0) &= LPB(0;1;1;0;0;1;0;0;0) = Sset(s) ; \\ L(1;1;0;0;1;1;0;0;0) &= B_{\text{tri}}(s) ; \\ L(0;1;1;1;0;1;1;0;0) &= Fish(s) ; \\ L(1;0;0;1;1;1;1;0;0) &= LPB(0;1;1;1;0;1;0;1;0) = W_{\text{edge}}(z;s) ; \\ L(1;1;0;0;1;1;1;0;0) &= LB_{\text{tri}}(z;s) ; \\ L(0;1;1;0;1;1;1;0;0) &= W_{\text{edgeF}}(z;s) ; \\ L(1;1;1;0;1;1;1;0;0) &= Zig(z;s) ; \\ L(1;1;1;1;1;1;1;0;0) &= P_{\text{tri}}(z;s) ; \\ L(1;1;1;1;1;2;1;0;0) &= P_{\text{tri}}(z;s) ; \\ L(1;0;0;1;1;1;1;0;0;1) &= LPB(0;1;1;0;1;1;0;1;0) \Big|_{z=1} = LPBW_{\text{edge}}(z;s) ; \\ LPB(0;1;1;1;1;2;1;1;0) &= LPBD_{\text{tri}}(z;s) ; \\ F(0;1;1;1;1;1;1;1;0) &= FD_{\text{tri}}(z;s) : \end{aligned} \quad (6.23)$$

$B_{\text{tie}}(s)$  is an integral with two independent one-loop triangles, which is trivially related to  $\text{Spec}(s)$ .

The master integrals are depicted in figure 31. The first three of the master integrals have no light-cone denominators present, so they do not depend on  $z$  and were encountered long ago in the computation of the quark form factor [90]. The next master integral,  $Fish(s)$ , has a light-cone denominator, but nevertheless does not depend on  $z$ . The remaining master integrals depend on  $z$ . The next six come from the L topology, although they can also come from other topologies. In the L topology labeling they have light-cone denominator 7, but not 9, present. The next master integral after that,  $LPBW_{\text{edge}}(z;s)$  can come from either the L or LPB topology, but in the L labeling it has light-cone denominator 9, but not 7, present. Finally, the last two master integrals come from the LPB and F topologies and have two light-cone denominators present, 7 and 8.

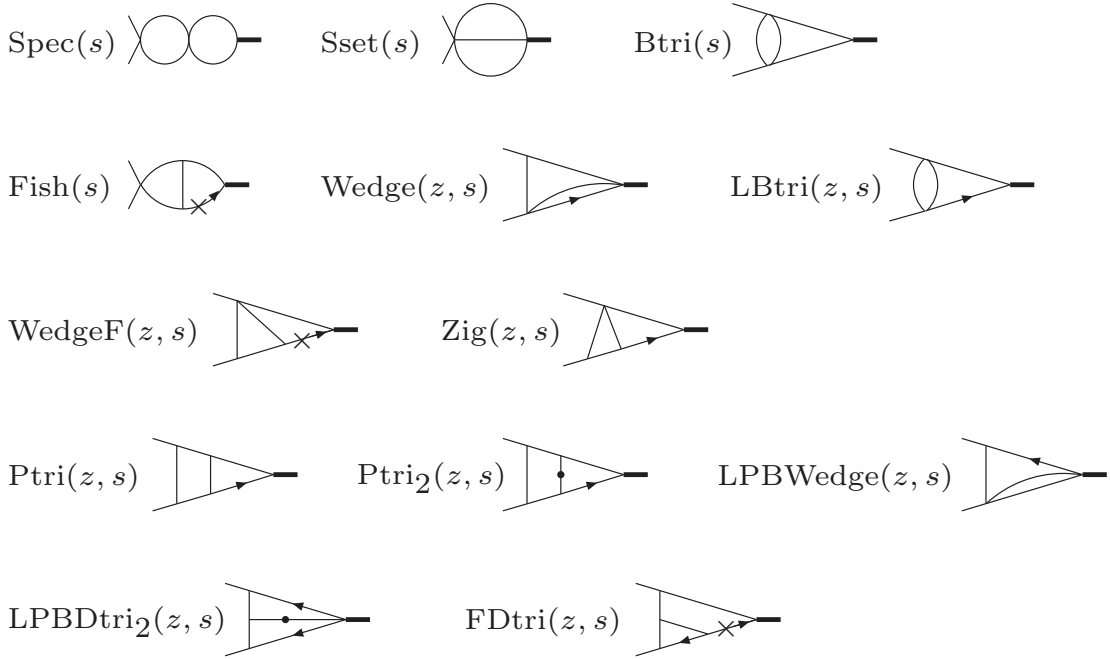


Figure 31: The planar master integrals required for computing two-loop leading-color splitting amplitudes. An arrow indicates a light-cone propagator, a dot indicates a doubled ordinary propagator, and a ' ' indicates an omitted ordinary propagator.

In intermediate steps, two other master integrals appear,  $J(0;1;1;1;1;1;1;1;0)$ ,  $JD\,tri(z;s)$  and  $M(0;1;1;1;1;1;1;1;0) - MD\,tri(z;s)$ . However, there is a partial fraction equation relating  $FD\,tri$ ,  $JD\,tri$  and  $MD\,tri$ . Consider the identity

$$\frac{1}{(p+q)} \frac{1}{nq} \frac{1}{n} = \frac{1}{p} \frac{1}{nq} \frac{1}{n} + \frac{1}{(p+q)} \frac{1}{np} \frac{1}{n}; \quad (6.24)$$

It implies, after inspecting figure 30, that

$$JD\,tri(z;s) = FD\,tri(z;s) + MD\,tri(1-z;s); \quad (6.25)$$

After using this relation to eliminate  $JD\,tri$ , we find that the coefficient of  $MD\,tri$  cancels out of all gg splitting amplitude expressions.

### 6.3 Differential Equations for Master Integrals

Since  $s$  is the only dimensionful scale entering the master integrals, their dependence on  $s$  is fixed simply by dimensional analysis. The  $z$ -dependence of the master integrals can be determined by differentiating their Schwinger-parametrized form with respect to  $z$ . This produces an integral where some of the indices and the dimension  $D$  have been shifted by integers ( $D$  is always shifted by an even integer). The effect of shifting  $D$  can also be converted into a shift of  $i$ . Integrals with shifted  $i$  are again reducible to master integrals. Thus we first derive 'dimension-shifting' relations, and then differential equations in  $z$ , for the master integrals.

Consider a case where all the  $t_i$  are non-negative. Schwinger parametrization is achieved by inserting (for  $t_i > 0$ )

$$\frac{1}{(p_i^2)^i} = \frac{(-1)^i}{(i)} \int_0^{t_i} dt_i t_i^{i-1} \exp(t_i p_i^2); \quad (6.26)$$

into the loop-momentum integrals, Wick rotating, and then performing the integrals over  $p$  and  $q$ , to arrive at the generic result

$$X_{(i)} = \int_0^{t_i} dt_i (-1)^i \frac{t_i^{i-1}}{(i)} \exp \left[ \frac{(s)Q_X(z; t_i)}{(t_i)} \right]^{\#}; \quad (6.27)$$

Here  $X$  stands for one of the integral topologies,  $n$  is the number of positive  $t_i$ , and  $Q_X(z; t_i)$  is a cubic polynomial in the  $t_i$ . Also,

$$(t_i) = T_p T_q + T_p T_{pq} + T_q T_{pq}; \quad (6.28)$$

where  $T_p$ ,  $T_q$ ,  $T_{pq}$  are the sums of Schwinger parameters along the lines carrying loop momenta  $p$ ,  $q$ ,  $p+q$ , respectively. For the  $L$ ,  $D$ ,  $G$  and  $H$  integrals,

$$T_p = t_3 + t_4 + t_5; \quad T_q = t_1 + t_2; \quad T_{pq} = t_6; \quad (6.29)$$

For the LP B, F, J and M integrals,

$$T_p = t_3 + t_5; \quad T_q = t_1 + t_2 + t_4; \quad T_{pq} = t_6; \quad (6.30)$$

From eq. (6.27) we see that shifting  $D \rightarrow D-2$  is equivalent to inserting a factor of  $t_i$  into the Schwinger-parametrized result. Breaking up  $X$  into monomials in the Schwinger parameters  $t_i$ , these integrals can be rewritten using shifted indices  $i$ . For example,

$$\begin{aligned} P_{tri}(z; s) &= L(1; 1; 1; 1; 1; 1; 1; 0; 0) \\ &= L(2; 1; 1; 1; 1; 2; 1; 0; 0) + L(1; 2; 1; 1; 1; 2; 1; 0; 0) + L(1; 1; 2; 1; 1; 2; 1; 0; 0) + \\ &\quad + L(1; 1; 1; 2; 1; 2; 1; 0; 0) + L(1; 1; 1; 1; 2; 2; 1; 0; 0) + L(2; 1; 2; 1; 1; 1; 1; 0; 0) + \\ &\quad + L(1; 2; 2; 1; 1; 1; 1; 0; 0) + L(2; 1; 1; 2; 1; 1; 1; 0; 0) + L(1; 2; 1; 2; 1; 1; 1; 0; 0) + \\ &\quad + L(2; 1; 1; 1; 2; 1; 1; 0; 0) + L(1; 2; 1; 1; 2; 1; 1; 0; 0); \end{aligned} \quad (6.31)$$

The latter combination of integrals can be reduced to a linear combination of  $P_{tri}(z; s)$ ,  $P_{tri_2}(z; s)$ , and the eight master integrals preceding them in eq. (6.23) or figure 31. We have worked out such dimension-shifting relations for all of the master integrals, but we refrain from presenting them all here. We shall give two examples in eqs. (6.43) and (6.44) below.

Once the  $z$ -dependence of  $Q_X(z; t_i)$  in eq. (6.27) is known, the derivative of  $X_{(i)}$  with respect to  $z$  may be computed from the parametric representation (6.27). The polynomial  $Q_X(z; t_i)$  is always linear in  $z$ ,

$$Q_X(z; t_i) = Q_X^0(t_i) + z Q_X^1(t_i); \quad (6.32)$$

where  $Q_X^0$  and  $Q_X^1$  are independent of  $z$ . For the integrals encountered in the calculation, the  $Q_X(z; t_i)$  have a definite sign for  $0 < z < 1$ . Hence all the master integrals are real in the time-like region, apart from the overall factor of  $(-s)^2$ . For the first ten master integrals in eq. (6.23),  $Q_X^1(t_i) = t_5 t_6 t_7$ , unless any of  $t_5, t_6, t_7$  vanishes. In these cases,  $Q_X^1(t_i) = 0$  and the master integral is independent of  $z$ . Thus  $Fish(s)$  is independent of  $z$ , despite containing a light-cone denominator. For the non-trivial cases where  $t_5, t_6, t_7 > 0$ , using eq. (6.27), the derivatives of the master integrals are simply obtained by inserting  $(-s)Q_X^1 = 0$  into the Schwinger parametrized form  $s$ . (There is an extra minus sign from Wick rotation.) For example,

$$\frac{\partial}{\partial z} P tri(z; s) = \frac{\partial}{\partial z} L(1; 1; 1; 1; 1; 1; 0; 0) = (-s)L(1; 1; 1; 1; 2; 2; 2; 0; 0)_{D+2} : \quad (6.33)$$

The shift  $D - D + 2$  comes from the factor of  $1 = 1$ . The effect of this shift is found by inverting the  $D - D - 2$  shift computed by inserting one factor of  $1$ .

For the integral  $LPBW edge(z; s)$ , we have  $Q_X^1(t_i) = t_4(t_3 + t_6)t_7$ . For  $LPBD tri_2(z; s)$  and  $FD tri(z; s)$ , we find  $Q_X^1(t_i) = [t_5(t_4 + t_6) + t_4(t_3 + t_6)]t_7 - [t_4(t_5 + t_6) + t_5(t_2 + t_6)]t_8$ .

Reducing the right-hand side of equations like (6.33) to linear combinations of master integrals, we obtain the following set of differential equations:

$$\frac{\partial}{\partial z} W edge(z; s) = \frac{z - 2}{z(1 - z)} W edge(z; s) + \frac{(1 - 2)(2 - 3)(1 - 3)}{2s^2 z(1 - z)} Sset(s); \quad (6.34)$$

$$\frac{\partial}{\partial z} LB tri(z; s) = \frac{2 - z}{z(1 - z)} LB tri(z; s) - \frac{1 - 3}{s z(1 - z)} B tri(s); \quad (6.35)$$

$$\begin{aligned} \frac{\partial}{\partial z} W edgeF(z; s) = & \frac{2(1 - 2) - z(2 - 3)}{2z(1 - z)} W edgeF(z; s) + \frac{s}{2(1 - z)} Z ig(z; s) + \\ & + \frac{3 - 1 - 2}{2z(1 - z)} LB tri(z; s) + \frac{3(1 - 2)(1 - 3)}{4s z(1 - z)} B tri(s) \\ & - \frac{(1 - 2)(1 - 3)(2 - 3)}{2^2 s^2 z(1 - z)} Sset(s); \end{aligned} \quad (6.36)$$

$$\begin{aligned} \frac{\partial}{\partial z} Z ig(z; s) = & \frac{3}{2s(1 - z)} W edgeF(z; s) - \frac{2 + 4 - z(2 + 3)}{2z(1 - z)} Z ig(z; s) \\ & - \frac{3 - 1 - 2}{2s z(1 - z)} LB tri(z; s) + \frac{3(1 - 2)(1 - 3)}{4s^2 z(1 - z)} B tri(s) + \\ & + \frac{3(1 - 2)(1 - 3)(2 - 3)}{2^2 s^3 z(1 - z)} Sset(s); \end{aligned} \quad (6.37)$$

$$\begin{aligned} \frac{\partial}{\partial z} P tri(z; s) = & \frac{1}{3 - 2z} \frac{3 + 6 - 2z}{z} P tri(z; s) + \frac{8(1 - 2)}{s} P tri_2^{(6)}(z; s) + \\ & + \frac{2}{s} Z ig(z; s) - \frac{2 - z}{s^2(1 - z)} W edgeF(z; s) + \\ & + \frac{2(1 - 2)(9 - 7z - 3z^2)}{s^2 z^2(1 - z)} LB tri(z; s) + \\ & + \frac{2(1 - z)(9 - 4z)}{s^2 z^2} W edge(z; s) + \frac{2(3 - 4z)}{s^2 z(1 - z)} Fish(s) + \end{aligned}$$

$$\begin{aligned}
& + \frac{(1 \quad 2 \quad)(1 \quad 3 \quad)(9 \quad 16z + 5z^2)}{s^3 z^2 (1 - z)} B_{\text{tri}}(s) \\
& + \frac{(1 \quad 2 \quad)(1 \quad 3 \quad)(2 \quad 3 \quad)(9 + 26z)}{s^2 z^4} S_{\text{set}}(s) \quad \frac{12}{s z} B_{\text{tie}}(s) ; \quad (6.38)
\end{aligned}$$

$$\begin{aligned}
\frac{\partial}{\partial z} P_{\text{tri}}^{(6)}(z; s) = & \frac{1}{3 - 2z} \frac{s}{2(1 - z)} P_{\text{tri}}(z; s) + \\
& + \frac{3(1 \quad ) \quad 2(3 \quad 2 \quad)z + 2z^2}{z(1 - z)} P_{\text{tri}}^{(6)}(z; s) \\
& - \frac{1}{4(1 - z)} Z_{\text{ig}}(z; s) \quad \frac{3}{4s(1 - z)} W_{\text{edgeF}}(z; s) \\
& - \frac{11(1 \quad 2 \quad)}{4s z(1 - z)} L_{\text{B tri}}(z; s) \quad \frac{1}{2s z} W_{\text{edge}}(z; s) \\
& - \frac{3}{2s z(1 - z)} F_{\text{ish}}(s) \quad \frac{5(1 \quad 2 \quad)(1 \quad 3 \quad)}{8^2 s^2 z(1 - z)} B_{\text{tri}}(s) + \\
& + \frac{2(1 \quad 3 \quad)(2 \quad 3 \quad)(2 \quad \quad 2z)}{3s^3 z(1 - z)} S_{\text{set}}(s) + \\
& + \frac{3 \quad 4 \quad z}{2(1 \quad 2 \quad)z(1 - z)} B_{\text{tie}}(s) ; \quad (6.39)
\end{aligned}$$

$$\frac{\partial}{\partial z} L_{\text{PBW edge}}(z; s) = \frac{z +}{z(1 - z)} L_{\text{PBW edge}}(z; s) \quad \frac{(1 \quad 3 \quad)(2 \quad 3 \quad)}{s^2 z(1 - z)} S_{\text{set}}(s) ; \quad (6.40)$$

$$\begin{aligned}
\frac{\partial}{\partial z} L_{\text{PBD tri}}^{(6)}(z; s) = & \frac{1 \quad 2z}{z(1 - z)} L_{\text{PBD tri}}^{(6)}(z; s) \\
& + \frac{1 \quad 2}{(1 \quad 3 \quad) s} \frac{L_{\text{PBW edge}}(z; s)}{z^2} \quad \frac{L_{\text{PBW edge}}(1 - z; s)}{(1 - z)^2} + \\
& + \frac{1}{(1 \quad 3 \quad) s z(1 - z)} W_{\text{edge}}(z; s) \quad W_{\text{edge}}(1 - z; s) + \\
& + \frac{(1 \quad 2 \quad)(2 \quad 3 \quad)(1 \quad 2z)}{2s^3 z^2 (1 - z)^2} S_{\text{set}}(s) ; \quad (6.41)
\end{aligned}$$

$$\begin{aligned}
\frac{\partial}{\partial z} F_{\text{D tri}}(z; s) = & 2 \frac{z +}{z(1 - z)} F_{\text{D tri}}(z; s) \quad 2 \frac{z}{s z(1 - z)} Z_{\text{ig}}(z; s) + \\
& + \frac{6(1 \quad 2 \quad)}{s^2 z^2 (1 - z)} z L_{\text{PBW edge}}(1 - z; s) \quad L_{\text{B tri}}(z; s) \\
& + \frac{1 \quad 3}{2 s} B_{\text{tri}}(s) : \quad (6.42)
\end{aligned}$$

In eqs. (6.38), (6.39) and (6.41), we have performed a change of basis: we exchange the (4 2)-dimensional integral  $P_{\text{tri}}(z; s) - P_{\text{tri}}^{(6)}(z; s)$  for its (6 2)-dimensional version,  $P_{\text{tri}}^{(6)}(z; s) - P_{\text{tri}}(z; s)$ , and similarly for  $L_{\text{PBD tri}}^{(6)}(z; s)$ . All of the integrals in this new basis are well-defined using ordinary dimensional regularization, following the same analysis as in section 3.4. The relations required to change the basis are examples of the dimension-shifting relations discussed previously,

$$P_{\text{tri}}^{(6)}(z; s) = \frac{3(1 - z) + (9 - 8z)}{2(1 - 2)(1 + 2)z(1 - z)} B_{\text{tie}}(s)$$

$$\begin{aligned}
& \frac{(1 \ 3 \ 2 \ 3)}{8^3 (1 + \ ) (1 + 2 \ ) s^3 z^2 (1 - z)} \frac{h}{9} \frac{47z + 38z^2 + (72 \ 373z + 270z^2)}{i} + \\
& + \frac{2 (171 \ 964z + 652z^2)}{s \text{set}(s)} + \\
& \frac{1 \ 3}{16^2 (1 + \ ) (1 + 2 \ ) s^2 z^2 (1 - z)} \frac{h}{54} \frac{92z + 34z^2 + (7 \ 8z) (54 \ 31z)}{i} + \\
& + \frac{2 (828 \ 1459z + 578z^2)}{B \text{tri}(s)} + \\
& \frac{3 \ 4z + (9 \ 10z)}{4 (1 \ 2 \ ) (1 + 2 \ ) s z (1 - z)} \text{Fish}(s) + \\
& + \frac{1 \ z}{4 (1 \ 2 \ ) (1 + \ ) (1 + 2 \ ) s^2 z} \frac{h}{9} \frac{8z + 6 \ (9 \ 7z) + 2 (63 \ 46z)}{i} \text{Wedge}(z; s) \\
& \frac{1}{8 (1 + \ ) (1 + 2 \ ) s^2 z (1 - z)} \frac{h}{2} \frac{(27 \ 37z + 9z^2) + 3 (90 \ 125z + 36z^2)}{i} + \\
& + \frac{2 (288 \ 403z + 126z^2)}{L \text{Btri}(z; s)} + \\
& + \frac{1}{8 (1 \ 2 \ ) (1 + \ ) (1 + 2 \ ) s (1 - z)} \frac{h}{2z} \frac{3 (9 \ 8z) + 2 (45 \ 34z)}{i} \text{WedgeF}(z; s) \\
& \frac{1}{8 (1 \ 2 \ ) (1 + \ ) (1 + 2 \ ) z (1 - z)} \frac{h}{2} \frac{(9 \ 11z + 3z^2) + (102 \ 125z + 36z^2)}{i} + \\
& + \frac{2 (120 \ 145z + 42z^2)}{Z \text{ig}(z; s)} \\
& \frac{s (3 \ 2z + (9 \ 8z))}{8 (1 \ 2 \ ) z (1 - z)} \text{Ptri}(z; s) - \frac{s^2 (1 + \ ) (3 \ 2z)}{8 (1 \ 2 \ ) (1 + 2 \ ) (1 - z)} \text{Ptri}_2(z; s); \quad (6.43)
\end{aligned}$$

and

$$\begin{aligned}
& \text{LPBDtri}_2^{(6)}(z; s) = \frac{(1 \ 2 \ ) (2 \ 3 \ )}{4^3 (1 + 2 \ )^2 s^3 z^2 (1 - z)^2} \frac{h}{5z (1 - z) \ 2 (1 - 12z (1 - z)) \ 4^2 (1 - 8z (1 - z)) \ \text{Sset}(s)} \\
& \frac{z \ 2 \ (1 - 2z)}{2 (1 + 2 \ ) (1 - 3 \ ) s^2 z} \text{Wedge}(z; s) - \frac{1 \ z + 2 \ (1 - 2z)}{2 (1 + 2 \ ) (1 - 3 \ ) s (1 - z)} \frac{h}{i} \text{Wedge}(1 - z; s) \\
& \frac{1 \ 2}{(1 - 3 \ ) s z} \text{LPBWedge}(z; s) - \frac{1 \ 2}{(1 - 3 \ ) s (1 - z)} \text{LPBWedge}(1 - z; s) \\
& \frac{s^2}{6 (1 - 3 \ ) (1 + 2 \ ) (1 + 3 \ )} \text{LPBDtri}_2(z; s); \quad (6.44)
\end{aligned}$$

We solve the differential equations (6.34)–(6.42) as Laurent expansions in  $\epsilon$ , beginning with the simplest cases, such as eq. (6.34), which only depends on  $\text{Wedge}(z; s)$  and the previously known integral  $\text{Sset}(s)$ . In a given differential equation (or a coupled pair of equations, in the case of eqs. (6.38) and (6.39)), we start with the most singular terms in the Laurent expansions, and proceed until we reach the order required for the expansion of the splitting amplitudes through  $O(\epsilon^0)$ . This order corresponds to transcendental weight 4, where each  $\ln(x)$  or  $\text{Li}_n(x)$  has weight 1, and  $\text{Li}_n(x)$  and  $\ln(\ln(1))$  have weight  $n$ . We insert into the differential equation an ansatz which is a linear combination of such functions, where  $x$  can be  $z$ ,  $1 - z$ , or  $(1 - z)/z$ . We adjust the coefficients in the

linear combination until the differential equation is satisfied. The constants of integration were determined by different techniques. In some cases the integrals could be performed analytically, at least for one value of  $z$ . It is also possible to evaluate the Schwinger parameter integrals numerically by Monte Carlo integration. To fix the constant, it is often sufficient to check that for a certain limiting value of  $z$ ,  $z = 0$  or  $z = 1$ , an integral remains finite.

We first give the Laurent expansions for the previously known master integrals, which constitute the inhomogeneous terms for the first set of non-trivial differential equations:

$$\begin{aligned} B_{\text{tri}}(s) &= (s)^{-1} \frac{(1+z)^2 (1-z)^2}{(1-2z)} \\ &= \frac{(s)^2}{s^2} - \frac{1}{4} + \frac{2}{2} + \frac{14}{3} z^3 + \frac{21}{4} z^4 + O(z^5); \end{aligned} \quad (6.45)$$

$$\begin{aligned} S_{\text{set}}(s) &= (s)^{-2} \frac{(1+2z)^3 (1-z)^3}{(3-3z)} \\ &= \frac{(s)^2 s}{(1-2z)(1-3z)(2-3z)} \frac{1}{2} - \frac{2}{2} - \frac{16}{3} z^2 - \frac{57}{8} z^3 + O(z^4); \end{aligned} \quad (6.46)$$

$$\begin{aligned} B_{\text{tri}}(s) &= (s)^{-2} \frac{(1-z)^2 (2z)^2 (1-z)^2 (1-2z)}{(2-2z)(2-3z)} \\ &= \frac{(s)^2}{(1-2z)(1-3z)} - \frac{1}{2^2} - \frac{2}{2} + \frac{13}{3} z^3 + \frac{41}{8} z^4 + O(z^5); \end{aligned} \quad (6.47)$$

For the remaining integrals we just give the Laurent expansions, omitting an overall factor of  $\exp(-2z)$ . The  $z$ -independent integral  $\text{Fish}(s)$  can be performed analytically, and the result is

$$\text{Fish}(s) = \frac{(s)^2}{s} - \frac{2}{2^2} + \frac{7}{2} z^3 + \frac{55}{4} z^4 : \quad (6.48)$$

The remaining,  $z$ -dependent Laurent expansions are

$$\begin{aligned} \text{Wedge}(z; s) &= \frac{(s)^2}{s(1-z)} - \frac{1}{2^3} - \frac{2}{2} - \frac{16}{3} z^3 \ln(z) + 2 \text{Li}_3(z) - \frac{1}{z} + \\ &\quad + 4 z^2 \text{Li}_3(z) - \frac{1}{z} + 8 z^3 \text{Li}_4(z) - \frac{1}{z}; \end{aligned} \quad (6.49)$$

$$\begin{aligned} \text{LBtri}(z; s) &= \frac{(s)^2}{s(1-2z)} - \frac{1}{2^3} - \frac{\ln z}{2^2} + \frac{1}{2} \text{Li}_2(\ln z) + \ln^2 z + \frac{1}{2} + \\ &\quad + \text{Li}_3(z) + \frac{1}{2} \text{Li}_3(\ln z) + \\ &\quad + \frac{1}{2} \ln^2 z \ln(\ln z) - \frac{1}{3} \ln^3 z - \frac{3}{2} z \ln z - \frac{16}{3} z^3 + \\ &\quad + \text{Li}_4(z) - \frac{1}{2} \text{Li}_4(\ln z) - \text{Li}_4(z) - \frac{1}{z} \\ &\quad - \frac{2}{2} \text{Li}_2(z) + \ln z \ln(\ln z) - 2 \ln^2 z + \\ &\quad + \frac{1}{8} \ln^4 z - \frac{1}{6} \ln^3 z \ln(\ln z) + \frac{16}{3} z^3 \ln z - \frac{23}{8} z^4; \end{aligned} \quad (6.50)$$

$$\begin{aligned}
W_{\text{edgeF}}(z; s) = & \frac{(\text{ s})^2}{s z} \left( \frac{1}{2^2} \text{Li}_2(1-z) \right)_2 + \\
& + \frac{1}{2} \left( 3 \text{Li}_3(z) + \frac{1}{2} \text{Li}_3(1-z) \right)_3 - 2 \text{Li}_2(1-z) \left( \frac{1}{2} \ln z \right) \\
& - \frac{3}{2} \ln^2 z \ln(1-z) \\
& - 11 \text{Li}_4(z) - \frac{5}{2} \text{Li}_4(1-z) - 3 \text{Li}_4 \left( \frac{1}{z} \right) + \\
& + 4 \ln z \text{Li}_3(1-z) \left( \frac{1}{3} \right) + 2 \text{Li}_3(z) + \\
& + \text{Li}_2(z) \left( \frac{3}{2} \text{Li}_2(z) \right)_2 - 2 \ln^2 z + 3 \ln z \ln(1-z) \\
& - \frac{1}{8} \ln^4 z + \frac{1}{6} \ln^3 z \ln(1-z) + \frac{3}{2} \ln^2 z \ln^2(1-z) \\
& - \frac{3}{2} \left( \frac{1}{2} \ln^2 z + \ln z \ln(1-z) \right) \left( \frac{11}{4} \right)_4 ; \tag{6.51}
\end{aligned}$$

$$\begin{aligned}
Z_{\text{ig}}(z; s) = & \frac{(\text{ s})^2}{s^2 z} \left( \frac{1}{4} \right)_4 + \frac{\ln z}{2^3} \left( \frac{1}{2} \right)_2 \ln^2 z + \frac{7}{2} \left( \frac{1}{2} \right)_2 + \\
& + \frac{1}{3} \left( \frac{1}{3} \right)_3 \ln^3 z + \frac{7}{2} \left( \frac{1}{2} \right)_2 \ln z \left( \frac{7}{3} \right)_3 + \\
& + 6 \text{Li}_4(z) - 6 \text{Li}_4(1-z) - 6 \text{Li}_4 \left( \frac{1}{z} \right) + 6 \text{Li}_3(1-z) \ln z + \\
& + 3 \text{Li}_2(z) \left( \frac{1}{2} \text{Li}_2(z) \right)_2 + \ln z \ln(1-z) + \left( \frac{5}{12} \right) \ln^4 z + \ln^3 z \ln(1-z) + \\
& + \frac{3}{2} \ln^2 z \ln^2(1-z) \left( \frac{13}{2} \right)_2 \ln^2 z - 3 \ln z \ln(1-z) \\
& - \frac{4}{3} \left( \frac{1}{3} \right)_3 \ln z \left( \frac{487}{16} \right)_4 ; \tag{6.52}
\end{aligned}$$

$$\begin{aligned}
P_{\text{tri}}(z; s) = & \frac{(\text{ s})^2}{s^3 z} \left( \frac{1}{4} \right)_2 - 2 \frac{\ln z}{3} + \frac{1}{2} \text{Li}_2(1-z) + 2 \ln^2 z + \frac{3}{2} \left( \frac{1}{2} \right)_2 + \\
& + \frac{1}{8} \left( 8 \text{Li}_3(z) - 3 \ln z \text{Li}_2(z) \right) \\
& - \frac{4}{3} \ln^3 z + \ln^2 z \ln(1-z) - 5 \left( \frac{1}{2} \right)_2 \ln z - \frac{25}{6} \left( \frac{1}{3} \right)_3 \\
& - 14 \text{Li}_4(z) - 8 \text{Li}_4(1-z) - 8 \text{Li}_4 \left( \frac{1}{z} \right) - \text{Li}_3(1-z) \ln z + \\
& + \text{Li}_2(z) \left( \frac{5}{2} \text{Li}_2(z) \right)_2 - 5 \ln z \ln(1-z) + 3 \ln^2 z + 6 \left( \frac{1}{2} \right)_2 + \\
& + \frac{1}{3} \ln^4 z + \frac{2}{3} \ln^3 z \ln(1-z) - \frac{5}{2} \ln^2 z \ln^2(1-z) \\
& + \left( \frac{28}{3} \right)_2 \ln^2 z + 6 \ln z \ln(1-z) + \frac{28}{3} \left( \frac{1}{3} \right)_3 \ln z + \frac{5}{2} \left( \frac{1}{2} \right)_4 ; \tag{6.53}
\end{aligned}$$

$$\begin{aligned}
P\text{tri}_2^{(6)}(z; s) = & \frac{1}{s^2} \left( \frac{1}{z} 4 \text{Li}_4(z) - 3 \text{Li}_4(1-z) - 4 \text{Li}_4 - \frac{1}{z} \right) + \\
& + 4 \text{Li}_3(1-z) - \frac{1}{3} \ln z + \text{Li}_2(z) \text{Li}_2(z) + 2 \ln z \ln(1-z) \\
& - \ln^2 z - \frac{1}{6} \ln^2 z - \frac{2}{3} \ln z \ln(1-z) - \ln^2(1-z) + 2 \text{Li}_2 - 4 \text{Li}_4 + \\
& + \frac{1}{1-z} 6 \text{Li}_4(z) - 2 \ln z \text{Li}_3(z) - \frac{1}{3} + \text{Li}_3(1-z) \ln z + \\
& + \frac{1}{2} \text{Li}_2(z) \text{Li}_2(z) + 2 \ln z \ln(1-z) - 2 \text{Li}_2 + \\
& + \frac{1}{2} \ln^2 z \ln^2(1-z) - \frac{1}{2} \ln z \ln(1-z) - \frac{19}{4} \text{Li}_4 ; \quad (6.54)
\end{aligned}$$

$$\begin{aligned}
\text{LPBW edge}(z; s) = & \frac{(\text{s})^2}{2s(1-z)(1-2)} \left( \frac{1}{3} \frac{\ln(1-z)}{2} + \frac{1}{2} \text{Li}_2(z) + \frac{1}{2} \ln^2(1-z) \right. \\
& + \text{Li}_3(z) + \text{Li}_3(1-z) + \frac{1}{2} \ln z \ln^2(1-z) - \frac{1}{6} \ln^3(1-z) - \frac{35}{3} \text{Li}_3 + \\
& + \text{Li}_4 \left( \frac{1}{z} \right) \text{Li}_2(z) + \ln z \ln(1-z) - \frac{1}{2} \ln^2 z + \\
& + \frac{1}{24} (\ln z - \ln(1-z))^4 + \frac{32}{3} \text{Li}_3 \ln(1-z) - \frac{25}{2} \text{Li}_4 ; \quad (6.55)
\end{aligned}$$

$$\begin{aligned}
\text{LPBD tri}_2^{(6)}(z; s) = & \frac{(\text{s})^2}{2s^2 z(1-z)(1-3)} \left( \frac{1}{2} \ln z \text{Li}_2(z) + \ln(1-z) \text{Li}_2(1-z) + \right. \\
& + \frac{1}{2} \ln z \ln(1-z) \ln z + \ln(1-z) + \\
& + 3 (\ln z + \ln(1-z)) \text{Li}_3(z) + \text{Li}_3(1-z) - \frac{1}{3} \\
& \text{Li}_2(z) \text{Li}_2(1-z) - \frac{1}{2} \ln^2 z \text{Li}_2(z) + \ln^2(1-z) \text{Li}_2(1-z) \\
& \left. - \frac{1}{6} \ln z \ln(1-z) \ln^2 z + \ln^2(1-z) - \frac{9}{2} \ln z \ln(1-z) + 12 \text{Li}_2 \right) ; \quad (6.56)
\end{aligned}$$

$$\begin{aligned}
\text{FD tri}(z; s) = & \frac{(\text{s})^2}{s^3 z^2} \left( \frac{1}{4} - 2 \frac{\ln z}{3} + \frac{1}{2} 3 \text{Li}_3(1-z) + 2 \ln^2 z - \frac{2}{2} \right) + \\
& + \frac{1}{2} 3 \text{Li}_3(z) + 6 \text{Li}_3(1-z) + 3 \ln z \text{Li}_2(z) \\
& - \frac{4}{3} \ln^3 z + \frac{9}{2} \ln^2 z \ln(1-z) - 5 \text{Li}_2 \ln z - \frac{61}{6} \text{Li}_3 + \\
& + 6 \text{Li}_4(z) + 3 \text{Li}_4(1-z) - 9 \text{Li}_4 \left( \frac{1}{z} \right) \\
& - 3 \ln z \text{Li}_3(z) + \text{Li}_3(1-z) +
\end{aligned}$$

$$+ \frac{3}{2} \operatorname{Li}_2(z) \operatorname{Li}_2(z) - \ln^2 z + 2 \ln z \ln(1-z) + \frac{7}{24} \ln^4 z \\ 2 \ln^3 z \ln(1-z) + \frac{3}{2} \ln^2 z \ln^2(1-z) + \frac{2}{2} \ln z^2 + \frac{34}{3} {}_3 \ln z - \frac{41}{4} {}_4 \quad : \quad (6.57)$$

The differential equations (6.34)–(6.42) are valid to all orders in  $\epsilon$ . Whereas eqs. (6.49)–(6.57) only give the solutions through transcendental weight 4, we have obtained the solutions through weight 5, up to integration constants. Beyond weight 4, the ordinary polylogarithms  $\text{Li}_n$  are insufficient to describe the solution space. Instead, one can use the harmonic polylogarithms (HPLs) [86, 20], denoted by  $H(m_w; z)$ . For transcendental weight  $w$  the vector  $m_w$  is a string of  $w$  entries, which (for our application) can only take on the values 0 or  $\pm 1$ . The HPLs obey the differential equations,

$$\frac{d}{dz} H(m_w; z) = f(a; z) H(m_{w-1}; z); \quad (6.58)$$

where  $a = m_w$  is the leftmost component of  $m_w$ ,  $m_{w-1}$  is obtained from  $m_w$  by omitting that component, and

$$f(0; z) = \frac{1}{z}; \quad f(+1; z) = \frac{1}{1-z}; \quad (6.59)$$

These 2<sup>nd</sup> HPLs succeed because the only true singularities in  $z$  on the right-hand side of the differential equations are those given in eq. (6.59). Actually, the differential equations (6.38) and (6.39) for  $P_{\text{tri}}(z; s)$  and  $P_{\text{tri}_2}(z; s)$  contain factors of  $1/(3 - 2z)$  on the right-hand side. However, these factors are artifacts of the change of basis (6.43) from  $P_{\text{tri}_2}(z; s)$  to  $P_{\text{tri}}^{(6)}(z; s)$ .

The 32 HPLs at  $w = 5$  can be written in terms of ordinary logarithms and polylogarithms, plus three more functions. Although a few of the  $z$ -dependent master integrals (W edge, LP BW edge, and LP BD tri<sub>2</sub><sup>(6)</sup>) do not require the three additional functions at the  $w = 5$  level of their expansions, the generic master integral requires all of them.

## 7. Splitting Amplitude Results

With the integrands obtained as described in section 5, and using the integrals obtained in the previous section, we can express the results for the splitting amplitudes in a variety of gauge theories. We will present results for QCD as well for  $N = 4$  and  $N = 1$  super-Yang-Mills theory. For QCD, both the integrands and the combination of master integrals are too lengthy to present here. We will present only the results expanded in  $\epsilon$  through  $O(\epsilon^0)$ .

The corresponding expressions for the  $N = 4$  maximally supersymmetric Yang-Mills (SYM) theory are relatively simple, and we shall present them in detail in section 7.1. We also give the results expanded through  $O(\epsilon^0)$ , which we presented previously [52]. The SYM results also serve as useful building blocks for the splitting amplitudes in  $N = 1$  super-Yang-Mills theory. In section 7.2 we give the  $N = 1$  results in terms of master integrals, and expanded in  $\epsilon$ . The  $N = 1$  results in turn form useful building blocks for representing the QCD results in section 7.3.

In the numerator algebra for the loop momentum polynomials, the dimensionality of the metric appears,

$$D_s \quad 4 \quad 2 \quad R : \quad (7.1)$$

As mentioned in section 2, setting  $R = 1$  defines the HV scheme, which has 2 physical states for external gluons, but 2 physical states for internal gluons. Setting  $R = 0$  defines the FDH scheme, which has 2 physical states for both internal and external gluons, matching the number of fermionic states, and which preserves supersymmetry [8, 69]. We therefore present the splitting amplitude results for supersymmetric theories in the FDH scheme.

The QCD results are given in both the HV and FDH schemes. The CDR scheme is often used in computations of unpolarized cross sections, or amplitude interferences. It has 2 physical states for external as well as internal gluons. The HV-scheme results could be converted to the CDR scheme by including splitting amplitudes for gluons carrying epsilonic helicities. In practice, the CDR results for the scattering amplitude interferences required for unpolarized cross sections agree, through two loops, with the sum over helicities of the HV results, after the infrared singularities are removed using the Catani formula [15, 33]. The tree and one-loop amplitudes in the Catani formula are different in the two schemes, but the finite remainders agree. Thus the collinear limits of the finite remainders in the CDR scheme should be obtainable from the HV-scheme results in section 8.

The results we will present in this section are for bare ("unrenormalized") splitting amplitudes. We will discuss their renormalization in section 8, where we also present a discussion of the collinear behavior of remainders after subtraction of infrared divergences.

## 7.1 $N = 4$ Super-Yang-Mills Theory Results

In super-Yang-Mills theory, scattering amplitudes are heavily constrained by supersymmetry Ward identities (SWI) [91, 92], and this has implications for the splitting amplitudes. First of all, amplitudes with only 0 or 1 negative-helicity gluon vanish at any loop order  $L$  in any supersymmetric theory [91],

$$A_n^{(L); \text{SUSY}} (1^-; 2^+; \dots; n^+) = 0; \quad (7.2)$$

Next consider the color-ordered amplitudes with two negative-helicity gluons,

$$A_n^{(L);SUSY} (1^+; 2^+; \dots; i^-; \dots; j^-; \dots; n^+); \quad (7.3)$$

known as maximally helicity-violating (MHV) amplitudes. In  $M$  SYM, the  $N = 4$  SW imply that eq. (7.3) is completely independent of the cyclic position of  $i$  and  $j$ , up to a trivial overall spinor-product factor of  $h_{ij} h_{ji}^4$  [92]. In  $N = 1$  super-Yang-Mills theory, this relation holds at tree level, but is violated at one loop.

What are the implications for supersymmetric splitting amplitudes? First consider the vanishing amplitude with 1 in eq. (7.2). Let two cyclically-adjacent legs  $a$  and  $b$  become collinear, so that the amplitude factorizes on the MHV amplitudes,

$$\sum_{l=0}^{X^L} \text{Splt}_{+}^{(l); \text{SUSY}}(z; a^+, b^+) = A_n^{(L-l)}(1^-; 2^+; \dots; p^-; \dots; n^+); \quad (7.4)$$

Since the amplitudes  $A_{n=1}^{(L-1)}$  in are nonvanishing, the helicity-ip splitting amplitudes for  $P^+ \rightarrow a^+ b^+$  must vanish to all orders in a supersymmetric theory. Using parity, we have

$$\text{Split}^{(L),\text{SUSY}}(z; a^+; b^+) = 0; \quad (7.5)$$

for all  $L$ . This result includes the tree-level vanishing (2.4), since tree-level n-gluon amplitudes are effectively  $(N = 4)$  supersymmetric.

Due to parity, we need to present results below only for the cases where  $P$  has positive helicity,  $P^+ \rightarrow a^+ b^+$ , which we shall denote by ' $a^+ b^+$ '. Two of these four cases,  $++$  and  $+-$ , are related to each other by exchanging legs  $a$  and  $b$ , which also exchanges  $z \leftrightarrow 1-z$ . As just noted, the  $+-$  case vanishes in any supersymmetric theory. The two independent non-vanishing supersymmetric splitting amplitudes are for  $P^+ \rightarrow a^+ b^+$  ( $++$ ) and  $P^+ \rightarrow a^- b^+$  ( $+-$ ). Since these two tree-level splitting amplitudes are nonzero, we define loop ratios  $r_s^{(L)}$  as in eqs. (2.14) and (2.20), or for  $L$  loops,

$$\text{Split}^{(L)}(a^+; b^+) = r_s^{(L)}(a^+; b^+) \quad \text{Split}^{(0)}(a^+; b^+); \quad (7.6)$$

In  $N = 4$  supersymmetry, the  $++$  and  $+-$  cases are related to each other by the fact that the expression (7.3) divided by  $h_{ij}i^4$  is independent of  $i$  and  $j$ . Thus the collinear limit  $P^+ \rightarrow i^+ (i+1)^+$  is essentially the same as that of  $P^+ \rightarrow 1^+ 2^+$ , up to overall spinor-product factors which are the same as at tree level. In other words, a universal  $r_s$  function describes both cases:

$$r_s^{(L);N=4}(z; s) = r_s^{(L);N=4}(z; s) \quad r_s^{(L);N=4}(z; s); \quad (7.7)$$

Using the Bose symmetry relation (2.9) for  $P^+ \rightarrow a^+ b^+$ , the universal function  $r_s^{(L);N=4}(z; s)$  must be symmetric,

$$r_s^{(L);N=4}(z; s) = r_s^{(L);N=4}(1-z; s); \quad (7.8)$$

This symmetry is not manifest in the one-loop expression (2.17), but it is easily demonstrated using polylogarithm identities.

After carrying out the unitarity-based sewing procedure for  $N = 4$  super-Yang-Mills theory, the integral required for the two-loop  $g^+ g^- \rightarrow gg$  splitting amplitude can be written as the sum of four terms, corresponding to the  $L$ ,  $D$ ,  $L_{PB}$  and  $F$  integral topologies, plus the same four terms with  $z \leftrightarrow 1-z$ :

$$r_s^{(2);N=4}(z; s) = I_A^{N=4}(z) + I_A^{N=4}(1-z); \quad (7.9)$$

where

$$I_A^{N=4}(z) = I_L + I_D + I_{L_{PB}} + I_F; \quad (7.10)$$

and

$$I_L = \frac{s^2}{8} \sum_{D=2}^Z \frac{d^D p}{D=2} \frac{d^D q}{D=2} \frac{sz + (1-z)(p_1^2 - p_2^2) + p_8^2 + \frac{p_2^2(s(1-z) + p_5^2)}{p_9^2}}{p_9^2} \frac{Y^7}{i=1} \frac{1}{p_i^2}; \quad (7.11)$$

$$I_D = \frac{s^2}{8} \sum_{D=2}^Z \frac{d^D p}{D=2} \frac{d^D q}{D=2} \frac{sz + p_5^2}{p_9^2} \frac{Y^7}{i=2} \frac{1}{p_i^2}; \quad (7.12)$$

$$I_{LPB} = \frac{s^2}{8} z (1-z)^Z \frac{d^D p}{D=2} \frac{d^D q}{D=2} p_1^2 \frac{Y^8}{i=2} \frac{1}{p_i^2}; \quad (7.13)$$

$$I_F = \frac{s^2}{8} z^Z \frac{d^D p}{D=2} \frac{d^D q}{D=2} (sz + (1-z)p_1^2) \frac{Y^8}{i=2} \frac{1}{p_i^2}; \quad (7.14)$$

The labeling of the propagators  $p_i^2$  is given in figure 29 and, in the case of the D and F topologies, figure 30. Note that the  $z \neq 1-z$  symmetry (7.8) is manifest in eq. (7.9). The result (7.9) is given in the FDH scheme,  $R = 0$ .

We can see explicitly from these expressions how the appearance of the light-cone propagators is restricted by unitarity. In eq. (7.11), whenever  $p_9^2$  appears in the denominator,  $p_2^2$  appears in the numerator. The appearance of  $p_2^2$  eliminates any two-particle cut (through lines 1 and 2) or any three-particle cut (through lines 2, 3 and 6) entirely to the right of propagator 9, in the terms containing that light-cone denominator. Exactly the same argument (after shifting the L integral over by letting  $k_1 \neq k_2$ ) explains why  $p_1^2$  cannot appear in the denominator of the D integrand in eq. (7.12) along with  $p_9^2$ . Finally, in eqs. (7.13) and (7.14),  $p_1^2$  never appears in the denominator. If it had, there would have been a two particle cut (through lines 1 and 2) entirely to the right of propagator 8, which is again forbidden by unitarity.

The result of reducing eq. (7.10) to master integrals is

$$\begin{aligned}
I_A^{N=4}(z) = & \frac{1}{16} \frac{s}{3} \frac{z}{2z} 4s z (1-z) s P \text{tri}(z; s) + 2(1-2) P \text{tri}_2^{(6)}(z; s) \\
& \frac{2}{3} z (3-z) s Z \text{ig}(z; s) + 3 W \text{edge}_F(z; s) \\
& 2 \frac{1-2}{2} (7-z) L B \text{tri}(z; s) \\
& \frac{4(1-z)(5-3z) W \text{edge}(z; s) - 4z F \text{ish}(s)}{(1-2)(1-3)(2-3)(5-14z) S \text{set}(s)} \\
& \frac{(1-2)(1-3)(16-9z)}{2s^2} B \text{tri}(s) - 2s(3-4z) B \text{tie}(s) + \\
& + 2s \frac{1-2}{2} \frac{h}{s} (1-z) L P B W \text{edge}(z; s) - z L P B W \text{edge}(1-z; s) \\
& 4s^2 z \frac{1}{3} s z F D \text{tri}(z; s) + (1-3)(1-z) L P B D \text{tri}_2^{(6)}(z; s) : \quad (7.15)
\end{aligned}$$

Inserting the Laurent expansions (6.45)–(6.57) into eq. (7.15), and adding the term with  $z \neq 1-z$ , we obtain,

$$\begin{aligned}
r_s^{(2); N=4}(z; s) = & \frac{1}{4} \frac{2}{s} \frac{2}{2} \frac{1}{2^4} - \frac{1}{3} \ln(z) + \ln(1-z) + \frac{1}{2} \ln^2(z) + \ln^2(1-z) + \frac{1}{2} + \\
& + \frac{1}{3} 2 \text{Li}_3(z) + \text{Li}_3(1-z) - \frac{2}{3} \ln^3(z) + \ln^3(1-z) +
\end{aligned}$$

$$\begin{aligned}
& + \ln(z) \ln(1-z) \quad 2_2 \quad \ln(z) + \ln(1-z) \quad \frac{23}{6} \quad 3 \\
& 2 \text{Li}_3(z) + \text{Li}_3(1-z) \quad \frac{17}{6} \quad 3 \quad \ln(z) + \ln(1-z) \quad + \\
& + \frac{1}{3} \ln^4(z) + \ln^4(1-z) \quad \ln(z) \ln(1-z) \quad 2_2 \quad \ln^2(z) + \ln^2(1-z) \\
& \quad ) \\
& 2_2 \ln(z) \ln(1-z) + \frac{7}{8} \quad 4 \quad :
\end{aligned} \tag{7.16}$$

This result can be cast into the suggestive form [52],

$$r_S^{(2);N=4}(z; s) = \frac{1}{2} r_S^{(1);N=4}(z; s)^2 + f(z) r_S^{(1);N=4}(2z; s) + O(z); \tag{7.17}$$

where

$$f(z) = (1-z)(1) = = \frac{1}{2} + \frac{1}{3} + \frac{1}{4}^2 + \dots \tag{7.18}$$

with  $(x) = (dx/dx) \ln(x)$ ,  $(1) = \dots$ . The iterative relation (7.17), along with a similar type of relation for the two-loop, leading-color, four-gluon amplitude in  $N = 4$  super-Yang-Mills theory, has led to an ansatz based on collinear limits for the two-loop, leading-color, n-gluon amplitude in  $N = 4$  super-Yang-Mills theory [52]. At least for the case of maximal helicity violation, we expect the following relation to hold,

$$M_n^{(2)}(z) = \frac{1}{2} M_n^{(1)}(z)^2 + f(z) M_n^{(1)}(2z) - \frac{5}{4} + O(z); \tag{7.19}$$

where  $M_n^{(L)}(z) = A_n^{(L)} = A_n^{(0)}$ .

For  $n = 4$ , we found that eq. (7.19) was violated at order  $^1$  [52]. To be more specific,  $M_4^{(1)}(z)$  contains at  $O(z^1)$  only two types of  $\text{Li}_5$  polylogarithms,  $\text{Li}_5(s=u)$  and  $\text{Li}_5(t=u)$ , whereas  $M_4^{(2)}(z)$  contains in addition the independent function  $\text{Li}_5(s=t)$ . We have now examined the  $z$ -dependence of the order  $^1$  term  $s$  in  $r_S^{(2);N=4}(z; s)$ . Again we find functions not present in the square of the corresponding one-loop quantity. At order  $^1$ ,  $r_S^{(1);N=4}(z; s)^2$  contains  $\text{Li}_5(1-z=z)$ , but no other  $\text{Li}_5$  functions. On the other hand,  $r_S^{(2);N=4}(z; s)$  contains all three  $\text{Li}_5(x)$  functions ( $x = z, 1-z, (1-z)=z$ ) as well as all three additional non- $\text{Li}_5$  functions required (in the basis we used). The violation of eq. (7.19) at  $O(z)$  is consistent with the intuition that conformal symmetry underlies this result, and so it should hold only for  $D = 4$ .

## 7.2 $N = 1$ Super-Yang-Mills Theory Results

For pure  $N = 1$  super-Yang-Mills theory, the ratio  $r_S^{(2);a-b;N=1}(z; s)$  now depends on the helicity configuration. The two independent nonvanishing cases are  $P^+ ! a^+ b^+ (+ +)$  and  $P^+ ! a^- b^+ (+ +)$ . The linear combinations of master integrals obtained are again relatively simple, and may be expressed as,

$$r_S^{(2);a-b;N=1}(z; s) = r_S^{(2);N=4}(z; s) + I_A^{(2);N=1}(z) + I_A^{(2);N=1}(1-z); \tag{7.20}$$

where

$$\begin{aligned} I_A^{++;N=1}(z) = & \frac{3}{8}s \frac{z}{1-z} s \text{Zig}(z;s) + W \text{edgeF}(z;s) - 2W \text{edge}(1-z;s) + \\ & + \text{LBtri}(z;s); \end{aligned} \quad (7.21)$$

and

$$\begin{aligned} r_S^{(2)++;N=1}(z;s) = & r_S^{(2)++;N=1}(z;s) + \\ & + \frac{3}{8}s \frac{2sz}{1-z} P\text{tri}_2^{(6)}(z;s) - P\text{tri}_2^{(6)}(1-z;s) \\ & - \frac{z^2}{1-z} \frac{s}{1-z} s \text{Zig}(z;s) + W \text{edgeF}(z;s) \\ & - (1-z) s \text{Zig}(1-z;s) + W \text{edgeF}(1-z;s) \\ & - \frac{z}{1-z} \text{LBtri}(z;s) + \text{LBtri}(1-z;s) \\ & - \frac{1}{2^2 s^2} \frac{1}{1-z} 2(2-3)S\text{set}(s) + s B\text{tri}(s); \end{aligned} \quad (7.22)$$

These expressions, like the  $N = 4$  results, are evaluated in the FDH scheme with  $D_s = 4$ , or  $R = 0$ .

At one loop, it happens that the splitting amplitude in  $N = 1$  super-Yang-Mills theory is the same for  $++$  as for  $++$ ,

$$r_S^{(1)++;N=1}(z;s) = r_S^{(1)++;N=1}(z;s); \quad (7.23)$$

This relation is spoiled at two loops, but we expect the difference to be finite as  $! 0$ , due to the one-loop relation. A form of eq. (7.22) which makes this property more manifest can be obtained by switching basis from  $\text{Zig}(z;s)$  to

$$\text{Zig}_2^{(6)}(z;s) - L(1;1;1;0;1;2;1;0;0)_{D=6-2}; \quad (7.24)$$

and defining

$$I_B^{N=1}(z;s) = (1-3) \text{Zig}_2^{(6)}(z;s) + \frac{W \text{edgeF}(z;s) + s P\text{tri}_2^{(6)}(z;s)}{1-z}; \quad (7.25)$$

Then

$$r_S^{(2)++;N=1}(z;s) = r_S^{(2)++;N=1}(z;s) + \frac{3}{4}s z I_B^{N=1}(z;s) - I_B^{N=1}(1-z;s); \quad (7.26)$$

The function  $I_B^{N=1}(z;s)$  is finite as  $! 0$ :  $P\text{tri}_2^{(6)}$  is finite, so it gives a vanishing contribution. There are 1= poles which cancel between  $\text{Zig}_2^{(6)}$  and  $W \text{edgeF}$ , yielding

$$I_B^{N=1}(z;s) = \frac{1}{s(1-z)} \frac{h}{2} L_{13}(z) - \frac{3}{3} \ln z L_{12}(z) - \frac{i}{2} + O(); \quad (7.27)$$

The result of performing the expansions in  $\epsilon$  of eqs. (7.20) and (7.26) is,

$$\begin{aligned}
r_s^{(2)++;N=1}(z;s) &= r_s^{(2);N=4}(z;s) + \\
&+ \frac{3}{8} \frac{z^2}{s^2} \left( \frac{1}{2^3} + \frac{1}{2} \ln(z) + \ln(1-z) \right) + \\
&+ \frac{1}{2} \left( \ln(z) \ln(1-z)^2 + 2 \ln(z) \ln(1-z) \right) + \frac{2}{2} \\
&+ 12 \text{Li}_3(z) + \text{Li}_3(1-z) + 2 \ln(z) \text{Li}_2(z) + \ln(1-z) \text{Li}_2(1-z) + \\
&+ \frac{2}{3} \ln^2(z) + \ln^2(1-z) - 4 \ln(z) \ln(1-z) + \frac{3}{2} \left( \ln(z) + \ln(1-z) \right) \\
&- 2 \ln(z) \ln(1-z)^2 + 4 \ln(z) \ln(1-z) + \frac{67}{3} \left( \frac{1}{2^3} + \frac{1}{2} \right); \quad (7.28)
\end{aligned}$$

$$\begin{aligned}
r_s^{(2)++;N=1}(z;s) &= r_s^{(2)++;N=1}(z;s) + \\
&+ \frac{3}{4} \left( 2 \text{Li}_3(1-z) - 3 \ln(1-z) \text{Li}_2(1-z) \right) \\
&- \frac{z}{1-z} \left( 2 \text{Li}_3(z) - 3 \ln(z) \text{Li}_2(z) \right); \quad (7.29)
\end{aligned}$$

### 7.3 QCD Results

We now present the  $g_1^+ gg$  splitting amplitudes in QCD, for a general value of the regularization-scheme parameter  $\epsilon$ . First we introduce some auxiliary functions describing the fermion-loop contributions and residual dependence on  $\epsilon$ .

The functions  $f_L^+$  describing the leading-color fermion-loop contributions to the QCD splitting amplitudes are similar to the differences between the  $N=1$  and  $N=4$  splitting amplitudes, so we write them as

$$\begin{aligned}
f_L^{++}(z;s) &= \frac{2}{9} \left( r_s^{(2)++;N=1}(z;s) - r_s^{(2);N=4}(z;s) \right) + \\
&+ \frac{1}{12} \frac{z^2}{s^2} \left( \frac{1}{2} z(1-z) - \frac{1}{6} \right) + \\
&+ \frac{1}{3} z(1-z) \ln(z) + \ln(1-z) + \frac{2}{3} + \frac{1}{3} \ln(z) + \ln(1-z) - \frac{17}{18} + \\
&+ z(1-z) \frac{1}{2} \ln(z) \ln(1-z)^2 - \frac{11}{3} \ln(z) + \ln(1-z) - \frac{187}{6} + \frac{R}{3} \\
&- \frac{1}{3} \ln(z) \ln(1-z)^2 + \frac{17}{9} z \ln(z) + \frac{8}{9} + z \ln(1-z) \\
&- \frac{2}{6} \frac{151}{54}; \quad (7.30)
\end{aligned}$$

and

$$f_L^{+-}(z;s) = \frac{2}{9} \left( r_s^{(2)++;N=1}(z;s) - r_s^{(2);N=4}(z;s) \right) +$$

$$\begin{aligned}
& + \frac{1}{12} \left( \frac{2}{s} \right)^2 \left( \frac{1}{6^2} + \frac{1}{3} \frac{1}{3} \ln(z) + \ln(1-z) - \frac{17}{18} + \right. \\
& + \frac{z(1+z)}{(1-z)^3} 2 \text{Li}_3(z) - 3 \ln(z) \text{Li}_2(z) - 2 \\
& \left. 2 \frac{z}{(1-z)^2} \text{Li}_2(1-z) - 2 \frac{1}{z} + \frac{\ln(z)}{1-z} \right) \\
& \frac{1}{3} \ln(z) \ln(1-z)^2 + \frac{8}{9} \ln(z) + \ln(1-z) - \frac{2}{6} - \frac{151}{54} : (7.31)
\end{aligned}$$

The functions  $f_{SL}$  describing the subleading-color fermion-loop and  $f_2$  describing the double fermion-loop contributions are very simple:

$$f_{SL}^{++}(z; s) = \frac{1}{8} z(1-z); \quad (7.32)$$

$$f_{SL}^+(z; s) = 0; \quad (7.33)$$

$$f_2^{++}(z; s) = \frac{1}{18} z(1-z) \frac{2}{s}^2 - \frac{1}{3} + \frac{16}{3}; \quad (7.34)$$

$$f_2^+(z; s) = 0; \quad (7.35)$$

There are also some functions describing the residual  $R$  dependence of the QCD results:

$$f_{SL}^{++}(z; s) = f_{SL}^+(z; s) + \frac{1}{12} z(1-z) \frac{2}{s}^2 - \frac{1}{3} \ln(z) \ln(1-z) + \frac{2}{3}; \quad (7.36)$$

$$\begin{aligned}
f_2^+(z; s) = & \frac{1}{24} \left( \frac{2}{s} \right)^2 \left( \frac{1}{2^2} + \frac{1}{3} \ln(z) + \ln(1-z) - \frac{4}{3} \ln(z) \ln(1-z) \right. \\
& \left. + \frac{8}{3} \ln(z) + \ln(1-z) - \frac{2}{2} - \frac{35}{9} \right) : \quad (7.37)
\end{aligned}$$

Then the unrenormalized two-loop QCD splitting amplitude  $r_s$  factors are given for both  $++$  and  $+$  by

$$\begin{aligned}
r_s^{(2);QCD} = & r_s^{(2);N=1} - 1 - \frac{N_f}{N_c} f_L - 1 + \frac{N_f}{N_c^3} f_{SL} - 1 - \frac{N_f^2}{N_c^2} f_2 + R; \\
= & ++ \text{ or } +;
\end{aligned} \quad (7.38)$$

For the helicity- $ip$  case,  $P^+ \rightarrow a \bar{b} ( \dots )$ , we similarly define

$$\begin{aligned}
f_L(z; s) = & \frac{1}{12} \left( \frac{2}{s} \right)^2 \left( \frac{1}{2} - \frac{1}{2} \ln(z) + \ln(1-z) + \frac{2}{3} + \frac{1}{2} \ln(z) \ln(1-z) \right. \\
& \left. - \frac{11}{3} \ln(z) + \ln(1-z) - 2 \frac{\ln(z)}{1-z} + \frac{\ln(1-z)}{z} - \frac{187}{6} + \frac{R}{3} \right) ;
\end{aligned} \quad (7.39)$$

$$f_{SL}(z; s) = \frac{1}{8}; \quad (7.40)$$

$$f_2(z; s) = \frac{1}{18} \frac{z^2}{s^2} \frac{1}{z} + \frac{16}{3} ; \quad (7.41)$$

$$(z; s) = \frac{1}{12} \frac{z^2}{s^2} \frac{1}{z} \ln(z) \ln(1-z) + \frac{2}{3} ; \quad (7.42)$$

Then the helicity- $\pm$  splitting amplitude in QCD is

$$\text{Split}^{(2); QCD}(z; a; b) = \frac{p}{z(1-z)} \frac{\text{habi}}{[ab]^2} \left[ 1 - \frac{N_f}{N_c} f_L \right] \left[ 1 + \frac{N_f}{N_c^3} f_{SL} \right] \left[ 1 - \frac{N_f^2}{N_c^2} f_2 \right] + \dots \quad (7.43)$$

We remark that the functions  $f_{SL}$  and  $f_2$  are so simple because no light-cone projectors on internal propagators are required to compute them. Clearly  $f_2$ , representing the double fermion-loop ( $N_f^2$ ) contribution, has no internal gluon lines, and only the simple master integral  $B_{11}(s)$  can appear. There is an internal gluon line in the graphs contributing to the subleading-color single-fermion loop ( $N_f^1$ ) contribution  $f_{SL}$ . However, this gluon always appears inside the fermion loop. All such graphs contribute with equal weight to  $f_{SL}$ , exactly as if the gluon were a photon. If we think of this gluon as a photon, it becomes clear that its gauge transformations can be separated from those of the on-shell external gluon with momentum  $k_P$ , and indeed, a covariant gauge could have been used for it. Therefore, in this special case we could have used a covariant propagator for the internal gluon, instead of a light-cone gauge propagator, which means that only the  $z$ -independent master integrals given in eqs. (6.45)–(6.47) can appear in  $f_{SL}$ . We have discussed in detail in sections 3 and 4 how unitarity can prevent certain light-cone denominators from ever appearing. The  $f_{SL}$  terms are examples of how color can occasionally do the same sort of thing.

Equations (7.38) and (7.43) give the dependence of the QCD results on  $N_f$  and  $N_c$ . The results can also be written in terms of general group Casimir constants (after multiplying by the extracted factor of  $N_c^2 = C_A^2$ ), using the substitution rules:

$$\begin{aligned} 1 & \rightarrow C_A^2 ; \\ \frac{N_f}{N_c} & \rightarrow 2C_A T_R N_f ; \\ \frac{N_f}{N_c^3} & \rightarrow 2(C_A - 2C_F) T_R N_f ; \\ \frac{N_f^2}{N_c^2} & \rightarrow (2C_A T_R N_f)^2 ; \end{aligned} \quad (7.44)$$

To recover pure  $N = 1$  super-Yang-Mills theory, which contains one Majorana fermion in the adjoint representation, we set  $C_F = C_A$ ,  $T_R = C_A$ , and  $N_f = 1 = 2$ . Thus  $N_f = N_c = 1$  and  $N_f = N_c^3 = 1$ , so that for  $R = 0$  each term in eq. (7.43) vanishes, and all but the first term in eq. (7.38) vanish, as required.

#### 7.4 Continuation to Space-Like Region

The preceding splitting amplitudes are for time-like kinematics,  $k_P^2 = s > 0$ . In the remainder of this section we briefly discuss the space-like case,  $s < 0$ . In the application

of splitting amplitudes to NNLO evolution kernels, the time-like region is relevant for the  $Q^2$  evolution of fragmentation functions. The space-like region is relevant for the evolution of parton distribution functions, which play a key role in the prediction of collider cross sections. (As mentioned in the introduction, the NNLO kernels for unpolarized space-like evolution have been computed very recently [48].)

The time-like results can be continued analytically into the space-like region. We take the space-like splitting process to be

$$(k_1)^{-1} ! (k_P)^{-p} + k_2^2; \quad (7.45)$$

with  $k_P^2 = s < 0$ . It is obtained from the time-like process by crossing leg 1 into the initial state, and leg  $P$  into the final state. The physical helicities of legs 1 and  $P$  flip under this crossing, but we retain the uncrossed labeling. Relative to  $(k_1)$ , the vectors  $(k_P)$  and  $k_2$  now carry longitudinal momentum fractions of  $x$  and  $1-x$  respectively. Comparing the ratio  $(k_1 \cdot n) / (k \cdot n)$  between the time-like and space-like cases, we identify  $z = 1-x$ . In principle, all we need to do to obtain the space-like splitting amplitude results from the above time-like formula is to let  $s$  be negative, and substitute  $z = 1-x$ , where  $0 < x < 1$ . For example, the tree-level splitting amplitude  $\text{Split}^{(0)}(z; a^+; b^+)$  given in eq. (2.5) becomes the space-like splitting amplitude for  $(k_1)^{-1} (k_P)^{-p} + k_2^2$ , which we denote by giving  $\text{Split}^{(0)}$  the argument  $x$ ,

$$\text{Split}^{(0)}(x; a^+; b^+) = p \frac{x}{1-x} \text{ habi} : \quad (7.46)$$

Note that in the construction of the space-like Altarelli-Parisi kernel, after squaring the  $x$ -dependent part of the splitting amplitude there is an additional factor of  $x$ ; see e.g. eq. (6.23) of ref. [74].) There are overall phases stemming from the factors  $\frac{p}{1-z}$  and  $\text{habi}$ , but they can be associated with the external states, and we neglect them in eq. (7.46).

At the loop-level, the preceding formula for  $r_s^{(L)}(z; s)$  have been written so that the logarithms and polylogarithms are manifestly real for  $0 < z < 1$ . To continue them to  $z > 1$ , one can apply polylogarithm identities so that the only function which is not manifestly real is  $\ln(1-z) = \ln(1-x) - \ln x$  i. For example, consider the one-loop splitting amplitudes  $r_s^{(1); N=4}(z; s)$  in eq. (2.17), which contain  $\text{Li}_{2m-1}(\frac{z}{z-1})$ . These functions develop branch cuts for  $z > 1$ . In this case, though, we can use the (non-manifest)  $z \not\in 1-z$  symmetry of  $r_s^{(1); N=4}(z; s)$ , eq. (7.8), to let  $z = 1-z$  in eq. (2.17) before substituting  $z = 1-x$ . (This amounts to using an infinite sequence of polylogarithm identities.) We obtain,

$$r_s^{(1); N=4}(x; s) = \hat{c} - \frac{2}{s} - \frac{1}{2} \left[ (1-x) \right] \frac{x^2}{\sin(\pi)} + \sum_{m=1}^{\infty} 2^{2m-1} \text{Li}_{2m-1}(1-x) : \quad (7.47)$$

In eq. (7.47), the factor  $(s^2 = -s)$  no longer contains any  $i$  terms, as  $s$  is now negative. However, in the expansion of  $[(1-x)]$  we must set  $\ln[(1-x)] = \ln(1-x) - i\pi$ . The presence of imaginary parts in the space-like region is a bit surprising, but it can be

traced back to integrand denominators that vanish in the interior of the integration region for  $z > 1$  | for example, the denominator of  $J^{(b)}(1-z)$  in eq. (3.19), as discussed in section 3.3. The appearance of an imaginary part can be verified from the explicit collinear behavior of one-loop amplitudes. From this verification, one also learns that the sign of the  $i$  term is ambiguous; it depends on whether the leg color-adjacent to leg 2 is incoming or outgoing. Fortunately, this sign is the same for all imaginary terms, and it drops out of the interferences required for the computation of evolution kernels. The  $^2$  factors from the product of two  $i$  terms do survive and are unambiguous. (Note that  $s(1-x)$  has the same negative sign in both space-like and time-like regions, so that the  $^2$  terms from the first term in eq. (7.47) are the same in both regions.)

At the two-loop level, eq. (7.47) and the squaring relation (7.17) provide a convenient way to continue  $r_s^{(2);N=4}(z;s)$  to  $z > 1$  (through  $O(^0)$ ). We refrain from giving the explicit continuations of the  $N = 1$  and QCD results, though they are straightforward to carry out.

## 8. Comparison to Catani's Formula and Finite Remainders

In this section we compare the pole terms in the two-loop splitting amplitudes to the expectation based on Catani's formula [38] for the two-loop infrared divergences of renormalized amplitudes, in order to establish their mutual consistency. More importantly, by examining the order  $^0$  terms in the splitting amplitudes, we derive relations that the finite remainders in the Catani formalism must obey in the collinear limit.

### 8.1 Singular Term Comparison

Catani's general formula includes color-space operators which have a fairly intricate structure in the trace-based color decomposition. In this section, to simplify the analysis we shall restrict attention to the single-trace coefficients  $A_n^{(L)}$  in the  $n$ -gluon amplitude, given explicitly in eq. (2.2), and to the terms in Catani's formula obtained by making the replacement,

$$T_i \cdot T_j = \begin{cases} \frac{N_c}{2} 1; & i, j \text{ color-adjacent,} \\ 0; & \text{otherwise.} \end{cases} \quad (8.1)$$

These terms include all the leading-color terms, as well as certain of the subleading-color terms (including all of the color dependence in  $H_i^{(2)}$  at order  $1=$ ). We refer to these terms as color trivial. In appendix A.4 we perform the full color-space analysis.

First we need to remove the ultraviolet divergences from the splitting amplitudes presented in section 7. The relation between the bare coupling  $s^u$  (implicitly used above) and renormalized coupling  $s(\mu) = g^2(\mu) = (4\pi)^2$ , through two-loop order, may be written as [38]

$$s^u \underset{2}{S} = s(\mu)^2 \underset{1}{1} - \frac{s(\mu)}{2} \underset{b_0}{b_0} + \frac{s(\mu)^2}{2} \underset{b_0^2}{b_0^2} \underset{b_1}{b_1} + O(\underset{3}{s}(\mu)); \quad (8.2)$$

where  $\mu$  is the renormalization scale, and  $S = \exp[-(\ln 4\pi + \gamma_E(1))]$ . The first two coefficients appearing in the beta function for QCD, or more generally  $SU(N_c)$  gauge theory with  $N_f$

avors of massless fundamental representation quarks, are

$$b_0 = \frac{11C_A - 4T_R N_f}{6}; \quad b_1 = \frac{17C_A^2 - (10C_A + 6C_F)T_R N_f}{6}; \quad (8.3)$$

where  $C_A = N_c$ ,  $C_F = (N_c^2 - 1)/(2N_c)$ , and  $T_R = 1=2$ . In pure  $N = 1$  super-Yang-Mills theory, the values are

$$b_0^{N=1} = \frac{3}{2}C_A; \quad b_1^{N=1} = \frac{3}{2}C_A^2; \quad (8.4)$$

In  $N = 4$  super-Yang-Mills theory, a conformal theory, the values are of course

$$b_0^{N=4} = b_1^{N=4} = 0; \quad (8.5)$$

One can define a 'perturbative expansion' of the gluon splitting amplitude as

$$\text{Split}_R(s) = g(s) \text{Split}^{(0)} + \frac{s(s)}{2} \text{Split}_R^{(1)} + \frac{s(s)^2}{2} \text{Split}_R^{(2)} + \mathcal{O}(\frac{3}{s}); \quad (8.6)$$

where  $\text{Split}_R^{(L)}$  is the  $L^{\text{th}}$  loop contribution. Equation (8.2) is equivalent to the following  $\overline{\text{MS}}$  renormalization prescriptions at one and two loops,

$$\text{Split}_R^{(1)} = s^{-1} \text{Split}^{(1)} - \frac{1}{2} \frac{b_0}{N_c} \text{Split}^{(0)}; \quad (8.7)$$

$$\text{Split}_R^{(2)} = s^{-2} \text{Split}^{(2)} - \frac{3}{2} \frac{b_0}{N_c} s^{-1} \text{Split}^{(1)} + \frac{3}{8} \frac{b_0^2}{N_c^2} - \frac{1}{4} \frac{b_1}{N_c^2} \text{Split}^{(0)}; \quad (8.8)$$

Here  $\text{Split}^{(L)}$  governs the collinear limits of unrenormalized amplitudes, while  $\text{Split}_R^{(L)}$  controls the limits of renormalized amplitudes. All quantities appearing in the remainder of this section are renormalized. In particular,  $A_n^{(L)}$  refers to renormalized  $L$ -loop amplitudes, in contrast to the unrenormalized ones used implicitly in previous sections. The renormalization of the splitting ratios  $r_s^{(L)}$  follows simply from eqs. (8.7) and (8.8). We will denote the renormalized splitting ratios by  $\bar{r}_s^{(L)}$ .

The full color-space forms of Catani's formula at one and two loops are given in eqs. (A.15) and (A.38). The color-trivial term  $s$ , defined by the replacements (8.1), are obtained by letting the operator  $I_n^{(L)}$  !  $N_c^L \hat{I}_n^{(L)} 1$ , in its action on the single-trace term  $A_n^{(L)}(1;2;:::;n)$  in the amplitude. The factor of  $N_c^L$  is extracted from  $I_n^{(L)}$  for consistency with the normalization of  $A_n^{(L)}$ ; we want both  $A_n^{(L)}$  and  $\hat{I}_n^{(L)}$  to be independent of  $N_c$  as  $N_c \rightarrow 1$  in the pure-glue case. At one loop, we have

$$\hat{I}_n^{(1)}(s) = \frac{1}{2} \frac{e^{-(1)}}{(1-s)_{i=1}^n} \frac{1}{2} + \frac{g}{N_c} \frac{1}{s_{i;i+1}} - \frac{2}{s_{i;i+1}}; \quad (8.9)$$

where  $g$  is given in eq. (A.17).

Similarly,  $\hat{I}_n^{(2)}$  is given by

$$\begin{aligned} \hat{I}_n^{(2)}(s) = & \frac{1}{2} \hat{I}_n^{(1)}(s) \hat{I}_n^{(1)}(s) + \frac{2}{N_c} b_0 + \frac{e^{-(1)}}{(1-s)_{i=1}^n} \frac{1}{N_c} b_0 + K_{\text{R:s.}} \hat{I}_n^{(1)}(2) + \\ & + \frac{e^{-(1)}}{4} \frac{H_g^{(2)}}{N_c^2} \frac{X^n}{s_{i;i+1}^2}; \end{aligned} \quad (8.10)$$

where  $K_{\text{RS}}$  is given in eq. (A.28) and  $H_g^{(2)}$  is given in eq. (A.33).

The singularities of the single-trace coefficients are,

$$A_n^{(1)} = \hat{I}_n^{(1)} A_n^{(0)} + A_n^{(1)} n ; \quad (8.11)$$

$$A_n^{(2)} = \hat{I}_n^{(1)} A_n^{(1)} + \hat{I}_n^{(2)} A_n^{(0)} + A_n^{(2)} n ; \quad (8.12)$$

Things become a bit simpler if we write the finite remainders in Catani's formula as multiples of the corresponding tree amplitudes:

$$A_n^{(L) n} (1; 2; \dots; n) = F_n^{(L)} (s_{ij}) A_n^{(0)} (1; 2; \dots; n) ; \quad (8.13)$$

Equations (8.11) and (8.12) become

$$A_n^{(1)} = \hat{I}_n^{(1)} + F_n^{(1)} A_n^{(0)} ; \quad (8.14)$$

$$A_n^{(2)} = \hat{I}_n^{(2)} + \hat{I}_n^{(1)} (\hat{I}_n^{(1)} + F_n^{(1)}) + F_n^{(2)} A_n^{(0)} ; \quad (8.15)$$

If the tree amplitude vanishes, we cannot perform this step. However, in this case the entire analysis is much simpler, essentially equivalent to the one-loop analysis.

Now consider the collinear limits. We will provide two independent forms for the pole terms in  $\hat{I}_n^{(2)}$ . The first form is similar to Catani's formula (8.10) for  $\hat{I}_n^{(2)}$ . The second form retains finite terms, so it can be used to predict the collinear behavior of the Catani finite remainders.

In the first derivation, we note that the  $\hat{I}_n^{(2)}$  term by itself does not have particularly enlightening collinear limits, because of contributions coming from  $O(\epsilon)$  parts of  $\hat{I}_n^{(1)}$ . However, this obscure behavior is balanced by similar behavior in the  $\hat{I}_n^{(1)} A_n^{(1)}$  term in eq. (8.15), suggesting that it is best to combine the first two terms in this equation:

$$\begin{aligned} A_n^{(2)} &= \frac{1}{2} \hat{I}_n^{(1)} (\ )^2 + \hat{I}_n^{(1)} (\ ) F_n^{(1)} - \frac{1}{N_c} \frac{b_0}{N_c} \hat{I}_n^{(1)} (\ ) + \\ &+ \frac{e^+}{(1-)} \frac{(1-2)1}{N_c} - \frac{b_0}{N_c} + K_{\text{RS}}: \hat{I}_n^{(1)} (2) + \\ &+ \frac{e}{(1-)} \sum_{i=1}^n \frac{X_i^{(2)}}{N_c^2} - \frac{2}{s_{ij;i+1}} A_n^{(0)} + O(\epsilon^0) \\ &= \frac{1}{2} \hat{I}_n^{(1)} (\ )^2 + F_n^{(1)} - \frac{1}{N_c} \frac{b_0}{N_c} \hat{I}_n^{(1)} (\ ) + F_n^{(1)} + \\ &+ \frac{e^+}{(1-)} \frac{(1-2)1}{N_c} - \frac{b_0}{N_c} + K_{\text{RS}}: \hat{I}_n^{(1)} (2) + F_n^{(1)} + \\ &+ \frac{n}{4} \frac{H_g^{(2)}}{N_c^2} A_n^{(0)} + O(\epsilon^0) : \end{aligned} \quad (8.16)$$

In the last step we added finite pieces, in particular ones proportional to  $F_n^{(1)2}$  and  $K_{\text{RS}}: F_n^{(1)}$ . Two singular terms proportional to  $(1-)^- b_0 F_n^{(1)}$  cancel against each other.

Now the combination  $\hat{I}_n^{(1)} (\ ) + F_n^{(1)}$  is just  $A_n^{(1)} (\ ) = A_n^{(0)}$ , so it has simple collinear limits. Indeed, inserting eq. (2.14) into eq. (2.10), we find that

$$\hat{I}_n^{(1)} (\ ) + F_n^{(1)} \stackrel{a \neq b}{=} \hat{I}_n^{(1)} (1) + F_n^{(1)} + \bar{I}_S^{(1)} (\ ) : \quad (8.17)$$

We use the behavior (8.17) to take the collinear limit of eq. (8.16), and compare the result with eq. (2.19). The terms quadratic and linear in  $\hat{I}_{n-1}^{(1)}( ) + F_{n-1}^{(1)}$  belong to  $A_n^{(2)}$   $\text{Split}^{(0)}$  and  $A_n^{(1)} \text{Split}_R^{(1)}$ . Most of the remaining terms belong to  $A_n^{(0)} \text{Split}_R^{(2)} = A_n^{(0)} \text{Split}^{(0)} \bar{r}_S^{(2)}( )$ . Collecting them, we see that the divergent parts of the two-loop splitting amplitude should be given by

$$\begin{aligned} \bar{r}_S^{(2)}( ) &= \frac{1}{2} (\bar{r}_S^{(1)}( ))^2 - \frac{1}{N_c} \bar{r}_S^{(1)}( ) + \frac{e^+}{(1- )} \frac{(1-2 )}{N_c} \frac{1}{N_c} \frac{b_0}{b_0} + K_{R:\text{s.}} \bar{r}_S^{(1)}(2 ) + \\ &+ \frac{1}{4} \frac{H_g^{(2)}}{N_c^2} + O^{(0)} : \end{aligned} \quad (8.18)$$

In the second derivation of the pole terms in  $\bar{r}_S^{(2)}( )$ , we shall retain the finite terms. Consider first the one-loop case. Equation (8.17) can be rewritten as

$$\bar{r}_S^{(1)} = \frac{h}{\hat{I}_{n-1}^{(1)} + F_{n-1}^{(1)}} \frac{i}{\text{akb}} \hat{I}_{n-1}^{(1)} F_{n-1}^{(1)} ; \quad (8.19)$$

which allows one to predict the singular terms in  $\bar{r}_S^{(1)}$  in terms of the collinear behavior of  $\hat{I}_n^{(1)}$ :

$$\bar{r}_S^{(1)} \Big|_{\text{pole}} = \frac{\hat{I}_n^{(1)}}{\text{akb}} \hat{I}_{n-1}^{(1)} : \quad (8.20)$$

But we can also solve eq. (8.19) for the collinear behavior  $F_{n-1}^{(1)} \Big|_{\text{akb}}$ , using also eq. (8.20). For definiteness, we will assume that  $a = 1$  and  $b = 2$ . We have then

$$F_{n-1}^{(1)} \Big|_{\text{akb}} = F_{n-1}^{(1)} + \frac{(1)}{(z; s_{n-1}; s_{n-3}; s)} ; \quad (8.21)$$

where

$$(1) (z; s_{n-1}; s_{n-3}; s) = \bar{r}_S^{(1)} \Big|_{\text{pole}} \bar{r}_S^{(1)} : \quad (8.22)$$

Note that the Mandelstam invariants involving the gluons which are color-adjacent to  $a = 1$  and  $b = 2$  appear, namely gluons 1 and 3. In evaluating eq. (8.22),  $\bar{r}_S^{(1)} \Big|_{\text{pole}}$  is given by eq. (8.20), including all terms at order  $0$ .

At two loops, the collinear limit as a  $\text{akb}$  of eq. (8.15) is, using eq. (2.19),

$$\begin{aligned} A_n^{(2)} \Big|_{\text{akb}} &= \frac{h}{\hat{I}_n^{(2)} + \hat{I}_n^{(1)} (\hat{I}_{n-1}^{(1)} + F_{n-1}^{(1)}) + F_{n-1}^{(2)} \Big|_{\text{akb}}} \text{Split}^{(0)} A_{n-1}^{(0)} \\ &= \frac{h}{\hat{I}_{n-1}^{(2)} + \hat{I}_{n-1}^{(1)} (\hat{I}_{n-1}^{(1)} + F_{n-1}^{(1)}) + F_{n-1}^{(2)} + \\ &+ \bar{r}_S^{(1)} (\hat{I}_{n-1}^{(1)} + F_{n-1}^{(1)}) + \\ &+ \bar{r}_S^{(2)} \text{Split}^{(0)} A_{n-1}^{(0)} :} \end{aligned} \quad (8.23)$$

Solving eq. (8.23) for  $\bar{r}_S^{(2)}$ , we find

$$\begin{aligned} \bar{r}_S^{(2)} &= \frac{h}{\hat{I}_n^{(2)} + \hat{I}_n^{(1)} (\hat{I}_{n-1}^{(1)} + F_{n-1}^{(1)}) + F_{n-1}^{(2)} \Big|_{\text{akb}}} \frac{i}{\hat{I}_{n-1}^{(2)} - \hat{I}_{n-1}^{(1)} (\hat{I}_{n-1}^{(1)} + F_{n-1}^{(1)}) - F_{n-1}^{(2)} - \bar{r}_S^{(1)} (\hat{I}_{n-1}^{(1)} + F_{n-1}^{(1)}) :} \end{aligned} \quad (8.24)$$

Equation (8.24) contains the one-loop finite remainder  $F_n^{(1)}$  multiplied by a singular factor  $\hat{I}_n^{(1)}$ . However, the pole terms in  $\bar{r}_s^{(2)}$  should not depend on any one-loop finite parts. Therefore we use eq. (8.19) to eliminate the  $\hat{I}_n^{(1)} F_n^{(1)}$  term. After a little algebra, we obtain

$$\bar{r}_s^{(2)} = \frac{h}{\hat{f}_{n-1}^{(2)} + (\bar{r}_s^{(1)} + \hat{f}_{n-1}^{(1)})\hat{f}_n^{(1)} + F_n^{(2)} - F_{n-1}^{(1)}F_n^{(1)}} \quad (8.25)$$

$$\hat{f}_{n-1}^{(2)} = (\bar{r}_s^{(1)} + \hat{f}_{n-1}^{(1)})\hat{f}_{n-1}^{(1)} - F_{n-1}^{(2)} + (F_{n-1}^{(1)})^2; \quad (8.25)$$

Now it is clear that the pole term  $s$  in  $\bar{r}_s^{(2)}$  have a universal form,

$$\bar{r}_s^{(2)} = \frac{h}{\hat{I}_n^{(2)} + (\bar{r}_s^{(1)} + \hat{I}_{n-1}^{(1)})\hat{I}_n^{(1)}} : \quad (8.26)$$

We have checked that the pole terms in this expression are equivalent to those in eq. (8.18) for  $N = 4$  and  $N = 1$  super-Yang-Mills theory, and for QCD. We have also verified that they agree with the singular parts of the  $g^! gg$  splitting amplitudes from our explicit results, eqs. (7.16), (7.28), (7.29), (7.38) and (7.43). Along with the full color-space discussion in appendix A.4, this shows that Catani's formula for the singular behavior of two-loop amplitudes is completely consistent with the collinear limits.

## 8.2 Finite Remainders

The next step is to use the finite parts of the two-loop splitting amplitudes to deduce the collinear limits of the finite remainder  $F_n^{(2)}$  in the color-trivial parts of Catani's formula. Again letting  $a = 1$  and  $b = 2$ , we rearrange eq. (8.24), with the help of eq. (8.26), to get

$$F_n^{(2)}_{1jj2} = F_{n-1}^{(2)} + F_n^{(1)}_{1jj2} - F_{n-1}^{(1)} F_{n-1}^{(1)} + \bar{r}_s^{(2)} \bar{r}_s^{(2)} \text{ pole} \quad (8.27)$$

$$= F_{n-1}^{(2)} + \overline{r}_s^{(1)} \overline{r}_s^{(1)} \underset{\text{pole}}{F_{n-1}^{(1)}} + \overline{r}_s^{(2)} \overline{r}_s^{(2)} \underset{\text{pole}}{F_{n-1}^{(1)}} ; \quad (8.28)$$

or

$$F_n^{(2)}_{1\bar{1}\bar{2}} = F_{n-1}^{(2)} + {}^{(1)}(z; s_{nP}; s_{P3}; s) F_{n-1}^{(1)} + {}^{(2)}(z; s_{nP}; s_{P3}; s); \quad (8.29)$$

where

$${}^{(2)}(z; s_{n_P}; s_{P_3}; s) = \frac{\bar{r}_S^{(2)}}{\bar{r}_S^{(2)} + \frac{1}{\text{pole}}}; \quad (8.30)$$

Here  $\bar{r}_s^{(2)} j$  pole is given by eq. (8.26), including all terms at order  $\epsilon^0$ . Equation (8.29) provides a useful check on finite remainders of two-loop scattering amplitudes, as any two external gluons become collinear.

Now we present the values of  $^{(1)}$  and  $^{(2)}$  for the various theories we have been considering. The values of  $^{(1)}$  are:

$$(1); N = 4 = \frac{1}{2} \ln(1-z) \ln \frac{s_{p3}}{s} + \ln(z) \ln \frac{s_{np}}{s} + \ln(z) \ln(1-z) \quad ; \quad (8.31)$$

$$(1)++;N=1 = (1) +;N=1 = (1);N=4 \frac{b_0^{N=1}}{2N_c} (\ln(z) + \ln(1-z) + \ln(-s)); \quad (8.32)$$

$$(1)++ ; QCD = (1) + ; QCD + \frac{1}{6} \cdot 1 \cdot \frac{N_f}{N_c} z (1 - z); \quad (8.33)$$

$$(1) + ; Q C D = (1); N = 4 \quad \frac{b_0}{2N_c} (\ln(z) + \ln(1-z) + \ln(-s)): \quad (8.34)$$

To get the proper analytic behavior of such expressions, one should apply the prescription (2.13) for logarithms of time-like invariants, after expanding the logarithmic ratios,  $\ln((s_1) = (s_2)) = \ln(s_1) - \ln(s_2)$ .

Next we quote the values of  $^{(2)}$ . For  $N = 4$  super-Yang-Mills theory,  $^{(2)}$  obeys an iterative equation in terms of  $^{(1)}$ , as a consequence of eq. (7.17),

$$^{(2)};N=4 = \frac{1}{2} \frac{h}{2} \frac{^{(1)};N=4}{2} \frac{i_2}{2} \frac{^{(1)};N=4}{2} \frac{11}{32} \frac{4}{4} : \quad (8.35)$$

For  $N = 1$  super-Yang-Mills theory, we first define the auxiliary function

$$\begin{aligned} (z; s_{n_P}; s_{P_3}; s) = & 2(L_{i_3}(z) + L_{i_3}(1-z)) + \frac{1}{2} \ln z L_{i_2}(z) + \ln(1-z) L_{i_2}(1-z) \\ & \frac{1}{2} \ln z \ln(1-z) - \frac{3}{2} \frac{1}{2} (\ln z + \ln(1-z) + \ln(s)) + \frac{85}{24} \frac{3}{3} \\ & \frac{1}{4} \ln z \ln \frac{s_{n_P}}{s} - \ln(s_{n_P}) + 2 \ln(s) + \\ & + \ln(1-z) \ln \frac{s_{P_3}}{s} - \ln(s_{P_3}) + 2 \ln(s) + \\ & + \ln z \ln(1-z) \ln(s_{n_P}) + \ln(s_{P_3}) \ln(s) + \\ & + 2 \ln^2 z \ln \frac{s_{n_P}}{s} + \ln^2(1-z) \ln \frac{s_{P_3}}{s} : \end{aligned} \quad (8.36)$$

Then the two functions required in eq. (8.29) are given by

$$\begin{aligned} (2)++\mathcal{A}N=1 = & (2);N=4 + \frac{b_0^{N=1}}{N_c} + \frac{1}{8} 42 \frac{^{(1)};N=4}{2} + \\ & + 3 \frac{b_0^{N=1}}{N_c} \frac{2h}{2} (\ln z + \ln(1-z) + \ln(s))^2 - \frac{8}{3} \ln z \ln(1-z) + \\ & + \frac{75}{4} \frac{6}{2} (\ln z + \ln(1-z) + \ln(s)) - \frac{40}{3} ; \end{aligned} \quad (8.37)$$

$$\begin{aligned} (2)+\mathcal{A}N=1 = & (2)++\mathcal{A}N=1 + \frac{3}{4} \frac{2}{2} L_{i_3}(1-z) \frac{3}{3} \ln(1-z) L_{i_2}(1-z) \frac{2}{2} \\ & \frac{z}{1-z} \frac{2}{2} L_{i_3}(z) \frac{3}{3} \ln(z) L_{i_2}(z) \frac{2}{2} : \end{aligned} \quad (8.38)$$

Equation (8.38) follows directly from eq. (7.29), because eq. (8.26) for the subtraction term  $\bar{r}_s^{(2)} j$  pole is the same for  $++$  and  $+$ .

For QCD, we define one more auxiliary function,

$$\begin{aligned} QCD = & (2);N=4 + \frac{b_0}{N_c} + \frac{1}{8} 2 \frac{83}{3} + \frac{2}{3} \frac{R}{R} \frac{64 N_f}{9 N_c} + \frac{4 N_f^2}{9 N_c^2} \frac{^{(1)};N=4}{2} + \\ & + 3 \frac{b_0}{N_c} \frac{2h}{2} (\ln z + \ln(1-z) + \ln(s))^2 - \frac{8}{3} \ln z \ln(1-z) + \\ & + \frac{925}{36} + \frac{5}{12} \frac{R}{R} \frac{15 N_f}{2 N_c} + \frac{5 N_f^2}{9 N_c^2} \frac{2}{2} \end{aligned}$$

$$\begin{aligned}
& \frac{34}{3} - \frac{13N_f}{3N_c} + \frac{N_f}{N_c^3} (\ln z + \ln(1-z) + \ln(-s)) \\
& \frac{1169}{81} + \frac{1}{3}^R + \frac{89}{81} \frac{8}{27}^R \frac{N_f}{N_c} : \quad (8.39)
\end{aligned}$$

In term  $s$  of this function, we have

$$\begin{aligned}
(2)_{++}^{\text{QCD}} &= \text{QCD} + z(1-z) \frac{1}{6} 1 \frac{N_f}{N_c} \quad (1); N=4 \\
&\quad + \frac{b_0}{2N_c} (\ln z + \ln(1-z) + 3\ln(-s)) + \frac{445}{36} + \frac{R}{6} \\
&\quad + \frac{1}{8} 1 + \frac{N_f}{N_c^3} + \frac{20}{27} 1 \frac{N_f^2}{N_c^2} + \\
&\quad + \frac{1}{12} 1 \frac{N_f}{N_c} z \ln z + (1-z) \ln(1-z) ; \quad (8.40)
\end{aligned}$$

$$\begin{aligned}
(2)_{+}^{\text{QCD}} &= \text{QCD} - \frac{z}{12} 1 \frac{N_f}{N_c} \frac{12 - 21z + 11z^2}{(1-z)^3} + \frac{9}{1} \frac{N_f}{z N_c} \\
&\quad + 2 \text{Li}_3(z) - 3 \ln z \text{Li}_2(z) - 2 + \\
&\quad + \frac{b_0}{2N_c} 2 \text{Li}_3(1-z) - 3 \ln(1-z) \text{Li}_2(1-z) - 2 + \\
&\quad + \frac{1}{6} 1 \frac{N_f}{N_c} \frac{z}{(1-z)^2} \text{Li}_2(1-z) - 2 - \frac{1}{2} \frac{z \ln z}{1-z} \ln(1-z) : \quad (8.41)
\end{aligned}$$

We can check some  $\lim$  properties of these results as  $z \rightarrow 0$  and  $z \rightarrow 1$ , using simple facts about soft limits of amplitudes. For example, in the  $\lim z \rightarrow 0$ , leg 1 becomes soft. The helicity of the hard leg should be conserved in the soft limit, and the limit should be independent of the helicity of the soft leg. Thus the cases  $P^+ \rightarrow 1^+ 2^+ (++)$  and  $P^+ \rightarrow 1 2^+ (+)$  should behave identically as  $z \rightarrow 0$ . The tree splitting amplitudes (2.5) and (2.7) are the same in this limit (up to an external phase associated with the soft external state). Hence the  $r_s$  factors, and also the Catani-subtracted functions, for  $++$  and  $+$  should behave identically as  $z \rightarrow 0$ . This property is obvious for  $N=4$  super-Yang-Mills theory; the two  $r_s$  factors are identical for all  $z$  due to the  $N=4$  supersymmetry Ward identity. For pure  $N=1$  super-Yang-Mills theory, one can inspect eq. (7.29) or eq. (8.38), recalling that  $\text{Li}_n(1) = 0$ , to see that the quantity in braces indeed vanishes as  $z \rightarrow 0$ . For QCD, the  $r_s^{(2)}$  factors in section 7.3 are not written in a particularly convenient way for checking the limit. However, one can easily compare  $(2)_{++}^{\text{QCD}}$  in eq. (8.40) with  $(2)_{+}^{\text{QCD}}$  in eq. (8.41). They do approach the same limit as  $z \rightarrow 0$ , namely the limit behavior of  $\text{QCD}$ .

For the  $++$  case, the limit  $z \rightarrow 1$  is the same as the limit  $z \rightarrow 0$ . For the  $+$  case, in the limit  $z \rightarrow 1$  the helicity of the hard leg, now leg 1, flips from  $+$  to  $-$ ; hence this splitting amplitude should be suppressed. Equation (2.7) shows that it is suppressed by two powers of  $1-z$  at tree-level. In the  $N=4$  and  $N=1$  supersymmetric cases, there is no additional  $1=(1-z)$  singularity in the  $r_s$  or  $\text{Li}_n$  factors. (There is an apparent  $1=(1-z)$  singularity in the quantity in braces in eqs. (7.29) and (8.38), but again recalling that  $\text{Li}_n(1) = 0$ ,

one sees that it cancels.) So, up to logs, the soft behavior is the same at the loop-level as at tree-level. In the case of QCD, the limiting behavior of  ${}^{(2)} + \mathcal{QCD}$  in eq. (8.41) looks quite singular as  $z \rightarrow 1$ , since powers of  $1/(1-z)^3$  and  $1/(1-z)^2$  appear. However, these cancel, and the actual behavior is

$${}^{(2)} + \mathcal{QCD} \sim \frac{1}{12} \ln \frac{N_f}{N_c} \frac{1}{1-z} + \dots \quad (8.42)$$

Taking into account the  $(1-z)^2$  behavior of the tree-level splitting amplitude, the one power of  $1/(1-z)$  in eq. (8.42) still means that the soft limit  $z \rightarrow 1$  for  $+$  is suppressed by a power of  $1-z$ , relative to that of  $++$ , as expected from the helicity flip on the hard line.

For the term corresponding to the helicity- $\pi$  splitting amplitude,  $P^+ \rightarrow 1 2$ , we should not remove the tree-amplitude factors. Instead we write

$$A_n^{(2) \text{ n}}_{1\bar{1}2} = \text{Split}_R^{(1)}(z; 1\bar{1}2) A_n^{(1) \text{ n}}_{1\bar{1}} + \frac{P}{z(1-z)} \frac{\ln 2i}{[12]^2} {}^{(2)} \mathcal{QCD} A_n^{(0)}_{1\bar{1}}; \quad (8.43)$$

where

$$\begin{aligned} {}^{(2)} \mathcal{QCD} = & \frac{1}{6} \ln \frac{N_f}{N_c} {}^{(1);N=4} + \frac{\ln z}{1-z} + \frac{\ln(1-z)}{z} \\ & \frac{b_0}{2N_c} (\ln z + \ln(1-z) + 3\ln(s)) + \frac{199}{18} + \frac{R}{6} - \frac{5N_f}{9N_c} \\ & \frac{1}{8} \frac{N_c^2 + 1}{N_c^3} N_f : \end{aligned} \quad (8.44)$$

For this helicity configuration, the tree-level splitting amplitude vanishes, so the one-loop renormalization is trivial:  $\text{Split}_R^{(1)}(z; 1\bar{1}2) = \text{Split}^{(1)}(z; 1\bar{1}2)$ . The expectation as  $z \rightarrow 0$  (or equivalently,  $z \rightarrow 1$ ) is that  ${}^{(2)} \mathcal{QCD}$  should have no power-law  $1=z$  singularity, since its prefactor  $P/z(1-z)$  in eq. (8.43) has only one power of  $z$  suppression relative to the  $++$  case. Indeed, in eq. (8.44)  $\ln(1-z)=z$  is finite as  $z \rightarrow 0$ .

Equations (8.21) and (8.29) govern the collinear behavior of finite remainders  $F_n^{(L)}$  for the case where only one intermediate helicity can contribute. If both helicities contribute, one needs to sum over the two, according to eqs. (2.10) and (2.19). Before doing this, it is best to multiply back by the tree amplitudes  $A_n^{(0)}(s)$ , because they are different for the two terms.

## 9. Dressing with Color

In this section we present the full color structure in the collinear limits. We will do this in the context of the trace-based color decomposition discussed in section 2 (and reviewed in refs. [66, 13]). An alternative, color-space language has been used by Catani to predict [38] and describe the infrared structure of two-loop amplitudes. In appendix A we re-express the collinear behavior in the color-space language, in order to demonstrate that the divergent parts of our splitting amplitudes are fully compatible with the structure of

infrared singularities predicted by Catani [38]. The color dressing here applies equally well to renormalized and unrenormalized amplitudes, but in the discussion in appendix A, all quantities are understood to be renormalized.

At tree level the trace-based color decomposition for an  $n$ -gluon amplitude is

$$A_n^{(0)a_1 a_2 \dots a_n} = \sum_{2S_n = Z_n}^X \text{Tr}(T^{a_1} \dots T^{a_n}) A_n^{(0)}(1; \dots; n); \quad (9.1)$$

where the  $A_n^{(0)}$  are tree-level color-ordered partial amplitudes and the notation is defined below eq. (2.2). On the left-hand side we have suppressed the dependence on helicities and momenta but have left the color dependence explicit, since that is what we focus on in this section.

The fully color-dressed tree amplitude has the following factorization property as the momenta of legs 1 and 2 become collinear,

$$A_n^{(0)a_1 a_2 \dots a_n} \stackrel{1k^2}{=} \text{if}^{a_1 a_2 a_p} \text{Split}^{(0)}(z; 1^1; 2^2) A_n^{(0)a_p a_3 \dots a_n}; \quad (9.2)$$

where  $\text{Split}^{(0)}$  is the tree-level splitting amplitude (2.3) defined for the color-ordered amplitude, and there is an implicit sum over the helicity of the intermediate state. Here  $\text{f}^{a_1 a_2 a_p}$  is the  $SU(N_c)$  structure constant corresponding to our normalization of the generators,  $\text{Tr}(T^a T^b) = \epsilon^{ab}$ :

$$f^{a_1 a_2 a_p} = i \text{Tr}(T^{a_1} T^{a_2} T^{a_p}) - \text{Tr}(T^{a_2} T^{a_1} T^{a_p}); \quad (9.3)$$

so that  $f^{abc} = \frac{p}{2} f^{abc}$ , where  $f^{abc}$  is the structure constant with conventional  $T^a$  normalizations.

By inserting eq. (9.1) into both sides of eq. (9.2), and using  $SU(N_c)$  Fierz identities on the right-hand side, we can see that this equation is equivalent to the collinear behavior of color-ordered amplitudes given in eq. (2.3). A given term in the amplitude (9.1) will contribute to the collinear limit only when the collinear legs 1 and 2 are cyclicly adjacent in the associated color trace. Alternatively, we can derive the color structure of eq. (9.2) directly from the fact that the only diagrams contributing to the collinear limit are of the type shown in figure 1, where  $a = 1$  and  $b = 2$ . The factor off  $\text{f}^{a_1 a_2 a_p}$  is precisely the color factor of the vertex joining legs 1;2 and  $P$ .

At one loop the full color decomposition of an  $n$ -gluon amplitude is,

$$A_n^{(1)a_1 a_2 \dots a_n} = \sum_{c=1}^{bn-2x+1} \sum_{2S_n = S_{n;c}}^X G r_{n;c}(1; 2; \dots; n) A_{n;c}(1; 2; \dots; n); \quad (9.4)$$

where  $b_{n;c}$  is the largest integer less than or equal to  $x$ . The leading-color structure factor

$$G r_{n;1}(1; 2; \dots; n) = N_c \text{Tr}(T^{a_1} \dots T^{a_n}); \quad (9.5)$$

is just  $N_c$  times the tree color factor, and the subleading-color structures are given by

$$G r_{n;j}(1; 2; \dots; n) = \text{Tr}(T^{a_1} \dots T^{a_{j-1}}) \text{Tr}(T^{a_j} \dots T^{a_n}); \quad j > 1; \quad (9.6)$$

Again  $S_n$  is the set of all permutations of  $n$  objects, and  $S_{n;c}$  is the subset leaving  $G_{r_{n;c}}$  invariant. In the trace-based color decomposition, fundamental representation quark loops will contribute only to  $A_{n;1}$ , with a relative factor of  $N_f = N_c$  compared to adjoint-representation gluon loops.

At one loop, the subleading-color amplitudes  $A_{n;c}$  are completely determined in terms of the leading-color ones  $A_{n;1}$  (see eq. (7.2) of ref. [10]). The collinear behavior of the leading-color amplitudes was given in eq. (2.10), where the notation  $A_n$  was used instead of  $A_{n;1}$ . The collinear behavior of the subleading-color amplitudes can be determined from the previously-mentioned relation, or from the observation that the two-particle collinear limit cannot reduce a pair of traces to a single trace. Therefore the tree-level ( $n = 1$ )-point amplitude  $A_{n=1}^{(0)}$  cannot enter into the limit. This implies that the one-loop splitting amplitude cannot appear either, and so the limit is (for  $c > 1$ ),

$$\begin{aligned} A_{n;c}^{(1)}(:::; a^a; b^b; :::) &\stackrel{a \neq b}{=} \text{Split}^{(0)}(z; a^a; b^b) A_{n-1;c-1}^{(1)}(:::; P; :::); \quad a; b < c; \\ A_{n;c}^{(1)}(:::; a^a; b^b; :::) &\stackrel{a \neq b}{=} \text{Split}^{(0)}(z; a^a; b^b) A_{n-1;c}^{(1)}(:::; P; :::); \quad a; b < c; \end{aligned} \quad (9.7)$$

Legs  $a$  and  $b$  must be cyclicly adjacent within the same color trace, otherwise the collinear limit is finite. In particular, the collinear limit is finite if the two legs lie in different traces.

We can reassemble these properties of  $A_{n;c}^{(1)}$  into a description of the collinear behavior of the full color-dressed amplitude,

$$\begin{aligned} A_n^{(1)a_1 a_2 a_3 \dots a_n} &\stackrel{1 \neq 2}{=} \text{if } a_1 a_2 a_p \text{ } \text{Split}^{(0)}(z; 1^1; 2^2) A_{n-1}^{(1)a_p a_3 \dots a_n} + \\ &\quad + N_c \text{Split}^{(1)}(z; 1^1; 2^2) A_{n-1}^{(0)a_p a_3 \dots a_n}; \end{aligned} \quad (9.8)$$

where  $\text{Split}^{(1)}(z; 1^1; 2^2)$  are precisely the color-stripped splitting amplitudes (2.15)–(2.17). Note that the  $c > 1$  contributions in eq. (9.7) all go into assembling  $A_{n-1}^{(1)}$  in the first term in brackets. We can also derive eq. (9.8) directly from argumentation using the unitarity sewing rules (or by using light-cone gauge, ignoring prescription issues). The diagrams in figure 2 correspond to a factorization of the process including color indices. The first term in the brackets corresponds to the left diagram, and the second term to the right diagram. The color factor in the first term is precisely the tree-level one. The color factor in the second term is that of a one-loop vertex,  $N_c f^{a_1 a_2 a_p}$  in the pure-glue case. (From the diagrammatic point of view, there are three types of color contributions obtained from color dressing the diagrams in figure 4. However, all these color factors are proportional to  $N_c f^{a_1 a_2 a_p}$ . Including fermions in the loop gives the  $N_f = N_c$  terms in eq. (2.15).)

If we examine the cuts of a color-stripped  $1 \neq 2$  splitting amplitude, each contribution has the product of a  $(j+2)$ -point scattering amplitude on the left and a  $1 \neq j$  lower-loop splitting amplitude on the right, where  $j$  is the number of particles crossing the cut. (See, for example, figure 27.) We can exchange the two final-state particles by reflecting through the horizontal axis. This produces a factor of  $(-1)^{j+2}$  on the left and  $(-1)^{j+1}$  on the right

because of the properties of the amplitudes under reflection [66, 5]. If the two final-state particles are gluons we get the same number of Fermi minus signs on the left and right from interchanging cut internal fermions, if there are any. Overall we always get a factor of 1; that is, the color-stripped splitting amplitude is antisymmetric when we exchange the two arguments, including their helicities and  $z \leftrightarrow 1-z$ . Bose symmetry then implies that the color factor must also be antisymmetric. The color-dressed splitting amplitude must be proportional to  $f^{a_1 a_2 a_p}$ , because there is no other antisymmetric invariant tensor. This argument holds to all loop orders.

Note from eqs. (2.11), (2.15) and (2.16) that there are no subleading-color corrections to the pure-glue ( $N_f = 0$ ) contributions to the one-loop splitting amplitude  $\text{Split}^{(1)}$ , which appears in the full-color collinear limit (9.8). To understand this fact, and the factor of  $N_c$  in front of the splitting amplitude, consider the color factors in a diagrammatic calculation. One can use the Jacobi identity to show that the result of the color algebra in any diagram is a linear combination of the results for its various possible parent diagrams. It is therefore sufficient to consider the parent diagrams. At one loop, for pure-glue contributions, there is only one kind of parent diagram, the triangle diagram shown in figure 4(a). Now, as far as the color algebra is concerned, any triangle subdiagram can be replaced by a factor of  $\frac{1}{2}C_A$  times a three-point color vertex. Similarly, any bubble subdiagram can be replaced by a factor of  $C_A$ . Thus at one loop we just obtain an overall coefficient of  $C_A = N_c$ , up to  $N_c$ -independent factors.

Now we turn to the two-loop case. The color decomposition generalizes in an obvious way,

$$A_n^{(2) a_1 a_2 \dots a_n} = \sum_{\substack{b_1 = 3c+1 \\ b_2 = 2c+1 \\ \dots \\ b_n = 2c+1}} \frac{G_{r_n; c_1; c_2} (1; 2; \dots; n)}{2 S_n = S_{n; c_1; c_2}} A_{n; c_1; c_2} (1; 2; \dots; n); \quad (9.9)$$

where

$$G_{r_n; c_1; c_2} (1; 2; \dots; n) = \text{Tr}(T^{a_1} \dots T^{a_{c_1-1}}) \text{Tr}(T^{a_{c_1}} \dots T^{a_{c_2-1}}) \text{Tr}(T^{a_{c_2}} \dots T^{a_n}); \quad (9.10)$$

and  $r_n$  runs over the set of permutations  $S_n$ , modulo those in  $S_{n; c_1; c_2}$  which leave  $G_{r_n; c_1; c_2}$  invariant. We identify  $\text{Tr}(1) = N_c$  so, for example,

$$G_{r_n; 1; 1} (1; 2; \dots; n) = N_c^2 \text{Tr}(T^{a_1} \dots T^{a_n}); \quad (9.11)$$

$$G_{r_n; 1; j} (1; 2; \dots; n) = N_c \text{Tr}(T^{a_1} \dots T^{a_{j-1}}) \text{Tr}(T^{a_j} \dots T^{a_n}); \quad j > 1; \quad (9.12)$$

The color-ordered amplitudes contain terms which depend on the number of quark flavors, for example, with factors  $N_f = N_c$  and  $(N_f = N_c)^2$ . In addition, at two loops  $A_{n; 1; 1}$  also contains terms of order  $1 = N_c^2$  arising from both planar and non-planar diagrams. In contrast, while the two-loop gluon splitting amplitude does contain contributions of  $O(N_f = N_c)$ ,  $O(N_f^2 = N_c^2)$ , and  $O(N_f^3 = N_c^3)$ , as we shall see below, it contains no contributions of  $O(1 = N_c^2)$ .

The collinear behavior of the leading-color amplitudes  $A_{n; 1; 1}$  was given in eq. (2.19), where the notation  $A_n$  was used instead of  $A_{n; 1; 1}'$ . At two loops the subleading-color

amplitudes cannot be determined solely from the leading-color ones. However, just as at one loop, consideration of the trace structure leads to the following collinear limits for the subleading-color amplitudes. The double-trace partial amplitudes behave as,

$$\begin{aligned}
A_{n;1;c}^{(2)}(\dots; a^a; b^b; \dots) &\stackrel{akb}{\underset{X}{\sim}} \text{Split}^{(0)}(z; a^a; b^b) A_{n-1;1;c-1}^{(2)}(\dots; P; \dots) + \\
&+ \text{Split}^{(1)}(z; a^a; b^b) A_{n-1;c-1}^{(1)}(\dots; P; \dots) ; \quad a;b < c; \\
A_{n;1;c}^{(2)}(\dots; a^a; b^b; \dots) &\stackrel{akb}{\underset{X}{\sim}} \text{Split}^{(0)}(z; a^a; b^b) A_{n-1;1;c}^{(2)}(\dots; P; \dots) + \\
&+ \text{Split}^{(1)}(z; a^a; b^b) A_{n-1;c}^{(1)}(\dots; P; \dots) ; \quad a;b < c;
\end{aligned} \tag{9.13}$$

while the triple-trace partial amplitudes behave as,

$$\begin{aligned}
A_{n;c_1;c_2}^{(2)}(\dots; a^a; b^b; \dots) &\stackrel{akb}{\underset{X}{\sim}} \text{Split}^{(0)}(z; a^a; b^b) A_{n-1;c_1-1;c_2-1}^{(2)}(\dots; P; \dots) ; \quad a;b < c_1; \\
A_{n;c_1;c_2}^{(2)}(\dots; a^a; b^b; \dots) &\stackrel{akb}{\underset{X}{\sim}} \text{Split}^{(0)}(z; a^a; b^b) A_{n-1;c_1;c_2-1}^{(2)}(\dots; P; \dots) ; \quad c_1 < a;b < c_2; \\
A_{n;c_1;c_2}^{(2)}(\dots; a^a; b^b; \dots) &\stackrel{akb}{\underset{X}{\sim}} \text{Split}^{(0)}(z; a^a; b^b) A_{n-1;c_1;c_2}^{(2)}(\dots; P; \dots) ; \quad a;b < c_2;
\end{aligned} \tag{9.14}$$

As at one loop, legs  $a$  and  $b$  must be cyclically adjacent within the same color trace, otherwise the collinear limit is finite.

At two loops, the generalization of the splitting amplitude from the leading-color structure to the fully color-dressed version would seem to be more complicated, because of the appearance of non-planar contributions, such as the ones depicted in figure 28. However, as already mentioned in section 5, all such non-planar contributions vanish for the  $g! gg$  case. The fully color-dressed splitting behavior is given simply in terms of the color-stripped splitting amplitudes of section 7 as,

$$A_n^{(2)a_1a_2a_3\dots a_n} \stackrel{1k^2}{\underset{N_c^1}{\sim}} \text{if}^{a_1a_2a_p} \underset{=0}{\stackrel{X^2}{\sim}} N_c^1 \text{Split}^{(1)}(z; 1^{-1}; 2^{-2}) A_{n-1}^{(2-1)a_p a_3 \dots a_n} : \tag{9.15}$$

The proportionality of the color dressing to  $f^{a_1a_2a_p}$  follows from the diagrammatic argument given after eq. (9.8), generalized to two loops. To see why the pure-glue contributions to the splitting amplitude just have an overall factor of  $N_c^2$  in front (as evidenced by eqs. (7.38) and (7.43)), consider again the parent diagrams. We have already seen in section 5 that the non-planar diagrams do not contribute at two loops to the splitting

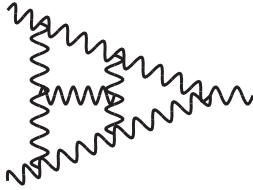


Figure 32: A diagram contributing to the three-loop  $g ! gg$  splitting amplitude which has subleading-color,  $1=N_c^2$  suppressed terms in its color factor.

amplitude to gluons, so we focus on the planar diagrams. At two loops there are four kinds of planar parent diagrams. Each of these has either a bubble or triangle subdiagram (the two parents with triangle subdiagrams are shown in Figure 29). Upon replacing the subdiagram factor of  $C_A$  or  $\frac{1}{2}C_A$  times a vertex, respectively, we are left with a triangle diagram, which generates a second factor of  $C_A$ , as at one loop. All pure-glue contributions are therefore homogeneous in  $N_c$  of degree two. This latter argument does not extend to higher loops. Beginning at three loops there are pure-glue diagrams, both planar and non-planar, which have no surviving triangle or bubble subdiagrams at some stage of this reduction. The simplest example is depicted in Figure 32. Such diagrams generally give rise to  $1=N_c^2$  suppressed terms. They correspond to the existence of other  $SU(N_c)$  group invariants, such as  $(d^{abc})^2$ , where  $d^{abc}$  is the fully symmetrized trace of three generator matrices, which are not homogeneous in  $N_c$ . Of course, the fermion-loop terms in the  $g ! gg$  splitting amplitudes have  $1=N_c^2$  suppressed contributions already at two loops, due to the existence of both  $C_A$  and  $C_F$  Casimir invariants.

## 10. Conclusions and Outlook

In this paper, we computed the behavior of a general two-loop amplitude in massless gauge theory as the momenta of two external gluons become collinear. (The behavior involving collinear fermions will be presented elsewhere [58].) This behavior is universal, and accordingly governed by a set of  $1 ! 2$  splitting amplitudes. For the  $g ! gg$  splitting there are three independent helicity configurations (the remainder are related by symmetry or parity). One of these configurations vanishes at tree level. In an  $N=4$  supersymmetric theory, the ratio of a non-vanishing two-loop splitting amplitude to the corresponding tree-level amplitude is helicity-independent, and given by eq. (7.16). In pure  $N=1$  super-Yang-Mills theory, the helicity configuration that vanishes at tree level also vanishes to all orders in perturbation theory. The ratios for the other two cases are given by eqs. (7.28) and (7.29). In QCD, all three helicity amplitudes are non-vanishing; the ratios to the tree for two of them are given by eq. (7.38), and the splitting amplitude for the remaining configuration by eq. (7.43). The finite remainders of amplitudes, after subtraction of poles predicted by Catani's formula, also have simple behavior in collinear limits in the color-trivial case. These limits are given at one and two loops by eqs. (8.21) and (8.29), respectively. The functions entering these limits are given by eqs. (8.31)–(8.34), (8.35), (8.37), (8.38), and (8.40)–(8.44).

These splitting amplitudes can be used as a check on calculations of higher-point two-loop QCD amplitudes; the collinear limits of these amplitudes must satisfy eqs. (7.38) and (7.43). One can also apply the checks to the finite terms after subtraction of the poles predicted by Catani's formula, using eq. (8.29). As mentioned previously, the compatibility of the divergent parts of our splitting amplitudes with Catani's formula provides an inductive proof of the latter, modulo some assumptions about the analytic behavior of the -singular terms in amplitudes.

The two-loop splitting amplitudes are also one of the ingredients required for computing the NNLO corrections to the Altarelli-Parisi kernel in an infrared approach. At NLO, one would add two terms [43]: the one-loop  $1! \cdot 2$  splitting amplitude interfered with its tree counterpart; and the tree-level  $1! \cdot 3$  splitting amplitude squared, integrated over the phase space of the unobserved partons. At NNLO, there are three ingredients: (a) the  $1! \cdot 2$  splitting amplitude computed here, interfered with its tree counterpart; (b) the interference of the one-loop [64] and tree-level [40, 41]  $1! \cdot 3$  splitting amplitudes, integrated over the unobserved phase space; and (c) the  $1! \cdot 4$  splitting amplitude squared [63], integrated over the four-particle unobserved phase space.

In  $N = 4$  supersymmetric gauge theories, the splitting amplitude has a remarkable property: it can be written as a polynomial in the one-loop and tree-level splitting amplitudes. This led to the conjecture that a similar property holds for two-loop amplitudes [52]. Explicit calculations showed that this conjecture is true for the four-point amplitude. This simplicity suggests that substantial parts of the theory may be solvable.

We performed this computation using the unitarity-based sewing method. The method has demonstrated many advantages over conventional diagrammatic techniques over the years. It has made possible, for example, the computation of series of amplitudes for arbitrarily many partons [10, 11]. The present computation demonstrates another advantage: it offers a pathway featuring the physical-projection advantages of light-cone gauge, while avoiding the need for cumbersome prescriptions for dealing with the ill-defined integrals of the latter. Because it effectively combines many diagrams at an early stage of the calculation, it also simplifies integrands considerably, and so minimizes the complexity of reducing loop integrals to master integrals.

## Acknowledgments

We thank Babis Anastasiou for key contributions at an early stage of this work. We also thank Thomas Gehrmann, Zoltan Kunszt and Marc Schreiber for helpful comments. L.D. thanks Cambridge University for hospitality when this work was begun, and we all thank the Kavli Institute for Theoretical Physics for its generous hospitality during completion of this paper. This research was supported in part by the National Science Foundation under Grant No. PHY-99-0794.

## A. Color-Space Collinear Limit of Catani's Formula

In section 8 we demonstrated the consistency of the divergent part of the splitting amplitudes with Catani's formula. This section provides a more detailed derivation of the color-space collinear limit of the splitting amplitudes, and shows that the divergent parts of the splitting amplitudes are consistent with Catani's formula.

tudes with the Catani formula at leading order in  $N_c$ , or more generally, for the color-trivial single-trace terms in the formula. In this appendix we demonstrate that the consistency also holds for the terms containing non-trivial color correlations. Because of these correlations, the collinear limits of the full Catani formula are a bit intricate. In this appendix, all quantities are understood to be renormalized.

### A.1 Color-Space Notation

In the color-space language of refs. [38, 93] an amplitude is expressed in terms of an abstract vector in color space,  $\mathbb{A}_n^{(L)} i$ . To convert to the more standard color notation one may use an orthogonal basis of unit vectors  $\mathbb{a}_1; a_2; \dots; a_n$  with the property that

$$\mathbb{A}_n^{(L)a_1 a_2 \dots a_n} (k_1; 1; k_2; 2; \dots; k_n; n) = a_1; a_2; \dots; a_n \mathbb{A}_n^{(L)} i; \quad (A.1)$$

Color interactions are represented by associating a color charge  $T_i$  with the emission of a gluon from each parton  $i$ . The color charge  $T_i = f T_R^a g$  is a vector with respect to the generator label  $a$ , and an  $SU(N_c)$  color matrix in the representation  $R$  of the outgoing parton  $i$ . For external gluons,  $R$  is the adjoint representation  $A$ , and  $T_{A,ab}^a = if^{cab}$ . (Note that the normalization of fundamental representation charge matrices is different in ref. [38] from that used elsewhere in the paper. In this appendix we normalize the  $T_i$  according to ref. [38].)

In this notation each vector  $\mathbb{A}_n i$  is a color singlet, so color conservation is simply

$$\sum_{i=1}^{N_c} T_i \mathbb{A}_n i = 0; \quad (A.2)$$

independent of the color representation of each leg. This identity incorporates the Jacobi identity and its generalizations very simply. Typical operators encountered in the discussion involve the combination

$$(T_i)^a (T_j)^a = T_i \cdot T_j; \quad (A.3)$$

For  $i = j$ , eq. (A.3) reduces to a Casimir operator,  $T_i^2 = C_i = C_A = N_c$  if leg  $i$  is a gluon, and  $T_i^2 = C_i = C_F = (N_c^2 - 1)/(2N_c)$  if leg  $i$  is a quark or anti-quark (with  $T_R = 1=2$ ). A useful property is

$$T_i \cdot T_j = T_j \cdot T_i; \quad (A.4)$$

which holds because charge matrices act on different index spaces.

In the collinear limit where  $k_1 \parallel z k_P$ ,  $k_2 \parallel (1-z) k_P$ , a tree-level color-space amplitude satisfies

$$\mathbb{A}_n^{(0)} i = \sum_{P} \text{Split}^{(0)} \mathbb{A}_{n-1}^{(0)} ( ) i; \quad (A.5)$$

where  $P$  denotes the helicity of  $P$  and the splitting functions  $\text{Split}^{(0)}$  are now operators acting on the color space. The operator  $\text{Split}^{(0)}$  links the color space with  $n-1$  legs to that of  $n$  legs. That is, we define

$$\begin{aligned} & a_1; a_2; a_3; \dots; a_n \text{Split}^{(0)} \mathbb{A}_{n-1}^{(1)} ( ) i \\ & = \text{if}^{a_1 a_2 a_P} \text{Split}^{(0)} \mathbb{A}_{n-1}^{(0) a_P a_3 \dots a_n} (k_P; ; k_3; ; \dots; k_n; n); \end{aligned} \quad (A.6)$$

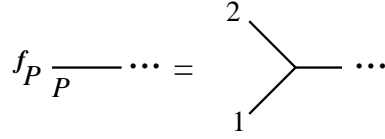


Figure 33: The action of  $f_P$  on the color index of leg  $P$  of an amplitude. The vertex represents a factor of  $if^{a_1 a_2 a_P}$ .

where  $\text{Split}^{(0)}$  is the color-ordered splitting function defined in eq. (2.3). We define an operator

$$\text{Split}^{(0)} = f_P \text{Split}^{(0)}; \quad (\text{A.7})$$

where for the pure-glue case we have

$$h_{a_1; a_2; a_3; \dots; a_n} f_P j_P; a_3; \dots; a_n i = if^{a_1 a_2 a_P}; \quad (\text{A.8})$$

The operator  $f_P$  is distinct from the operator  $T_P$  because it links color spaces of different dimensions. The action of the operator  $f_P$  on an amplitude is illustrated in figure 33.

Color conservation on the three-vertex implies that

$$f_P T_P = (T_1 + T_2) f_P; \quad (\text{A.9})$$

which is a special case of eq. (A.2) (up to a sign due to a swap of incoming and outgoing indices). This equation is equivalent to the Jacobi identity.

From eq. (9.8), it is apparent that the behavior of the one-loop amplitude in color space in the collinear limit is very similar to that of the tree amplitude,

$$\begin{array}{ccc} \mathcal{A}_n^{(1)} i ! & \xrightarrow{X} & \text{Split}^{(0)} \mathcal{A}_{n-1}^{(1)} ( ) i + \\ = & & = \\ & & \text{Split}^{(1)} \mathcal{A}_{n-1}^{(0)} ( ) i; \end{array} \quad (\text{A.10})$$

where

$$\text{Split}^{(1)} (1^1; 2^2) = N_c \text{Split}^{(1)} (1^1; 2^2) f_P; \quad (\text{A.11})$$

with  $\text{Split}^{(1)}$  the color-stripped splitting amplitude. For helicity contributions where the tree splitting amplitude does not vanish, it is convenient to re-express this as

$$\text{Split}^{(1)} (1^1; 2^2) = N_c \bar{r}_S^{(1); 1^2} (z; s) \text{Split}^{(0)} (1^1; 2^2); \quad (\text{A.12})$$

where  $\bar{r}_S^{(1)}$  is given as  $r_S^{(1)}$  in eqs. (2.15)–(2.17), and is renormalized according to eq. (8.7).

The  $L$ -loop generalization is the obvious one,

$$\begin{array}{ccc} \mathcal{A}_n^{(L)} i ! & \xrightarrow{X} & \text{Split}^{(1)} \mathcal{A}_{n-1}^{(L-1)} ( ) i; \\ \xrightarrow{L=0} & & = \end{array} \quad (\text{A.13})$$

where

$$\text{Split}^{(L)} = N_c^L \text{Split}^{(L)} f_P; \quad (\text{A.14})$$

In the two-loop case,  $\text{Split}^{(2)}$  is the color-trivial splitting amplitude defined in eq. (2.19).

Next we shall demonstrate that the full color-space dependence of Catani's formula for the divergences of one- and two-loop amplitudes is completely compatible with the divergent parts of our color-dressed splitting amplitudes.

## A.2 One-Loop Warm Up

At one loop, the infrared divergences of renormalized  $n$ -point amplitudes can be written compactly in color-space notation as [38],

$$\mathcal{A}_n^{(1)} i_{\text{R:s:}} = I_n^{(1)}( ) \mathcal{A}_n^{(0)} i_{\text{R:s:}} + \mathcal{A}_n^{(1)} n i_{\text{R:s:}} : \quad (\text{A.15})$$

The color operator  $I_n^{(1)}$  is

$$I_n^{(1)}( ) = \frac{1}{2} \frac{e}{(1)} \sum_{i=1}^{(1)} \sum_{j \neq i} X^n T_i T_j \frac{1}{2} + \frac{i}{T_i^2} \frac{1}{-} \frac{2}{s_{ij}} : \quad (\text{A.16})$$

The sum runs over pairs of external legs. For external gluons  $i$ , we set  $T_i$  equal to

$$g = \frac{11C_A}{6} \frac{4T_R N_f}{6} : \quad (\text{A.17})$$

(For external fermions, the ratio  $q=T_i^2 = 3=2$  is independent of the representation.) The subscript  $\text{R:s:}$  indicates that a quantity depends on the regularization and renormalization scheme.

Now consider the limit of the  $I_n^{(1)}$  operator as the momenta of legs 1 and 2 become collinear. Inserting the decomposition of the amplitude into divergent and finite parts, eq. (A.15), into both sides of eq. (A.10) and taking the collinear limit, we find that the divergent parts must satisfy

$$I_n^{(1)}( ) \text{Split}^{(0)} \mathcal{A}_{n-1}^{(0)}( ) i_{\text{R:s:}} = \text{Split}^{(1)} \mathcal{A}_{n-1}^{(0)}( ) i_{\text{R:s:}} + \text{Split}^{(0)} I_{n-1}^{(1)}( ) \mathcal{A}_{n-1}^{(0)}( ) i_{\text{R:s:}} + \text{finite}; \quad (\text{A.18})$$

where collinear kinematics are implicit. On the left-hand side of the equation  $I_n^{(1)}( )$  acts on an  $n$ -dimensional color space, while on the right-hand side  $I_{n-1}^{(1)}( )$  acts on an  $(n-1)$ -dimensional color space. A compact way to write the same equation is

$$\text{Split}^{(1)} = I_n^{(1)}( ) \text{Split}^{(0)} \text{Split}^{(0)} I_{n-1}^{(1)}( ) + \text{finite} : \quad (\text{A.19})$$

To make this more explicit, consider an  $n$ -gluon amplitude, for simplicity. Inserting the explicit forms of the operators, we have that the infrared-divergent parts of the renormalized one-loop splitting amplitude must be

$$\begin{aligned} \text{Split}^{(1)} &= \frac{e}{(1)} \frac{1}{2} + \frac{g}{C_A} \frac{1}{-} \\ &\quad \left( \sum_{j=3}^{(1)} X^n T_1 T_j \frac{2}{z s_{Pj}} + \sum_{j=3}^{(1)} X^n T_2 T_j \frac{2}{(1-z) s_{Pj}} \right. \\ &\quad \left. + T_1 T_2 \frac{2}{s_{12}} + \frac{1}{2} \sum_{i \neq j=3} X^n T_i T_j \frac{2}{s_{ij}} \text{Split}^{(0)} \right. \\ &\quad \left. + \sum_{j=3}^{(1)} X^n T_P T_j \frac{2}{s_{Pj}} + \frac{1}{2} \sum_{i \neq j=3} X^n T_i T_j \frac{2}{s_{ij}} \right) \\ &\quad + \text{finite}; \end{aligned} \quad (\text{A.20})$$

where we have separated the term  $s$  into those involving the collinear legs and those not involving them. The term  $s$  that do not involve the collinear legs simply cancel, since  $\text{Split}^{(0)}$  commutes with any  $T_j$  where  $j > 3$ . After separating term  $s$  that involve  $s_{p,j}$  from those that do not (allowing for shifts in the finite terms), we find,

$$\begin{aligned} \text{Split}^{(1)} = & \frac{e^{(1)}}{(1)} \frac{1}{2} + \frac{g}{C_A} \frac{1}{2} \ln z \sum_{j=3}^{X^n} T_1 T_j + \ln(1-z) \sum_{j=3}^{X^n} T_2 T_j + \\ & + T_1 T_2 \frac{2}{s_{12}} \text{Split}^{(0)} + \\ & + \sum_{j=3}^{X^n} (T_1 + T_2) T_j \text{Split}^{(0)} \text{Split}^{(0)} T_p T_j \frac{2}{s_{p,j}} \\ & + \text{finite:} \end{aligned} \quad (A 21)$$

In the above, we have been careful in the placement of  $\text{Split}^{(0)}$  since it links  $(n-1)$ -point color space to  $n$ -point color space. To simplify eq. (A 21) we use eq. (A 9). Furthermore, using color conservation, eq. (A 2), we have

$$\begin{aligned} \sum_{j=3}^{X^n} T_1 T_j \text{Split}^{(0)} &= T_1 (T_1 + T_2) \text{Split}^{(0)} \\ &= \frac{1}{2} (T_1 + T_2)^2 + T_1^2 T_2^2 \text{Split}^{(0)} \\ &= \frac{1}{2} C_A \text{Split}^{(0)}; \end{aligned} \quad (A 22)$$

with a similar equation with leg 1 replaced by 2. Also,  $T_1 T_2 \frac{1}{2} ((T_1 + T_2)^2 - T_1^2 - T_2^2) = \frac{1}{2} C_A$ . Inserting these relations into the divergent parts of the renormalized splitting amplitude gives us

$$\begin{aligned} \text{Split}^{(1)} = & C_A \frac{1}{2} \frac{e^{(1)}}{(1)} \frac{1}{2} + \frac{g}{C_A} \frac{1}{2} \frac{2}{z(1-z)s_{12}} \text{Split}^{(0)} + \\ & + \text{finite:} \end{aligned} \quad (A 23)$$

This result is in complete agreement with the divergent parts of the one-loop color-space splitting amplitude, as given in eqs. (2.14) and (A 12), after renormalization according to eq. (8.7). (Renormalization produces the term proportional to  $g = b_0$  in eq. (A 23).) A similar analysis using mixed quark-gluon amplitudes yields the same result for the  $g \rightarrow gg$  splitting amplitudes. This demonstrates that the expression (A 15) for the divergences of one-loop amplitudes is fully compatible with the splitting amplitudes.

### A.3 Review of Catani's Two-Loop Divergence Formula

In a beautiful yet mysterious paper, Catani expressed the infrared-divergent parts of two-loop amplitudes as [38]

$$\mathcal{A}_n^{(2)} i_{\text{R:S.}} = I_{n;\text{R:S.}}^{(2)} ( ) \mathcal{A}_n^{(0)} i_{\text{R:S.}} + I_n^{(1)} ( ) \mathcal{A}_n^{(1)} i_{\text{R:S.}} + \mathcal{A}_n^{(2)} n_{\text{R:S.}}; \quad (A 24)$$

where  $\mathcal{A}_n^{(2)}(n_{\text{R:S}})$  is the finite remainder and the operator  $I_{n;\text{R:S}}^{(2)}(\cdot)$  is

$$I_{n;\text{R:S}}^{(2)}(\cdot) = \frac{1}{2} I_n^{(1)}(\cdot) I_n^{(1)}(\cdot) + \frac{2b_0}{2} + + \frac{e^+}{(1-\cdot)} \frac{(1-2)}{2} \frac{b_0}{2} + K_{\text{R:S}} I_n^{(1)}(2; \cdot; \text{fpg}) + H_{n;\text{R:S}}^{(2)}(\cdot); \quad (\text{A 25})$$

An argument for this general structure has been given in ref. [61]. The quantity  $K_{\text{R:S}}$  depends on the variant of dimensional regularization through the parameter  $\text{R}$  [15]. It is given by [38, 15]

$$K_{\text{FDH}}^{N=4} = -2 C_A; \quad (\text{A 26})$$

$$K_{\text{FDH}}^{N=1} = 3 - 2 - \frac{4}{9} C_A; \quad (\text{A 27})$$

$$K_{\text{R:S}}^{\text{QCD}} = \frac{67}{18} - 2 - \frac{1}{6} + \frac{4}{9} (1 - \text{R}) C_A - \frac{10}{9} T_R N_f; \quad (\text{A 28})$$

Note that in passing to the  $N = 4$  case we have switched away from the conventions of ref. [15], with regard to assigning  $\text{R}$ -dependent terms to  $K_{\text{FDH}}$ . (We did not want to destroy the uniform transcendental weight which all functions have in the  $N = 4$  case.)

The function  $H_{n;\text{R:S}}^{(2)}$  contains only single poles. It splits into two types of terms,

$$H_{n;\text{R:S}}^{(2)}(\cdot) = \frac{e}{4} \frac{(1-\cdot)}{(1-\cdot)} \sum_{i=1}^n \sum_{j \neq i} \frac{X^n}{T_i} \frac{X^n}{T_j} \frac{H_i^{(2)}}{\frac{T_j}{T_i}^2} - \frac{2}{s_{ij}} + H_n^{(2)}; \quad (\text{A 29})$$

where  $H_i^{(2)}$  is either  $H_g^{(2)}$  or  $H_q^{(2)}$ , depending on whether particle  $i$  is a gluon or a quark. The constants  $H_g^{(2)}$  and  $H_q^{(2)}$  are given by [26, 27, 28, 15, 33]

$$H_q^{(2)} = \frac{13}{2} - 3 - \frac{23}{8} - 2 + \frac{245}{216} C_A C_F + 6 - 3 - 2 - \frac{3}{8} C_F^2 + \frac{2}{2} - \frac{25}{54} C_F T_R N_f + + \frac{4}{3} C_A C_F + \frac{1}{2} C_F^2 + \frac{1}{6} C_F T_R N_f (1 - \text{R}); \quad (\text{A 30})$$

and (including also the supersymmetric cases here [15, 33]),

$$H_g^{(2);N=4} = \frac{3}{2} C_A^2; \quad (\text{A 31})$$

$$H_g^{(2);N=1} = \frac{3}{2} + \frac{3}{8} - 2 - \frac{2}{9} C_A^2; \quad (\text{A 32})$$

$$H_g^{(2);QCD} = \frac{3}{2} + \frac{11}{24} - 2 + \frac{5}{12} C_A^2 - \frac{2}{6} + \frac{58}{27} C_A T_R N_f + C_F T_R N_f + \frac{20}{27} T_R^2 N_f^2 + + \frac{11}{36} C_A^2 + \frac{1}{9} C_A T_R N_f (1 - \text{R}); \quad (\text{A 33})$$

There is no real proof that eq. (A 29) is the precise form of the  $n$ -point divergences, but previous calculations strongly indicate that it is right. There are several conventions in

the literature for ‘dressing’ the term  $s$  proportional to  $H_i^{(2)}$  with factors of ( $^2=(s_{ij})$ ) to make them dimensionally consistent. Dimensional conventions agree at 0 (1=), but generate divergent finite remainders, which would have divergent collinear behavior, affecting the results of section 8. Here we adopt a convention motivated by Catani’s treatment [38] of the 1= poles proportional to  $i$  at one loop in eq. (A.16). Note that the 1= pole part of the term  $s$  containing  $H_i^{(2)}$  in eq. (A.29) is actually proportional to the color identity matrix 1, since  $\sum_{j \neq i} T_i \cdot T_j = T_i^2$ , due to eq. (A.2).

Less is known about the function  $\hat{H}_n^{(2)}( )$ , which contains genuinely non-trivial color structure at 0 (1=). For the four-point amplitudes it is given by [15, 33]

$$\hat{H}_4^{(2)}( ) = 4 \ln \frac{s_{12}}{s_{23}} \ln \frac{s_{23}}{s_{13}} \ln \frac{s_{13}}{s_{12}} \frac{h}{T_1} \frac{i}{T_2; T_2} \frac{i}{T_3}; \quad (\text{A.34})$$

with  $\ln((s_{12})/(s_{23})) = \ln s_{12} - \ln(s_{23})$  in the s-channel, etc. A simple ansatz, generalizing eq. (A.34) to arbitrary n-parton amplitudes, is

$$\hat{H}_n^{(2)}( ) = \sum_{(i_1, i_2, i_3)} f^{a_1 a_2 a_3} T_{i_1}^{a_1} T_{i_2}^{a_2} T_{i_3}^{a_3} \ln \frac{s_{i_1 i_2}}{s_{i_2 i_3}} \ln \frac{s_{i_2 i_3}}{s_{i_1 i_3}} \ln \frac{s_{i_1 i_3}}{s_{i_1 i_2}}; \quad (\text{A.35})$$

where the sum is over distinct triplets of external legs, with  $i_1 \neq i_2 \neq i_3$ . For  $n = 4$ , there are four such triplets (omit any one of the four partons). Using  $[T_i^a; T_i^b] = if^{abc}T_i^c$ , color conservation (A.2), and antisymmetry of  $f^{abc}$ , it is easy to see that each triplet gives an equal contribution, and eq. (A.34) is recovered.

#### A.4 Collinear Compatibility with Catani’s Two-loop Divergence Formula

Next let us verify that the poles in the collinear splitting amplitudes match those predicted by Catani for the full color-space two-loop amplitude. In order to analyze these divergent terms, it is convenient to define the one-loop amplitude as being a color operator acting on the tree amplitude (assume it does not vanish),

$$\begin{aligned} \mathcal{A}_n^{(1)} i_{\text{RS}} &= M_n^{(1)}( ) \mathcal{A}_n^{(0)} i_{\text{RS}} \\ &= (I_n^{(1)}( ) + M_n^{(1)}( )) \mathcal{A}_n^{(0)} i_{\text{RS}}; \end{aligned} \quad (\text{A.36})$$

since we want to combine divergent and finite parts into a single entity. We do not actually need the explicit form of the  $M_n^{(1)}( )$  operator, although it is straightforward to construct this operator in one’s favorite color basis.

The full color-space two-loop amplitude is

$$\begin{aligned} \mathcal{A}_n^{(2)} i_{\text{RS}} &= I_n^{(1)}( ) \mathcal{A}_n^{(1)} i_{\text{RS}} + I_{n; \text{RS}}^{(2)}( ) \mathcal{A}_n^{(0)} i_{\text{RS}} + \mathcal{A}_n^{(2)} n i_{\text{RS}} \\ &= I_n^{(1)}( ) I_n^{(1)}( ) + M_n^{(1)}( ) \mathcal{A}_n^{(0)} i_{\text{RS}} + \\ &\quad + \frac{1}{2} I_n^{(1)}( ) I_n^{(1)}( ) + \frac{2b_0}{(1)} + \frac{e^+}{(1)} \frac{(1-2)}{(1)} \frac{b_0}{(1)} + K_{\text{RS}} \cdot I_n^{(1)}(2) + \\ &\quad \# \\ &\quad + H_{n; \text{RS}}^{(2)}( ) \mathcal{A}_n^{(0)} i_{\text{RS}} + \text{finite}; \end{aligned} \quad (\text{A.37})$$

After adding and subtracting finite terms to combine the  $(I_n^{(1)})^2$  term with finite pieces, in much the same way as was done for the color trivial parts in eq. (8.16), we obtain,

$$\begin{aligned} \mathcal{A}_n^{(2)} i_{\text{R:s}} = & \frac{1}{2} M_n^{(1)}( )^2 \mathcal{A}_n^{(0)} i_{\text{R:s}} + \\ & + \frac{1}{2} h I_n^{(1)}( ) M_n^{(1)}( ) + \frac{1}{4} H_n^{(2)}( ) \mathcal{A}_n^{(0)} i_{\text{R:s}} + \\ & + \frac{b_0}{4} I_n^{(1)}( ) + \frac{e^+}{4} \frac{(1-2)}{(1-)} \frac{b_0}{2} + K_{\text{R:s}} I_n^{(1)}(2) \mathcal{A}_n^{(0)} i_{\text{R:s}} \\ & - \frac{e}{4} \frac{(1)}{(1-)} \sum_{i=1}^n \sum_{j \neq i} T_i T_j \frac{H_i^{(2)}}{T_i^2} - \frac{2}{s_{ij}} \mathcal{A}_n^{(0)} i_{\text{R:s}} + \text{finite:} \quad (\text{A.38}) \end{aligned}$$

First consider the terms on the penultimate line in eq. (A.38) containing the operator  $I_n^{(1)}$ . Since the same operator appears as in the one-loop case, the collinear limit of these terms may be determined in the same way as the one-loop case, using eqs. (A.19) and (A.12) in particular. Equation (A.19) says nothing about the  $O(0)$  terms in  $I_n^{(1)}$ . Fortunately these terms are identical for  $I_n^{(1)}( )$  and  $I_n^{(1)}(2)$ ; hence their contribution to the singular terms in eq. (A.38), when they are multiplied by  $b_0 = 0$ , cancels. Following the one-loop discussion, we obtain contributions to the two-loop splitting amplitude of the form

$$N_c - \frac{b_0}{4} \bar{r}_s^{(1)}( ) + \frac{e^+}{4} \frac{(1-2)}{(1-)} \frac{b_0}{2} + K_{\text{R:s}} \bar{r}_s^{(1)}(2) \text{Split}^{(0)} + \text{finite:} \quad (\text{A.39})$$

(Recall that  $\bar{r}_s^{(1)}$ , introduced in section 8, denotes the renormalized splitting ratio.)

Now consider the terms containing  $H_i^{(2)}$  on the last line of eq. (A.38). These terms are written in the same form as  $I_n^{(1)}$ , but with one less power of  $1-0$ , so their collinear behavior again follows from the one-loop discussion. Their contribution to the two-loop splitting amplitude is just

$$\frac{H_g^{(2)}}{4} \text{Split}^{(0)} + \text{finite:} \quad (\text{A.40})$$

where  $H_g^{(2)}$  is given in eq. (A.33).

Next consider the  $(M_n^{(1)}( ))^2$  term in eq. (A.38). In the collinear limits for this term we have,

$$\frac{1}{2} M_n^{(1)}( )^2 \text{Split}^{(0)} \mathcal{A}_{n-1}^{(0)} i: \quad (\text{A.41})$$

In order to evaluate this we use the collinear relation,

$$M_n^{(1)} \text{Split}^{(0)} : \text{Split}^{(0)} M_{n-1}^{(1)} + \text{Split}^{(1)}; \quad (\text{A.42})$$

which is a rewriting of eq. (A.10) after acting on  $\mathcal{A}_{n-1}^{(0)} i$  and using eq. (A.36). Using eq. (A.42), we find that in the collinear limit,

$$\frac{1}{2} M_n^{(1)}( )^2 \text{Split}^{(0)} : \frac{1}{2} M_n^{(1)} \text{Split}^{(0)} M_{n-1}^{(1)} + \text{Split}^{(1)} : \quad (\text{A.43})$$

To simplify the  $\text{Split}^{(1)}$  term we may multiply eq. (A.42) by  $N_c \bar{r}_S^{(1)}(\cdot)$  to obtain

$$M_n^{(1)} \text{Split}^{(1)} ! \text{Split}^{(1)} M_{n-1}^{(1)} + \text{Split}^{(1)} N_c \bar{r}_S^{(1)}(\cdot); \quad (\text{A.44})$$

where we used eq. (A.12). Then applying eqs. (A.42) and (A.44) to eq. (A.43) yields

$$\begin{aligned} \frac{1}{2} M_n^{(1)} {}^2 \text{Split}^{(0)} ! \frac{1}{2} \text{Split}^{(0)} M_{n-1}^{(1)} M_{n-1}^{(1)} + 2 \text{Split}^{(1)} M_{n-1}^{(1)} + \text{Split}^{(1)} N_c \bar{r}_S^{(1)}(\cdot) \\ = \text{Split}^{(0)} \frac{1}{2} M_{n-1}^{(1)} M_{n-1}^{(1)} + \text{Split}^{(1)} M_{n-1}^{(1)} + \frac{1}{2} (N_c \bar{r}_S^{(1)}(\cdot))^2 \text{Split}^{(0)} : \end{aligned} \quad (\text{A.45})$$

The first term on the last line may be identified as a contribution to  $\text{Split}^{(0)} \mathcal{A}_{n-1}^{(2)} i$ , the second as a contribution to  $\text{Split}^{(1)} \mathcal{A}_{n-1}^{(1)} i$ , while the third is the contribution we include in  $\text{Split}^{(2)} \mathcal{A}_{n-1}^{(0)} i$ .

Finally we examine the second line of eq. (A.38), containing the commutator term and  $\hat{H}_n^{(2)}$ . After some manipulations involving eqs. (A.42) and (A.44) we may write the part of the commutator term that does not contribute to  $\text{Split}^{(0)} \mathcal{A}_{n-1}^{(2)} i$  as

$$\begin{aligned} \frac{1}{2} M_n^{(1)} I_n^{(1)} \text{Split}^{(0)} & \text{Split}^{(0)} I_{n-1}^{(1)} \text{Split}^{(1)} + \\ + \frac{1}{2} I_n^{(1)} \text{Split}^{(0)} & \text{Split}^{(0)} I_{n-1}^{(1)} \text{Split}^{(1)} (M_{n-1}^{(1)} + N_c \bar{r}_S^{(1)}); \end{aligned} \quad (\text{A.46})$$

where the finite combination appearing is,

$$\begin{aligned} I_n^{(1)} \text{Split}^{(0)} & \text{Split}^{(0)} I_{n-1}^{(1)} \text{Split}^{(1)} \\ h & i x^n \\ = \ln z T_1 + \ln(1-z) T_2 & T_j \ln(s_{p,j}) \text{Split}^{(0)} + O(\cdot) : \end{aligned} \quad (\text{A.47})$$

Only the universal  $1 =$  terms in  $M_n^{(1)}$  contribute in eq. (A.46) to the order we need, and we may obtain these terms from  $I_n^{(1)}$ . Inserting these terms, and moving them to the right with the help of color commutators, the total contribution to  $\text{Split}^{(2)} \mathcal{A}_{n-1}^{(0)} i$  from the commutator term is

$$\begin{aligned} \frac{i}{2} \ln \frac{z}{1-z} & \sum_{i=3}^{X^n} f^{abc} T_1^a T_2^b T_i^c \ln(s_{p,i}) \ln(s_{p,i}) + \ln z + \ln(1-z) \ln(s_{12}) + \\ & \# \\ + \sum_{i=3}^{X^n} \sum_{j=3; j \neq i}^{X^n} f^{abc} & \ln z T_1^a + \ln(1-z) T_2^a T_i^b T_j^c \ln(s_{p,i}) \ln(s_{ij}) \text{Split}^{(0)} : \end{aligned} \quad (\text{A.48})$$

This result turns out to be precisely the negative of the corresponding contribution from the  $\hat{H}_n^{(2)}$  term. Thus the second line of eq. (A.38) only contributes to the tree-level splitting amplitude term,  $\text{Split}^{(0)} \mathcal{A}_{n-1}^{(2)}(\cdot) i$ , in eq. (A.13).

Combining the contributions to  $\text{Split}^{(2)}$  in eqs. (A.39) and (A.40) and (A.45), we obtain,

$$\text{Split}^{(2)}(1^1; 2^2) = N_c^2 \text{Split}^{(2)}(1^1; 2^2) f_p$$

$$\begin{aligned}
&= N_c^2 \frac{1}{2} (\bar{r}_S^{(1)}(\ ))^2 \\
&\quad + \frac{b_0}{N_c} \bar{r}_S^{(1)}(\ ) + \frac{e^+}{N_c} \frac{(1 \ 2)}{(1 \ )} \frac{b_0}{b_0 + K_{R:S:}} \bar{r}_S^{(1)}(2 \ ) + \\
&\quad + \frac{1}{4} \frac{H_g^{(2)}}{N_c^2} + \text{nite } \text{Split}^{(0)}(1^1; 2^2) f_P \\
&= N_c^2 \bar{r}_S^{(2)}(\ ) \text{Split}^{(0)}(1^1; 2^2) f_P + \text{nite}; \tag{A.49}
\end{aligned}$$

where  $\bar{r}_S^{(2)}(\ )$  is given in eq. (8.18). This in turn agrees with the divergent parts of the splitting amplitudes for  $N = 4$  and  $N = 1$  supersymmetric theories, and for QCD, as given in section 7, after they are renormalized according to eq. (8.8). Thus our splitting amplitudes are fully compatible with Catani's color-space formula for the infrared divergences of scattering amplitudes.

As noted already, this agreement may be turned around to prove the validity of Catani's formula inductively, up to reasonable assumptions about the analytic structure of the - singular parts, i.e. such that they do not have vanishing collinear limits in all channels.

## B . R elabeling A lgorithm

For completeness, in this appendix we review a simple procedure for mechanically performing relabelings. For the splitting amplitude problem discussed in this paper, it is not difficult to identify the diagrammatic structure of a given term and map the momentum labels used in the cuts to those used in the integration. However, for more general problems it may be useful to perform these steps algorithmically. To do so, first one chooses a set of parent diagrams and momentum labels used in the integration. To sort the terms into diagrams it is useful to collect the terms on each propagator or light-cone denominator type. The propagators and light-cone denominators encode the diagram type, but with labels not matching the ones used in integration. Assuming the external legs are ordered the same way in the cut and integration labels (if not, one should permute the external legs), the problem amounts to finding a mapping between a given term in the cuts and the diagram to which it belongs. For an  $n$ -point  $L$  loop diagram there are  $L$  independent loop momenta and  $n - 1$  independent external momenta, under momentum conservation. If the loop propagators carry momenta  $p_i$  in one set of labelings and  $q_i$  in another labeling, then a change of variables should exist relating the two of the form,

$$q_i = \sum_{j=1}^{X^L} a_{ij} p_j + \sum_{j=1}^{X^1} b_{ij} k_j; \tag{B.1}$$

where the  $a_{ij}$  and  $b_{ij}$  are in the set  $\{1; 0; 1g\}$ . This form assumes that for both the original and final momentum labels the momentum of each internal leg is a sum or difference of the independent momenta, as naturally arises either in cut or Feynman diagram momentum routings. One sweeps over all changes of variables in eq. (B.1) until a match is found. If no change of variables matches then the subsequent diagrams should be checked until a

match is found. A convenient way to rule out putative changes of variables is to first set all external momenta to zero, then re-introduce them one by one, eliminating candidate diagrams and solving for the  $b_{ij}$ .

As a simple example, consider the double triangle diagram with a light-cone denominator occurring in our calculation of the two-loop splitting amplitude. From its origin in the three-particle cuts shown in figure 26(b), where the cut momenta are  $f q_1$ ;  $q_1 - q_2 - k_1 - k_2$ ;  $q_2 g$ , this diagram is described by the set of propagators and light-cone denominators

$$f q_1^2; q_2^2; (q_2 + k_2)^2; (q_2 + k_1 + k_2)^2; (q_2 + q_1 + k_1 + k_2)^2; (q_1 + k_1 + k_2)^2; q_1 \text{ ng:} \quad (B.2)$$

The denominator variables used in the integration routines, shown in figure 29(a), are

$$f p_1^2; (p_1 + k_1 + k_2)^2; p_2^2; (p_2 - k_1 - k_2)^2; (p_2 - k_1)^2; (p_1 + p_2)^2; p_1 \text{ ng} \quad (B.3)$$

where  $p_2$  is labeled as  $p_3$  in the figure. After sweeping through the change of variables in eq. (B.1) one finds that the two sets of momenta are related by

$$q_1 = p_1; \quad q_2 = p_2 - k_1 - k_2; \quad (B.4)$$

With this change of variable the two sets of propagators and denominators in eqs. (B.2) and (B.3) are identical, except for the order in which they appear.

## References

- [1] F.A. Berends, R.K. Ellis, P. De Causmaecker, R. Gastmans and T.T. Wu, *Phys. Lett. B* 103, 124 (1981);  
P. De Causmaecker, R. Gastmans, W. Troost and T.T. Wu, *Phys. Lett. B* 105, 215 (1981);  
J.F. Gunion and Z. Kunszt, *Phys. Lett. B* 161, 333 (1985);  
Z. Xu, D. Zhang and L. Chang, *Nucl. Phys. B* 291, 392 (1987).
- [2] J.E. Paton and H.-M. Chan, *Nucl. Phys. B* 10, 516 (1969);  
P. Cvitanovic, P.G. Lauwers and P.N. Scharbach, *Nucl. Phys. B* 186, 165 (1981);  
M. L. Mangano, *Nucl. Phys. B* 309, 461 (1988).
- [3] F.A. Berends and W.T.Giele, *Nucl. Phys. B* 294, 700 (1987).
- [4] M. L. Mangano, S.J. Parke and Z. Xu, *Nucl. Phys. B* 298, 653 (1988).
- [5] Z. Bern and D.A. Kosower, *Nucl. Phys. B* 362, 389 (1991).
- [6] V. Del Duca, L.J. Dixon and F. Maltoni, *Nucl. Phys. B* 571, 51 (2000)  
[arXiv:hep-ph/9910563].
- [7] F.A. Berends and W.T.Giele, *Nucl. Phys. B* 306, 759 (1988);  
D.A. Kosower, *Nucl. Phys. B* 335, 23 (1990);  
G. Mahlon and T.M. Yan, *Phys. Rev. D* 47, 1776 (1993) [arXiv:hep-ph/9210213];  
G. Mahlon, T.M. Yan and C. Dunn, *Phys. Rev. D* 48, 1337 (1993) [arXiv:hep-ph/9210212].
- [8] Z. Bern and D.A. Kosower, *Nucl. Phys. B* 379, 451 (1992).
- [9] E.W.itten, arXiv:hep-th/0312171;  
F. Cachazo, P. Svrcek and E.W.itten, arXiv:hep-th/0403047.

[10] Z. Bem, L.J.D. Dixon, D.C. Dunbar and D.A. Kosower, *Nucl. Phys. B* 425, 217 (1994) [[arXiv:hep-ph/9403226](#)].

[11] Z. Bem, L.J.D. Dixon, D.C. Dunbar and D.A. Kosower, *Nucl. Phys. B* 435, 59 (1995) [[arXiv:hep-ph/9409265](#)].

[12] Z. Bem and A.G. M. Organ, *Nucl. Phys. B* 467, 479 (1996) [[arXiv:hep-ph/9511336](#)].

[13] Z. Bem, L.J.D. Dixon and D.A. Kosower, *Ann. Rev. Nucl. Part. Sci.* 46, 109 (1996) [[arXiv:hep-ph/9602280](#)].

[14] Z. Bem, L.J.D. Dixon and D.A. Kosower, *JHEP* 0001, 027 (2000) [[arXiv:hep-ph/0001001](#)].

[15] Z. Bem, A. De Freitas and L.J.D. Dixon, *JHEP* 0203, 018 (2002) [[arXiv:hep-ph/0201161](#)].

[16] V.A. Smirnov, *Phys. Lett. B* 460, 397 (1999) [[arXiv:hep-ph/9905323](#)].

[17] J.B. Tausk, *Phys. Lett. B* 469, 225 (1999) [[arXiv:hep-ph/9909506](#)].

[18] V.A. Smirnov and O.L. Veretin, *Nucl. Phys. B* 566, 469 (2000) [[arXiv:hep-ph/9907385](#)].

[19] C. Anastasiou, T. Gehrmann, C. Oleari, E. Remiddi and J.B. Tausk, *Nucl. Phys. B* 580, 577 (2000) [[arXiv:hep-ph/0003261](#)].

[20] T. Gehrmann and E. Remiddi, *Nucl. Phys. B* 580, 485 (2000) [[arXiv:hep-ph/9912329](#)].

[21] T. Gehrmann and E. Remiddi, *Nucl. Phys. B* 601, 248 (2001) [[arXiv:hep-ph/0008287](#)]; *Nucl. Phys. B* 601, 287 (2001) [[arXiv:hep-ph/0101124](#)].

[22] T. Gehrmann and E. Remiddi, *Nucl. Phys. B* 640, 379 (2002) [[arXiv:hep-ph/0207020](#)].

[23] S. Laporta, *Int. J. Mod. Phys. A* 15, 5087 (2000) [[arXiv:hep-ph/0102033](#)].

[24] S. Moch, P. Uwer and S. Weinzierl, *J. Math. Phys.* 43, 3363 (2002) [[arXiv:hep-ph/0110083](#)].

[25] Z. Bem, L.J.D. Dixon and A.G. Hinculov, *Phys. Rev. D* 63, 053007 (2001) [[arXiv:hep-ph/0010075](#)].

[26] C. Anastasiou, E.W.N. Glover, C. Oleari and M.E. Tejeda-Yeomans, *Nucl. Phys. B* 601, 318 (2001) [[hep-ph/0010212](#)]; *Nucl. Phys. B* 601, 341 (2001) [[hep-ph/0011094](#)].

[27] C. Anastasiou, E.W.N. Glover, C. Oleari and M.E. Tejeda-Yeomans, *Nucl. Phys. B* 605, 486 (2001) [[hep-ph/0101304](#)].

[28] E.W.N. Glover, C. Oleari and M.E. Tejeda-Yeomans, *Nucl. Phys. B* 605, 467 (2001) [[arXiv:hep-ph/0102201](#)].

[29] Z. Bem, A. De Freitas and L.J.D. Dixon, *JHEP* 0109, 037 (2001) [[arXiv:hep-ph/0109078](#)].

[30] Z. Bem, A. De Freitas, L.J.D. Dixon, A.G. Hinculov and H.L. Wong, *JHEP* 0111, 031 (2001) [[arXiv:hep-ph/0109079](#)].

[31] C. Anastasiou, E.W.N. Glover and M.E. Tejeda-Yeomans, *Nucl. Phys. B* 629, 255 (2002) [[arXiv:hep-ph/0201274](#)].

[32] T. Binoth, E.W.N. Glover, P.M. Harland and J.J. van der Bij, *JHEP* 0205, 060 (2002) [[arXiv:hep-ph/0202266](#)].

[33] Z. Bem, A. De Freitas and L.J.D. Dixon, *JHEP* 0306, 028 (2003) [[arXiv:hep-ph/0304168](#)].

[34] E.W.N. Glover and M.E. Tejeda-Yeomans, *JHEP* 0306, 033 (2003) [[arXiv:hep-ph/0304169](#)].

[35] E.W.N. Glover, arXiv:hep-ph/0401119.

[36] L.W.Garland, T.Gehrmann, E.W.N. Glover, A.Koukoutsakis and E.Remiddi, Nucl. Phys. B 627, 107 (2002) [arXiv:hep-ph/0112081].

[37] L.W.Garland, T.Gehrmann, E.W.N. Glover, A.Koukoutsakis and E.Remiddi, Nucl. Phys. B 642, 227 (2002) [arXiv:hep-ph/0206067];  
S.Moch, P.Uwer and S.Weinzierl, Acta Phys. Polon. B 33, 2921 (2002) [arXiv:hep-ph/0207167].

[38] S.Catani, Phys. Lett. B 427, 161 (1998) [arXiv:hep-ph/9802439].

[39] F.A.Berends and W.T.Giele, Nucl. Phys. B 313, 595 (1989).

[40] J.M.Campbell and E.W.N. Glover, Nucl. Phys. B 527, 264 (1998) [arXiv:hep-ph/9710255].

[41] S.Catani and M.Grazzini, Phys. Lett. B 446, 143 (1999) [arXiv:hep-ph/9810389];  
Nucl. Phys. B 570, 287 (2000) [arXiv:hep-ph/9908523].

[42] Z.Bern, V.Delduc and C.R.Schmidt, Phys. Lett. B 445, 168 (1998) [arXiv:hep-ph/9810409];  
Z.Bern, V.Delduc, W.B.Kilgore and C.R.Schmidt, Phys. Rev. D 60, 116001 (1999) [arXiv:hep-ph/9903516].

[43] D.A.Kosower and P.Uwer, Nucl. Phys. B 563, 477 (1999) [arXiv:hep-ph/9903515];

[44] S.Weinzierl, JHEP 0307, 052 (2003) [arXiv:hep-ph/0306248].

[45] G.Altarelli and G.Parisi, Nucl. Phys. B 126, 298 (1977).

[46] W.L.van Neerven and A.Vogt, Nucl. Phys. B 568, 263 (2000) [arXiv:hep-ph/9907472];  
Nucl. Phys. B 588, 345 (2000) [arXiv:hep-ph/0006154];  
Phys. Lett. B 490, 111 (2000) [arXiv:hep-ph/0007362];

[47] S.Moch, J.A.M.Vermaseren and A.Vogt, Nucl. Phys. B 646, 181 (2002) [arXiv:hep-ph/0209100].

[48] S.Moch, J.A.M.Vermaseren and A.Vogt, arXiv:hep-ph/0403192;  
A.Vogt, S.Moch and J.A.M.Vermaseren, arXiv:hep-ph/0404111.

[49] D.A.Kosower and P.Uwer, in proceedings of International Europhysics Conference on High-Energy Physics (EPS-HEP 99), Tampere, Finland (1999); Nucl. Phys. B 674, 365 (2003) [arXiv:hep-ph/0307031].

[50] D.deFlorian and M.Grazzini, Nucl. Phys. B 616, 247 (2001) [arXiv:hep-ph/0108273].

[51] J.A.Minhaan and K.Zarembo, JHEP 0303, 013 (2003) [hep-th/0212208]; N.Beisert,  
S.Frolov, M.Staudacher and A.A.Tseytlin, JHEP 0310, 037 (2003), and references therein.

[52] C.Anastasiou, Z.Bern, L.J.Dixon and D.A.Kosower, Phys. Rev. Lett. 91, 251602 (2003) [arXiv:hep-th/0309040].

[53] Z.Bern, L.J.Dixon, M.Perelstein and J.S.Rozowsky, Nucl. Phys. B 546, 423 (1999) [arXiv:hep-th/9811140].

[54] J.C.Collins, D.E.Soper and G.Sterman, Phys. Lett. B 134, 263 (1984); Nucl. Phys. B 261, 104 (1985); in Perturbative Quantum Chromodynamics, ed. by A.H.Mueller, World Scientific (1989), Singapore.

[55] Z.Bern and G.Chalmers, Nucl. Phys. B 447, 465 (1995) [arXiv:hep-ph/9503236].

[56] A. Bassutto, G. Nardelli and R. Soldati, *Yang-Mills Theories in Algebraic Noncovariant Gauges: Canonical Quantization and Renormalization*, World Scientific (1991), Singapore; G. Leibbrandt, *Noncovariant Gauges: Quantization of Yang-Mills and Chern-Simons Theory in Axial-Type Gauges*, World Scientific (1994), Singapore.

[57] A. Andrasik and J.C. Taylor, *Nucl. Phys. B* 310, 222 (1988).

[58] Z. Bern, L.J. Dixon, D.A. Kosower and M. Schreiber, in progress.

[59] F.V. Tkachov, *Phys. Lett. B* 100, 65 (1981);  
K.G. Chetyrkin and F.V. Tkachov, *Nucl. Phys. B* 192, 159 (1981).

[60] C. Anastasiou and A. Lazopoulos, [arXiv:hep-ph/0404258](https://arxiv.org/abs/hep-ph/0404258).

[61] G. Sterman and M. E. Tejeda-Yeomans, *Phys. Lett. B* 552, 48 (2003) [[arXiv:hep-ph/0210130](https://arxiv.org/abs/hep-ph/0210130)].

[62] A. Koukoutsakis, Ph.D. thesis, U. Durham (2003).

[63] V. Del Duca, A. Frizzo and F. Maltoni, *Nucl. Phys. B* 568, 211 (2000) [[arXiv:hep-ph/9909464](https://arxiv.org/abs/hep-ph/9909464)].

[64] S. Catani, D. de Florian and G. Rodrigo, *Phys. Lett. B* 586, 323 (2004) [[arXiv:hep-ph/0312067](https://arxiv.org/abs/hep-ph/0312067)].

[65] D.A. Kosower, *Nucl. Phys. B* 552, 319 (1999) [[arXiv:hep-ph/9901201](https://arxiv.org/abs/hep-ph/9901201)].

[66] M. L.M. Angano and S.J. Parke, *Phys. Rept.* 200, 301 (1991);  
L.J. Dixon, [arXiv:hep-ph/9601359](https://arxiv.org/abs/hep-ph/9601359).

[67] S.J. Parke and T.R. Taylor, *Phys. Rev. Lett.* 56, 2459 (1986).

[68] G. 't Hooft and M.J.G. Veltman, *Nucl. Phys. B* 44, 189 (1972).

[69] Z. Bern, A.D. de Freitas, L.J. Dixon and H.L.Wong, *Phys. Rev. D* 66, 085002 (2002) [[arXiv:hep-ph/0202271](https://arxiv.org/abs/hep-ph/0202271)].

[70] W. Siegel, *Phys. Lett. B* 84, 193 (1979);  
D.M. Capper, D.R.T. Jones and P. van Nieuwenhuizen, *Nucl. Phys. B* 167, 479 (1980);  
I. Jack, D.R.T. Jones and K.L. Roberts, *Z. Phys. C* 63, 151 (1994) [[arXiv:hep-ph/9401349](https://arxiv.org/abs/hep-ph/9401349)].

[71] Z. Bern, J.S. Rozowsky and B. Yan, *Phys. Lett. B* 401, 273 (1997) [[arXiv:hep-ph/9702424](https://arxiv.org/abs/hep-ph/9702424)];  
Z. Bern, L.J. Dixon, D.C. Dunbar, M. Perelstein and J.S. Rozowsky, *Nucl. Phys. B* 530, 401 (1998) [[arXiv:hep-th/9802162](https://arxiv.org/abs/hep-th/9802162)].

[72] J.-L. Gervais and A. Neveu, *Nucl. Phys. B* 46, 381 (1972).

[73] R.K. Ellis, H. Georgi, M.M.achacek, H.D. Politzer and G.G. Ross, *Phys. Lett. B* 78, 281 (1978); *Nucl. Phys. B* 152, 285 (1979).

[74] G. Curci, W. Furryanski and R. Petronzio, *Nucl. Phys. B* 175, 27 (1980).

[75] W. Furryanski and R. Petronzio, *Phys. Lett. B* 97, 437 (1980).

[76] R.K. Ellis and W. Vogelsang, [arXiv:hep-ph/9602356](https://arxiv.org/abs/hep-ph/9602356).

[77] S. Mandelstam, *Nucl. Phys. B* 213, 149 (1983).

[78] G. Heinrich and Z. Kunszt, *Nucl. Phys. B* 519, 405 (1998) [[arXiv:hep-ph/9708334](https://arxiv.org/abs/hep-ph/9708334)].

[79] L.D. Landau, *Nucl. Phys.* 13, 181 (1959);  
S. Mandelstam, *Phys. Rev.* 112, 1344 (1958); 115, 1741 (1959);  
R.E. Cutkosky, *J. Math. Phys.* 1, 429 (1960).

[80] M. E. Peskin and D. V. Schroeder, *An Introduction to Quantum Field Theory*, Addison-Wesley (1995), Menlo Park.

[81] W. L. van Neerven, *Nucl. Phys. B* 268, 453 (1986).

[82] Z. Bern, L.J. Dixon and D.A. Kosower, *Nucl. Phys. B* 412, 751 (1994) [[arXiv:hep-ph/9306240](#)];  
 J.M. Campbell, E.W.N. Glover and D.J.M. Miller, *Phys. Lett. B* 409, 503 (1997) [[arXiv:hep-ph/9706297](#)];  
 T. Binoth, J.P. Guillet and G. Heinrich, *Nucl. Phys. B* 572, 361 (2000) [[arXiv:hep-ph/9911342](#)].

[83] J.C. Collins, *Renormalization: an Introduction to the Renormalization Group and the Operator-Product Expansion*, Cambridge Monographs on Mathematical Physics, Cambridge University Press (1984), Cambridge.

[84] D.A. Kosower, *Phys. Rev. D* 67, 116003 (2003) [[arXiv:hep-ph/0212097](#)];  
 S. Weinzierl, *JHEP* 0303, 062 (2003) [[arXiv:hep-ph/0302180](#)].

[85] L. Lewin, *Di logarithms and Associated Functions*, Macdonald (1958), London.

[86] E. Remiddi and J.A.M. Vermaasen, *Int. J. Mod. Phys. A* 15, 725 (2000) [[arXiv:hep-ph/9905237](#)].

[87] C. Anastasiou, E.W.N. Glover and C.O. Lepage, *Nucl. Phys. B* 575, 416 (2000), err. *ibid. B* 585, 763 (2000) [[arXiv:hep-ph/9912251](#)].

[88] MAPLE, <http://www.maplesoft.com>

[89] J.A.M. Vermaasen, [arXiv:math-ph/0010025](#).

[90] R.J. Gonzalves, *Phys. Rev. D* 28, 1542 (1983).

[91] M.T. Grisaru, H.N. Pendleton and P. van Nieuwenhuizen, *Phys. Rev. D* 15, 996 (1977);  
 M.T. Grisaru and H.N. Pendleton, *Nucl. Phys. B* 124, 81 (1977);  
 S.J. Parke and T.R. Taylor, *Phys. Lett. B* 157, 81 (1985), err. *ibid. B* 174, 465 (1985).

[92] Z. Bern, L.J. Dixon, D.C. Dunbar and D.A. Kosower, *Phys. Lett. B* 394, 105 (1997) [[arXiv:hep-th/9611127](#)].

[93] S. Catani and M.G. Razzini, *Nucl. Phys. B* 591, 435 (2000) [[arXiv:hep-ph/0007142](#)].